INFORMATION TO USERS

This manuscript has been reproduced from the microfilm master. UMI films the text directly from the original or copy submitted. Thus, some thesis and dissertation copies are in typewriter face, while others may be from any type of computer printer.

The quality of this reproduction is dependent upon the quality of the copy submitted. Broken or indistinct print, colored or poor quality illustrations and photographs, print bleedthrough, substandard margins, and improper alignment can adversely affect reproduction.

In the unlikely event that the author did not send UMI a complete manuscript and there are missing pages, these will be noted. Also, if unauthorized copyright material had to be removed, a note will indicate the deletion.

Oversize materials (e.g., maps, drawings, charts) are reproduced by sectioning the original, beginning at the upper left-hand corner and continuing from left to right in equal sections with small overlaps.

Photographs included in the original manuscript have been reproduced xerographically in this copy. Higher quality 6" x 9" black and white photographic prints are available for any photographs or illustrations appearing in this copy for an additional charge. Contact UMI directly to order.

ProQuest Information and Learning
300 North Zeeb Road, Ann Arbor, MI 48106-1346 USA
800-521-0600

RICE UNIVERSITY

CHEMISTRY OF GROUP 13 LEWIS ACIDS

by

CATHERINE S. BRANCH

A THESIS SUBMITTED
IN PARTIAL FULFILLMENT OF THE
REQUIREMENTS FOR THE DEGREE
DOCTOR OF PHILOSOPHY

APPROVED, THESIS COMMITTEE

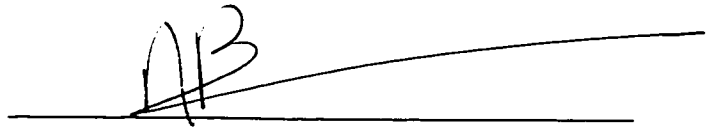

Andrew R. Barron, Chairman
Charles W. Duncan, Jr. – Welch Chair of
Chemistry and Professor of Materials Science

Lon J. Wilson,
Professor of Chemistry

Peter J. A. Nordlander,
Professor of Physics and Astronomy

Houston, Texas
April, 2002

UMI Number: 3047293

UMI®

UMI Microform 3047293

Copyright 2002 by ProQuest Information and Learning Company.
All rights reserved. This microform edition is protected against
unauthorized copying under Title 17, United States Code.

ProQuest Information and Learning Company
300 North Zeeb Road
P.O. Box 1346
Ann Arbor, MI 48106-1346

Abstract

Chemistry of Group 13 Lewis Acids

by

Catherine S. Branch

Reaction of 9-fluorenone with a Group 13 Lewis acid, MX_3 (M = B, Al, Ga; X = Cl, Br), yields a Lewis acid-base adduct, $MX_3(9\text{-fluorenone})_n$. Bond dissociation energies for MX_3(9-fluorenone) in solution have been determined. BDE and other thermodynamic values are good indicators of the strength of a Lewis acid-base interaction. Correlating these values with various spectroscopic data should lead to a simple test of Lewis acidity.

Hydrogen/deuterium exchange between naphthalene and C_6D_6 is catalyzed by $Hg(C_6D_6)_2(GaCl_4)_2$ and occurs by electrophilic substitution. In this regard, we have studied the kinetics of H/D exchange, using ^1H NMR. There are two distinct first order regimes, separated by a non-first order regime. In the first regime, $Hg(C_6D_6)_2(GaCl_4)_2$ deuterates free naphthalene. As the reaction progresses, a ligand exchange occurs between C_6D_6 and naphthalene, resulting in the protonation of C_6D_6 by $Hg(C_{10}H_8)_2(GaCl_4)_2$. This ligand exchange has been confirmed by ^{13}C CPMAS NMR of

$Hg(C_{10}H_8)_2(GaCl_4)_2$, as well as by DFT calculations, UV-visible spectroscopy, and MS. The rates of not only H/D exhange, but also the rate of ligand exchange has been determined.

Reaction of $M(^tBu)_3$ with anthranilic, salicylic, and *ortho*-toluic acids yields $[(^tBu)_2M(\mu\text{-}O_2CC_6H_4\text{-}2\text{-}NH_2)]_2$, M = Al, Ga; $[(^tBu)_2Ga(\mu\text{-}O_2CC_6H_4\text{-}2\text{-}OH)]_2$, and $[(^tBu)_2Ga(\mu\text{-}O_2CC_6H_4\text{-}2\text{-}Me)]_2$, respectively. Reaction of anthranilic acid with two equivalents of $Al(^tBu)_3$ allows for the isolation of $(^tBu)_2Al(\mu\text{-}O_2CC_6H_4\text{-}2\text{-}NH_2)Al(^tBu)_3$. Based on this compound's isolation and its conversion to $[(^tBu)_2Al(\mu\text{-}O_2CC_6H_4\text{-}2\text{-}NH_2)]_2$ during physical grinding, a proposal that the formation of $[(^tBu)_2M(\mu\text{-}O_2CC_6H_4\text{-}2\text{-}X)]_2$ occurs *via* a chelate species can be made. Additionally, intra-molecular hydrogen bonding, found in the anthranilate and salicylate ligands, remains present in the Group 13 compounds but is not enhanced.

"What if the hokey pokey is all it really is about?"

-Jimmy Buffett

For Aunt Cat.

Acknowledgements

I'd like to thank my advisor, Professor Andrew Barron, for his seemingly endless supply of both insight and patience. I would not have come to Rice without his being here, and I certainly would not have finished. Lotus is now more than a bug...or a flower.

Thanks to Larry Alemany and to Xiao for always being a step away when the 200 didn't do what I thought it was supposed to.

Thank you, Simon Bott, for all your work on my crystal structures. UGA!

Thank you, Niamh McMahon. Like someone once said to Donna Shalala: "You rock!" All other post-docs were shadows of you. I've never met a teacher with more patience with inane questions and mistakes. Your guidance in my first year was invaluable.

The Barron group, past and present: Julie, crossword puzzles were never so fun. Cullen, a fellow yellow-dog Democrat. Chris and Rhonda, corruptors in New Orleans! Max, that Scout. And running the Houston Marathon. And for making everything hard look easy. Alex, you didn't kill me when I asked you DFT Question Number 236,542,543. You are a better person than I. Steve, whenever I needed an ear, you were there. Whether you wanted to be or not. Liz, nothing seems to bother you. Famine, pestilence, three piles of my NMR spectra on your desk. Ryan, you could always make

me laugh. Naureen, you believed that I knew anything about coating this, that, and the other. Doug, Robin and Chris, play hard.

John Thurston, while we were talking about the CCD, you became a friend.

Thanks to all the non-Parrotheads who went to Buffett shows with me: Regina, Neil, Ric, Thierry, Kim, Laura, Steve, Max, Ryan, Doug, Laura B., Robin. May they soon see the light. **FINS UP!**

Thank you, Mama. Even a thousand miles away, you were there to listen to me vent, to rage, to cry. You believed in me when I didn't. You told me it would be okay, and you were right. You told me that things happen for a reason, and they do. You've been more of a support for me out here than you could ever imagine.

And now, the other two Andy's Angels...what can I say? We drank more while writing up than we should. We ate vegetables either in pizza or spring roll form. We sang The Sound of Music in Andy's office the moment he left lab (and while he was there). We went to Lubbock, of all places. We saw a zebra outside Austin. We took a detour to New Orleans. We made up stories about Swamp People. We never Checked the Children. We sat on the steps at Valhalla in the middle of the day. Kim and Laura, y'all made this whole adventure what it was. When we're on opposite sides of the country, I'm going to miss you both terribly.

Table of Contents

List of Figures x

List of Tables xv

List of Compounds xvii

Abbreviations and Glossary ixx

Introduction 1

Chapter 1. Group 13 Trihalide Complexes of 9-Fluorenone:

A Comparison of Methods for Assigning Relative Lewis Acidity

Introduction 15

Results and Discussion 18

Characterization of 9-fluorenone complexes 18

Bond dissociation energies for MX_3(9-fluorenone) 28

Is there a simple parameter for Lewis acidity? 32

Conclusions 40

Experimental 40

References 49

Chapter 2. Aluminum and Gallium Compounds of Salicylic and Anthranilic Acids: Examples of Weak Intra-Molecular Hydrogen Bonding

Introduction 54

Results and Discussion 55

Conclusions 65

Experimental 65

References 72

Chapter 3. Arene-Mercury Complexes Stabilized by Gallium Chloride: Relative Rates of H/D and Arene Exchange

Introduction 75

Results and Discussion 77

Conclusions 94

Experimental 94

References 96

Appendix 100

List of Figures

Chapter 1

Figure 1.1. MX_3(9-fluorenone) complexes are brightly colored: (**a**) 9-fluorenone, (**b**) $GaCl_3$(9-fluorenone), and (**c**) $AlBr_3$(9-fluorenone). 19

Figure 1.2. Molecular structure of BCl_3(9-fluorenone) (**1.1**). Thermal ellipsoids are shown at the 30% level. 21

Figure 1.3. Molecular structure of $AlBr_3$(9-fluorenone) (**1.2**). Thermal ellipsoids are shown at the 30% level. 22

Figure 1.4. Molecular structure of $GaCl_3$(9-fluorenone) (**1.5**). Thermal ellipsoids are shown at the 30% level. 22

Figure 1.5. Molecular structure of $GaBr_3$(9-fluorenone) (**1.6**). Thermal ellipsoids are shown at the 30% level. 23

Figure 1.6. Molecular structure of $AlBr_3$(9-fluorenone)$_2$ (**1.3**). Thermal ellipsoids are shown at the 30% level. 24

Figure 1.7. Coordination sphere of $AlBr_3$(9-fluorenone)$_2$ (**1.3**) viewed along the O(1)-Al(1)-O(1A) vector, showing the orientation of the two 9-fluorenones with respect to each other and the $AlBr_3$ unit. 26

Figure 1.8. Molecular structure of VO(Cl)(9-fluorenone)$_2$(H_2O)(μ-O)($VOCl_2$) (**1.12**). Thermal ellipsoids are shown at the 30% level. 26

Figure 1.9. Concentration dependence of the ^{1}H NMR shift of the 1-C<u>H</u> in 9-fluorenone (R = 0.995). 30

Figure 1.10. Temperature dependence of the ^{1}H NMR shift of the 1-C<u>H</u> in 9-fluorenone (R = 0.993). 31

Figure 1.11. Temperature dependence of the equilibrium constant, K_{eq}, for the dissociation of $GaCl_3$(9-fluorenone) (R = 0.995). 31

Figure 1.12. Plot showing the relationship between M-O bond distance in the complexes MX_3(9-fluorenone) (M = B, Al, Ga; X = Cl, Br) and the ionic radii for M (R = 0.986). 36

Figure 1.13. Plot showing the relationship between experimental M-O (a) and M-X (b) bond distance in the complexes MX_3(9-fluorenone) (M = B, Al, Ga; X = Cl, Br) and the sum of the ionic radii (□) and covalent radii (■) ($R_{(a)}$ = 0.979; $R_{(b)}$ = 0.986). 37

Figure 1.14. Plot of the deviation from planarity of the Group 13 element in MX_3(9-fluorenone) (M = B, Al, Ga; X = Cl, Br) as a function of the M-O bond distance (R = 0.851). 39

Chapter 2

Figure 2.1. Molecular structure of $[(^tBu)_2Ga(\mu\text{-}O_2CC_6H_4\text{-}2\text{-}NH_2)]_2$ (**2.2**).

Thermal ellipsoids are shown at the 20% level, and hydrogen atoms bound to carbon are omitted for clarity. Hydrogen bonding interactions are denoted by a dashed line. 56

Figure 2.2. Molecular structure of $[(^tBu)_2Ga(\mu\text{-}O_2CC_6H_4\text{-}2\text{-}OH)]_2$ (**2.3**). Thermal ellipsoids are shown at the 30% level, and hydrogen atoms bound to carbon are omitted for clarity. Hydrogen bonding interactions are denoted by a dashed line. 58

Figure 2.3. Molecular structure of $[(^tBu)_2Ga(\mu\text{-}O_2CC_6H_4\text{-}2\text{-}Me)]_2$ (**2.4**). Thermal ellipsoids are shown at the 20% level, and hydrogen atoms bound to carbon are omitted for clarity. 60

Figure 2.4. IR spectra of $[(^tBu)_2Ga(\mu\text{-}O_2CC_6H_4\text{-}2\text{-}NH_2)]_2$ (**2.2**) in toluene solution (a) and solid state (b), showing the presence of discrete hydrogen bonded and non-hydrogen bonded N-H groups. 61

Figure 2.5. Molecular structure of $[(^tBu)_2Ga(\mu\text{-}O_2CC_6H_4\text{-}2\text{-}OH)]_2$ (**2.5**). Thermal ellipsoids are shown at the 30% level, and hydrogen atoms bound to carbon are omitted for clarity. 63

Chapter 3

Figure 3.1. Representative plot of $-\ln[C\text{-}H_1]$ versus time (s) for the

$Hg(arene)_2(GaCl_4)_2$ catalyzed H/D exchange between C_6D_6 and $C_{10}H_8$ at 308 K (R = 0.991). 79

Figure 3.2. Plot of k_{obs} versus catalyst concentration for the $Hg(arene)_2(GaCl_4)_2$ catalyzed H/D exchange between C_6D_6 and $C_{10}H_8$ at 298 K (R = 0.997). 80

Figure 3.3. An Eyring plot of $\ln(k_1/T)$ versus 1/T for the initial $Hg(arene)_2(GaCl_4)_2$ catalyzed H/D exchange between C_6D_6 and $C_{10}H_8$: 1-position (■, R = 0.993) and the 2-position (□, R = 0.993). 81

Figure 3.4. Representative plot of $-\ln[C\text{-}H_1]$ (■) and $-\ln[C\text{-}H_2]$ (□) versus time (s) for the $Hg(arene)_2(GaCl_4)_2$ catalyzed H/D exchange between C_6D_6 and $C_{10}H_8$ at 308 K. 83

Figure 3.5. ^{13}C CPMAS NMR spectra of $Hg(C_{10}H_8)_2(GaCl_4)_2$ (**3.1**). 84

Figure 3.6. Calculated structure for $Hg(C_{10}H_8)_2(GaCl_4)_2$. 85

Figure 3.7. Calculated structure for $Hg(C_6H_6)_2(GaCl_4)_2$. 88

Figure 3.8. Representative plot of $-\ln[Hg(C_6D_6)_2(GaCl_4)_2]$ versus time (s) at 298 K (R = 0.956). 90

Figure 3.9. An Eyring plot of the $\ln(k_{ex}/T)$ versus 1/T for the $C_6D_6/C_{10}H_8$ ligand exchange reaction (R = 0.976). 91

Figure 3.10. Schematic representation of relative reactivity of the hydrogens in the 1- and 2-position of naphthalene towards H/D exchange. 91

Figure 3.11. Calculated charge distribution on the aromatic C and H atoms in $Hg(C_{10}H_8)_2(GaCl_4)_2$. 92

Figure 3.12. Liquid clathrate formed from the reaction of $Hg(C_6H_5Me)_2(GaCl_4)_2$ with C_6Me_6 in toluene. 93

List of Tables

Introduction

Table I.1. Coordination numbers of metal atoms of Group 13 halides in the solid state. 2

Table I.2. Substituent Contribution to ν_{CO} (A_1) of $Ni(CO)_3PX_1X_2X_3$. 4

Table I.3. Relative acceptor strengths of the Group 13 metal trihalides. 5

Chapter 1

Table 1.1. Carbonyl stretching frequencies, 13C NMR shifts, and λ_{max} for $MX_n(9\text{-fluorenone})_{n'}$. 20

Table 1.2. Selected bond lengths (Å) and angles (°) for $MX_3(9\text{-fluorenone})_n$. 25

Table 1.3. Selected Bond Lengths (Å) and Angles (°) in VO(Cl)(9-fluorenone)$_2$(H_2O)(μ-O)($VOCl_2$) (**1.12**). 27

Table 1.4. Determination of K_{eq} for the ligand dissociation of $GaCl_3$(9-fluorenone) from the ^1H NMR chemical shift of the 9-fluorenone's 1-C<u>H</u> proton.[a] 32

Table 1.5. Thermodynamic data for Group 13 halide complexes of 9-fluorenone. 33

Table 1.6. Summary of spectroscopic data and structural trends for

MX_3(9-fluorenone). 34

Table 1.7. Summary of X-ray diffraction data. 46

Chapter 2

Table 2.1. Selected Bond Lengths (Å) and Angles (°) in $[(^tBu_2M)_2(\mu\text{-}O_2CC_6H_4\text{-}2\text{-}X)]_2$. 57

Table 2.2. Selected Bond Lengths (Å) and Angles (°) in $(^tBu_2)Al(\mu\text{-}O_2CC_6H_4\text{-}2\text{-}NH_2)Al(^tBu)_3$ (**2.5**). 64

Table 2.3. Summary of X-ray diffraction data. 69

Chapter 3

Table 3.1. Summary of activation enthalpy and entropy for the $Hg(C_6H_5Me)_2(GaCl_4)_2$ catalyzed H/D exchange reaction. 80

Table 3.2. Experimental and calculated (DFT) ^{13}C NMR spectra for $Hg(C_{10}H_8)_2(GaCl_4)_2$. 86

Table 3.3. Calculated bond lengths (Å) and angles (°) in $Hg(arene)_2(GaCl_4)_2$. 87

List of Compounds

1.1	BCl_3(9-fluorenone)
1.2	$AlBr_3$(9-fluorenone)
1.3	$AlBr_3$(9-fluorenone)$_2$
1.4	AlI_3(9-fluorenone)$_2$
1.5	$GaCl_3$(9-fluorenone)
1.6	$GaBr_3$(9-fluorenone)
1.7	GaI_3(9-fluorenone)$_2$
1.8	$MgCl_2$(9-fluorenone)$_n$
1.9	$HgCl_2$(9-fluorenone)$_n$
1.10	$ZrCl_4$(9-fluorenone)$_n$
1.11	$SnCl_4$(9-fluorenone)$_n$
1.12	VO(Cl)-O=$VOCl_2$(9-fluorenone)$_2$
2.1	$[(^tBu)_2Al(\mu\text{-}O_2CC_6H_4\text{-}2\text{-}NH_2)]_2$
2.2	$[(^tBu)_2Ga(\mu\text{-}O_2CC_6H_4\text{-}2\text{-}NH_2)]_2$
2.3	$[(^tBu)_2Ga(\mu\text{-}O_2CC_6H_4\text{-}2\text{-}OH)]_2$
2.4	$[(^tBu)_2Ga(\mu\text{-}O_2CC_6H_4\text{-}2\text{-}Me)]_2$

2.5 $(^tBu)_2Al(\mu\text{-}O_2CC_6H_4\text{-}2\text{-}NH_2)Al(^tBu)_3$

3.1 $Hg(C_{10}H_8)_2(GaCl_4)_2$

3.2 $Hg(C_6Me_6)_2(GaCl_4)_2$

Abbreviations and Glossary

Å	angstrom
Anal.	analysis
avg.	average
BDE	bond dissociation energy
br.	bridging
^{t}Bu	*tert*-butyl, t-C_4H_9
cf.	confer, compare
Calc'd	calculated
CP	cross-polarization (NMR)
°C	degrees centigrade
ca.	circa, approximately
d	doublet (NMR)
δ	delta, chemical shift (NMR)
DFT	density functional theory
e.g.	exempli gratia, for the sake of example
equiv.	equivalent
E	element

Eq.	equation
Et	ethyl
et al.	*et alia*, and others
F_c	calculated structure factor
F_o	observed structure factor
g	gram
h	hour
ΔH	enthalpy
Hz	hertz
IR	infrared spectroscopy
kJ	kilojoule(s)
L	Lewis base
λ	wavelength
m	minute(s), medium (IR)
mg	milligram(s)
min.	minute(s)
mL	milliliter(s)
mm	millimeter(s)
mmol	millimole(s)

ms	millisecond(s)
μg	microgram(s)
m	meta
M	metal
MAS	magic angle spinning (NMR)
Me	methyl, CH_3
MS	mass spectrometry
NMR	nuclear magnetic resonance spectroscopy
o	ortho
ppm	parts per million
p	para
R	alkyl
rpm	revolutions per minute
s	singlet (NMR), strong (IR), second(s)
t	triplet (NMR)
tr.	terminal
w	weak (IR)
$W_{1/2}$	width at half hight (^{27}Al NMR)
xs	excess

basis set	Mathematical functions that describe a LCAO-MO (linear combination of atomic orbitals-molecular orbitals
clathrate	Non-stoichiometric liquid inclusion compound that forms upon the interaction of aromatic molecules with certain ionic moities
Lewis acid	A substance that can accept an electron pair to form a coordinate bond.
Lewis base	A substance that can donate an electron pair to form a coordinate bond.

Introduction

The concepts of acid and base are fundamental in chemistry. Early definitions of acids and bases, postulated by Arrhenius, were based upon the generation of hydrogen and hydroxide ions in aqueous solutions.[1] Brønsted and Lowry expanded this limited concept of acids and bases, defining an acid as a proton donor and a base as a proton acceptor. The broadest definition, however, was provided by Lewis: "a basic substance is one which has a lone pair of electrons which may be used to complete the stable group of another atom, and an acidic substance is one which can employ a lone pair from another molecule in completing the stable group of one of its own atoms".[2] In practice, substances meeting this definition of an acid, with the exception of protic compounds, are specifically referred to as Lewis acids.

Trihalides of Group 13 elements are among the strongest and most widely used Lewis acids.[3] The structures of these species are determined by the nature of the halide and existing conditions. Table I.1 lists the coordination numbers of the Group 13 halides in the solid state.[4] For example, the structure of $AlCl_3$ changes at the melting point from a 6-coordinate polymer (**I**) to a 4-coordinate dimer (**II**), which also exists in the gas phase.[4]

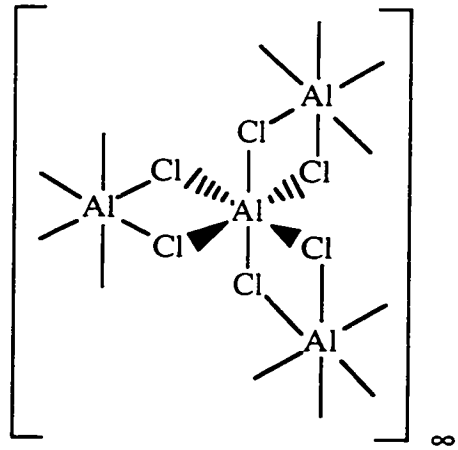

(**I**)

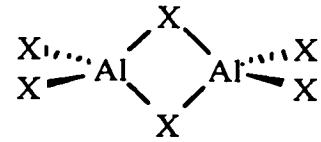

(**II**)

Table I.1 Coordination numbers of metal atoms of Group13 halides in the solid state.

	F	Cl	Br	I
Al	6	6	4	4
Ga	6	4	4	4
In	6	6	6	4
Tl	6	6	4	4

Al_2Br_6 and Ga_2Cl_6 form dimeric molecular units (**II**) in the crystalline phase as well as in the liquid and gaseous states.[5] At high temperatures, the dimers, $[X_2Al(\mu\text{-}X)]_2$, dissociate into monomers with dissociation enthalpies of 46 – 63 $kJ.mol^{-1}$ (X = Cl, Br, I).[4] Generally, the halides are soluble in aromatic solvents, in which they are also dimeric. An exception is AlF_3, which is nonvolatile and insoluble.[5] Other than several hydrates ($AlF_3 \cdot nH_2O$; n = 1, 3, 9), no neutral complexes of AlF_3 are known, which is consistent with its ionic nature. GaF_3 and InF_3 are also essentially ionic, with few known neutral adducts.[6]

The ability of trihalides to form adducts with a great variety of Lewis bases is the most important aspect of the chemistry of the Group 13 elements. The bridging metal-halide bond energies are *ca.* 30% lower than that of the terminal metal-halogen bonds. Therefore, an interaction of a trihalide with a Lewis base is initiated by the cleaving of the bridging metal-halide bond. While tetrahedral 4-coordinate Lewis base adducts $MX_3(L)$ are the most common, particularly for aluminum and gallium, 5- and 6-coordinate adducts are also known, mainly for the heavier members of the group.[4] The wide range of compounds that have been reported to coordinate includes both organic (amines, nitriles, ethers,

ketones, organosulfur compounds, etc.) and inorganic species (ammonia, nitric oxide, hydrogen cyanide, phosphorus pentoxide, etc.).[7]

The strength of Brønsted acid-base interactions has been thoroughly explored, and much progress has been made in quantifying the strengths of Lewis bases. Tolman developed a convenient technique for measuring donor-acceptor properties of phosphorus ligands. It was found that, by examining the A_1 carbonyl frequency by infrared spectroscopy of $Ni(CO)_3(PX_1X_2X_3)$, altering the substituents (X_n) resulted in an incremental change in the carbonyl shift.[8] From this, Tolman was able to devise both an equation to describe the contribution of any given substituent (Eq. I.1) and a substituent contribution scale (see Table I.2). Success in devising a definitive scale for Lewis acids has not proven so easy. Much work has been done to define acceptor strengths of the Group 13 metal halides based on their gas-phase enthalpies of association with various donor groups. Table I.3 lists several types of electron donors with their corresponding Group 13 metal halide acceptor sequence.[7]

$$\nu_{CO}\,(A_1) = 2056.1 + \sum_{i=1}^{3} \chi_i \text{ cm}^{-1} \qquad \text{(I.1)}$$

Studying the gas-phase reactions of Group 13 metal trihalides is made difficult, however, by the low volatility of certain complexes.[9] Simple tests for the strength of Lewis acids are needed, and some workers have been successful in devising such tests. Solution techniques (e.g., multinuclear NMR, IR and UV/visible spectroscopy), which are more accessible than those of the gas-phase, will be discussed in greater detail in Chapter 1.

Lewis acids are widely used as catalysts for a large number of organic reactions. The Friedel-Crafts reaction (Eq. I.2), the ene reaction (Eq. I.3), the Diels-Alder reaction (Eq I.4), and other reactions are efficiently catalyzed by Group 13 Lewis acids.[10]

Table I.2. Substituent Contribution to ν_{CO} (A_1) of $Ni(CO)_3PX_1X_2X_3$.[8]

Substituent	χ_i, cm^{-1}	Substituent	χ_i, cm^{-1}
^tBu	0.0	H	8.3
^nBu	1.4	C_6F_5	11.2
Me	2.6	Cl	14.8
Ph	4.3	F	18.2
OEt	6.8	CF_3	19.6

Table I.3. Relative acceptor strengths of the Group 13 metal trihalides.[11]

Donor	Acceptor sequence
amines, ethers	$MCl_3 > MBr_3 > MI_3$ (M = Al, Ga, or In)
phosphines	$MCl_3 > MBr_3 > MI_3$ (M = Ga)
Me_2S, Et_2S	$MCl_3 > MBr_3 > MI_3$ (M = Al)
C_4H_8S	$MCl_3 > MBr_3 > MCl_3$ (M = Ga or In)
N, O donors	AlX_3, GaX_3 (X = Cl or Br)
S donors	$GaX_3 > AlX_3$ (X = Cl or Br)
MeC(O)OEt	$BCl_3 > AlCl_3 > GaCl_3 > InCl_3$
py	$AlPh_3 > GaPh_3 > BPh_3 = InPh_3$
py	$AlX_3 > BX_3 > GaX_3$ (X = Cl or Br)
Me_2S	$GaX_3 > AlX_3 > BX_3$ (X = Cl or Br)

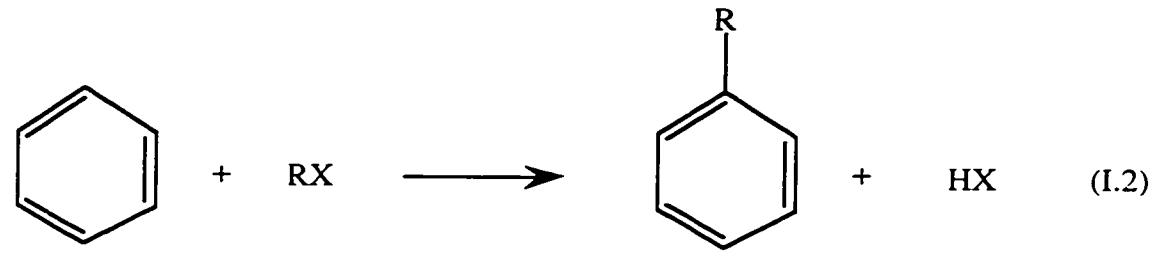

(I.2)

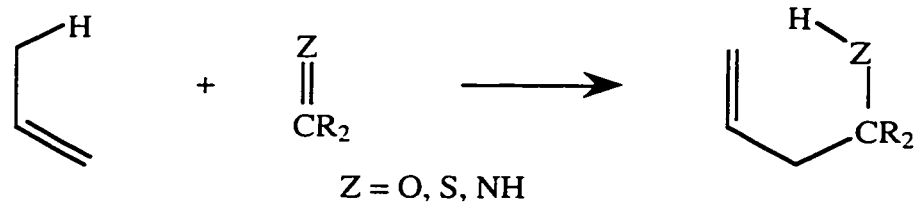

(I.3)

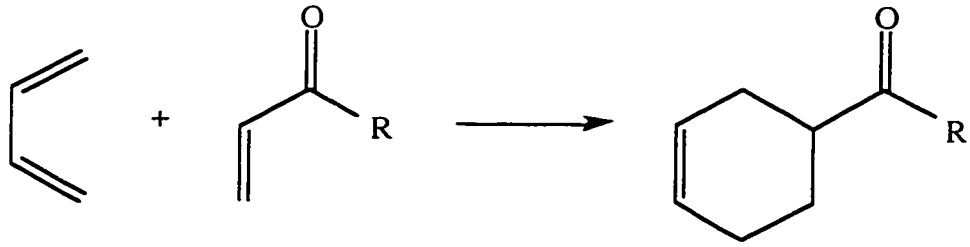

(I.4)

The general pathway for a Lewis acid-promoted reaction is the activation of the substrate by coordination to its basic site and polarization of the carbon–heteroatom bond (Eq. I.5). Ionization then generates a cationic species, which can either revert to starting material or be trapped by the nucleophile, yielding the product. For example, the highly

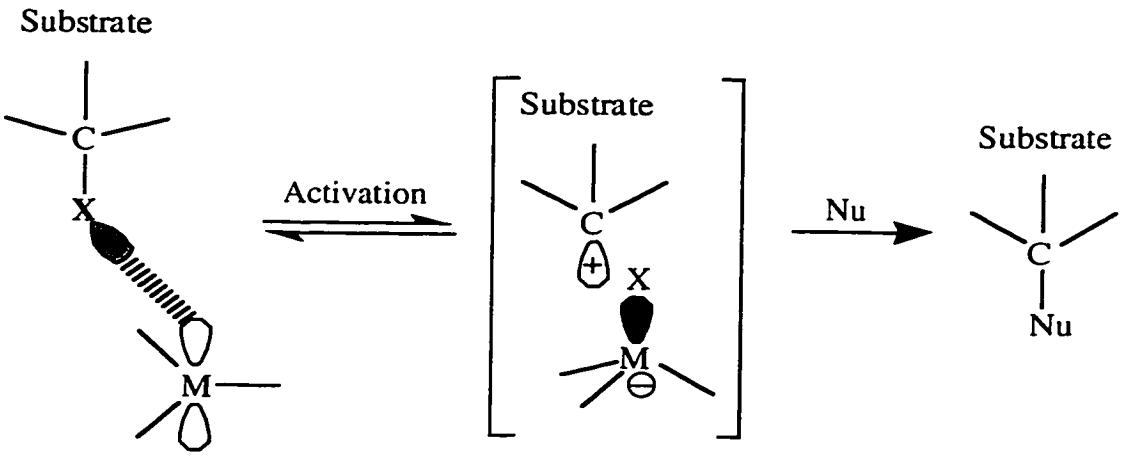

(I.5)

Lewis acidic Group 13 halide, $AlCl_3$, activates an alkyl or acyl halide *via* either complexation or ionization (Eq. I.6) by placing a positive charge on the β-substituent (**III**).[12]

$$RCl + AlCl_3 \longrightarrow RCl\cdots AlCl_3 \longrightarrow [R]^+[AlCl_4]^- \qquad (I.6)$$

The increase in positive charge on the β-substituent is a general effect of the coordination of aluminum Lewis acids to both organic (**IV**) and inorganic (**V**) carbonyls.

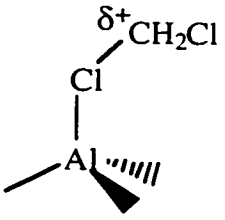

(**III**)

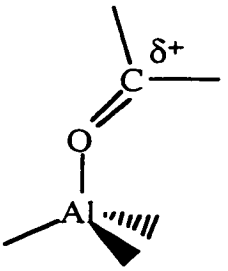

(**IV**)

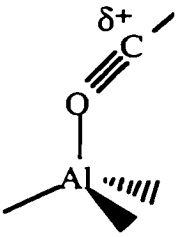

(**V**)

Examples include not only activation of ketones to alkylation and reduction,[13] but also activation of transition metal carbonyl ligands towards methyl migration,[14] respectively. Recently, Maruoka and co-workers demonstrated that carbonyl activation could be increased by using bidentate Lewis acids.[15]

The Barron group has previously observed that the coordination of an alcohol to an aluminum Lewis acid results in an increase of the pK_a of the alcohol O–H by at least 7 units (and possibly as high as 30).[16] This activation may be considered to be another example of increasing the positive charge on the β-substituent, in this case, the alcohol hydrogen (**VI**).

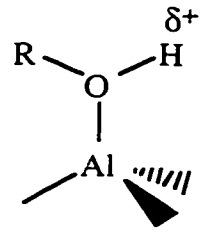

(**VI**)

The proton's electrophilicity is increased, making it more susceptible to reaction with nucleophiles (i.e., aluminum alkyls).

Work in the Barron group has shown that stable Lewis acid-base complexes between aluminum alkyls and primary and secondary amines may be isolated if at least one heteroatom donor ligand is already present on aluminum [e.g., $AlR_n(OR)_{3-n}(HNR_2)$, where n = 1 or 2].[17] It was proposed that the presence of a heteroatom donor ligand (e.g., alkoxide, aryloxide, amide, etc.) significantly reduces the basicity of the aluminum alkyl group as a result of the high electronegativity at the aluminum atom.[18] While these complexes appear to be special cases of stability, Robinson *et al.*[19] have reported that a cyclic secondary amine, 1,4,8,11-tetraazacyclotetradecane([14]andN_4), forms a stable

adduct with $AlMe_3$ as a consequence of the intramolecular hydrogen bonding between the N-H of the nitrogen coordinated to aluminum and an adjacent uncomplexed nitrogen center. Hydrogen bonding allowed for the isolation of alcohol complexes of AlR_3.[15] In Chapter 2, the investigation of intramolecular hydrogen bonding in complexes of benzoic acid derivatives and AlR_3 is presented.

Lewis acid–base interaction has been the focus of several theoretical studies, e.g., AlX_3 with H_2O, HX, benzene, and ethene.[20] One of the major outcomes of the benzene-AlX_3 interaction is that a charge reorganization is induced on the benzene atoms due to complexation. As a result, the carbon atom closest to the aluminum atom becomes highly nucleophilic, and the activation energy of the aromatic substrate–electrophile interaction is significantly lowered.[21]

There has been an increased interest in the development of new Lewis acidic compounds with respect to molecular recognition.[22] Among various organoaluminum derivatives, exceptionally bulky aryloxides are monomeric in organic solvents and show excellent sensitivity.[23] The Lewis acid mediated chelation control is one of the most important concepts in inorganic chemistry.[9] It is well accepted that the chelating controlled reaction proceeds through the coordination of a lone electron pair of a heteroatom (i.e., the oxygen of an aldehyde or the nitrogen of an imine) to a Lewis acid. Recently, it was reported that bidentate chelation of a Lewis acid to either an olefinic[24] or acetylenic[25] π-bond can be achieved.

Lewis acids are also widely used as co-catalysts, especially with regard to olefin polymerization. To form active catalysts, metallocenes may be activated by a methylalumoxane (MAO) co-catalyst. Although many of its features remain unclear, MAO is currently the most effective metallocene co-catalyst. MAO is generally thought to act as a

Lewis acid, abstracting a methide (alkide) anion, facilitating the formation of a 14-electron, unsaturated "cation-like" catalytic metal center (see Eq I.7).

$$Cp_2ZrMe_2 + (AlMeO)_n \rightleftharpoons [Cp_2ZrMe]^+[Me(AlMeO)n]^- \qquad (I.7)$$

Large MAO/catalyst ratios (Al:Zr ≈ 10^4:1) are necessary for acceptable polymerization activity. In contrast, strong Lewis acids with electron-withdrawing substituents[26] can be successfully used for the direct synthesis of catalytically active species.

As an alternative approach, we have become interested in applying the concept of increasing the Lewis acidity of metals through their "activation" by another Lewis acid (**VII**). Aluminum halides have been previously employed as activators for transition metals through a similar complexation (**VIII**).[27]

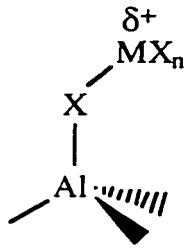

(**VII**)

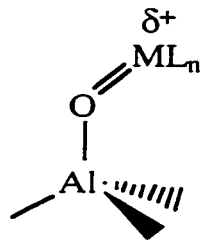

(**VIII**)

Although the Lewis acidic behavior of mercuracarboranes has been extensively studied by Hawthorne and co-workers,[28] the Lewis acidic nature of Group 12 halides, in particular, those of mercury, has been studied less than that of the Group 13 halides.[29] The chemistry of mercury (II) salts with aromatic hydrocarbons, however, is well developed regarding electrophilic attack on aromatic compounds (aromatic mercuration), and Olah *et al.* have shown that Hg—arene complexes are involved as intermediates.[30] Kochi and co-

workers have shown that the activation of the arene is related to a charge-transfer transition in the π-complex.[31,32] Crabtree and co-workers have proposed a π-complex as a key intermediate in a variety of photochemical C—C bond forming reactions,[33] while the characterization of a series of Hg(I)—arene complexes has been reported.[34] Mercury (II) —arene complexes are well established as important intermediates, but simple complexes have been characterized only spectroscopically.[35] The only structural characterization of a nonsolvate mercury (II) complex was reported by Kochi and co-workers with a highly electronegative trifluoroacetate ligand.[36]

Chapter 3 describes recent work in the Barron group in which we have shown that Group 13 Lewis acids activate weaker Lewis acids, specifically $HgCl_2$, by preparing stable Hg···arene complexes (Eq. I.8).[37]

$$HgCl_2 + MCl_3 \longrightarrow Hg(arene)_2(MCl_4)_2 \qquad (I.8)$$

References

1 S. Arrhenius, *Z. Phys. Chem.*, 1887, **1**, 631.

2 G. N. Lewis, *Valence and the Structure of Atoms and Molecules*, Chemical Catalogue, Inc., New York, 1923.

3 K. Wade and J. Banister, in *Comprehensive Inorganic Chemistry*, Vol. 1, Pergamon Press, Oxford, 1973, Chapter 2.

4 F. A. Cotton, G. Wilkinson, C. A. Murillo, and M. Bochmann, *Advanced Inorganic Chemistry*, Sixth Edition, Wiley-Interscience, New York, 1999, Part 2.6.

5 N. N. Greenwood and A. Earnshaw, *Chemistry of the Elements*, Second Edition,

Butterworth-Heinemann, Oxford, 1998, Chapter 7.

6 D. G. Tuck in A. J. Downs, *Chemistry of Aluminium, Gallium, Indium, and Thallium*, Blackie Academic and Professional, London, 1993, Chapter 8.

7 N. N. Greenwood and K. Wade, in G. A. Olah, *Friedel-Crafts and Related Reactions*, Vol. 1, Interscience, New York, 1963.

8 C. A. Tolman, *J. Am. Chem. Soc.*, 1970, **92**, 2953.

9 D. P. N. Satchell and R. S. Satchell, *Chem. Rev.*, 1969, **69**, 251.

10 H. Yamamoto, *Lewis Acid Reagents: A Practical Approach*, Oxford University Press, New York, 1999.

11 N. N. Greenwood and A. Earnshaw, *Chemistry of the Elements*, Pergamon, Oxford, 1984, p. 269 and references therein.

12 (a) F. C. Whitmore, *J. Am. Chem. Soc.*, 1932, **54**, 3274.

(b) G. A. Olah, S. J. Kuhn, and S. H. Flood, *J. Am. Chem. Soc.*, 1962, **84**, 1688.

(c) G. A. Olah, S. Kobayashi, and m. Tashiro, *J. Am. Chem. Soc.*, 1972, **94**, 7448.

13 (a) M. B. Power, J. R. Nash, M. D. Healy, and A. R. Barron, *Organometallics*, 1992, **11**, 1830.

(b) M. B. Power, S. G. Bott, J. L. Atwood, and A. R. Barron, *J. Am. Chem. Soc.*, 1990, **112**, 3446.

(c) M. B. Power, S. G. Bott, D. L. Clark, J. L. Atwood, and A. R. Barron, *Organometallics*, 1990, **9**, 3086, and references therein.

14 (a) S. B. Butts, E. M. Holt, S. H. Strauss, N. W. Alcock, R. E. Stimson, and D. F. Shriver, *J. Am. Chem. Soc.*, 1979, **101**, 5864.

(b) S. B. Butts, S. H. Strauss, E. M. Holt, R. E. Stimson, N. W. Alcock, and D.

F. Shriver, *J. Am. Chem. Soc.*, 1980, **102**, 5093.

15 (a) H. Hanawa, S. Kii, N. Asao, and K. Maruoka, *Tetrahedron Lett.*, 2000, **41**, 5543.

(b) T. Ooi, T. Miura, and K. Maruoka, *Angew. Chem. Int. Ed.*, 1998, **37**, 2347.

16 C. N. McMahon, S. G. Bott, and A. R. Barron, *J. Chem. Soc., Dalton Trans.*, 1997, 3129.

17 M. D. Healy, J. W. Ziller, and A. R. Barron, *Organometallics*, 1991, **10**, 597.

18 M. D. Healy, M. B. Power, and A. R. Barron, *Coord. Chem. Rev.*, 1994, **130**, 63.

19 G. H. Robinson, W. T. Pennington, B. Lee, M. F. Self, and D. C. Hrncir, *Inorg. Chem.*, 1991, **30**, 809.

20 P. Tarakeshwar and K. S. Kim, *J. Phys. Chem., A*, 1999, **103**, 9116.

21 P. Tarakeshwar, J. Y. Lee, and K. S. Kim, *J. Phys. Chem. A*, 1998, **102**, 2253.

22 See, for example, (a) S. Saito and H. Yamamoto, *J. Chem. Soc., Chem. Commun.*, 1997, 1585.

(b) H. Yamamoto and S. Saito, *Pure Appl. Chem.*, 1994, **116**, 4131.

23 (a) K. Maruoka, H. Imoto, S. Saito, and H. Yamamoto, *J. Am. Chem. Soc.*, 1994, **116**, 4131.

(b) T. Ooi, Y. Kondo, and K. Maruoka, *Angew. Chem. Int. Ed.*, 1998, **37**, 3039.

24 N. Asao, T. Shimada, and Y. Yamamoto, *Tetrahedron Lett.*, 2000, **41**, 9533.

25 N. Asao, T. Shimada, and Y. Yamamoto, *J. Am. Chem. Soc.*, 2000, **122**, 4817.

26 See, for example, (a) L. Li and T. J. Marks, *Organometallics*, 1998, **17**, 3996.

(b) L. Li, C. L. Stern, and T. J. Marks, *Organometallics*, 2000, **19**, 3332.

27 (a) N. Le, P. Jean, M. T. Youinou, and J. A. Osborn, *Organometallics*, 1992,

11, 2413.

(b) N. Le, P. Jean, and J. A. Osborn, *Organometallics*, 1991, **10**, 1546.

28 See, for example, (a) M. F. Hawthorne and Z. Zheng, *Acc. Chem. Res.*, 1997, **30**, 267.

(b) M. F. Hawthorne, X. Yang, and Z. Zheng, *Pure Appl. Chem.*, 1994, **66**, 245.

(c) H. Lee, M. Diaz, and M. F. Hawthorne, *Angew. Chem. Int. Ed.*, 2000, **39**, 776.

(d) H. Lee, M. Diaz, and M. F. Hawthorne, *Tetrahedron Lett.*, 1999, **40**, 7651.

(e) I. H. A. Badr, M. Diaz, M. F. Hawthorne, and L. G. Bachas, *Anal. Chem.*, 1999, **71**, 1371, and references therein.

29 (a) *The Chemistry of Mercury*, C. A. McAuliffe, Ed., Macmillan, Toronto, 1977.

(b) P. A. W. Dean, *Prog. Inorg. Chem.*, 1978, **24**, 109.

(c) M. Tschinkl, A. Schier, J. Riede, and F. P. Gabbaï, *Organometallics*, 1999, **18**, 2040.

(d) S. Saito, J. Zhang, and T. J. Koizumi, *J. Org. Chem.*, 1998, **63**, 6029.

(e) R. Zhuang and A. H. E. Mueller, *Macromolecules*, 1995, **28**, 8043.

(f) I. Persson, M. Sandstroem, and P. L. Goggin, *Inorg. Chim. Acta*, 1987, **129**, 183.

(g) J. D. Wuest and B. Zacharie, *Organometallics*, 1985, **4**, 410, and references therein.

30 See, for example, G. A. Olah, S. H. Yu, and D. G. Parker, *J. Org. Chem.*, 1976, **41**, 1983, and references therein.

31 W. Lau and J. K. Kochi, *J. Am. Chem. Soc.*, 1986, **108**, 6720.

32 S. Fukuzumi, J. K. Kochi, *J. Org. Chem*, 1981, **46**, 4116.

33 L. A. Fowley, J. C. Less, Jr., R. H. Crabtree, and P. E. M. Siegbahn, *J.*

Organomet. Chem., 1995, **505**, 57.

34 W. Frank and B. Dincher, *Z. Naturforsch*, 1987, **42b**, 828.

35 (a) L. C. Damude and P. A. W. Dean, *J. Organomet. Chem.*, 1979, **181**, 1.

(b) L. C. Damude, P. A. W. Dean, M. D. Sefcik, and J. Schaefer, *J. Organomet. Chem.*, 1982, **226**, 105.

36 W. Lau, J. C. Huffman, and J. K. Kochi, *J. Am. Chem. Soc.*, 1982, **104**, 5515.

37 A. S. Borovik, S. G. Bott, and A. R. Barron, *J. Am. Chem. Soc.*, 2001, **123**, 11219.

Chapter 1

Group 13 Trihalide Complexes of 9-Fluorenone: A Comparison of Methods for Assigning Relative Lewis Acidity

Introduction

Forty years ago, Lappert noted that the one drawback with Lewis' theory of acids and bases is its failure to "come to terms with quantitative aspects".[1] Despite attempts by many researchers, there is still no clear quantitative measure of Lewis acidity. The measurement of the strength of a Lewis base is actually more refined. Tolman developed a simple approach for the measurement of the electron donor ability properties of phosphorous ligands towards transition metals,[2] which in combination with his concepts of cone angle,[3] may be used to predict relative reactivity and structures of Lewis acid-base complexes, including those for main group metals.[4]

The strength of Brønsted acid-base interactions has been thoroughly explored, but quantifying the strengths of Lewis acid-base has proven much more difficult.[5] Olah *et al.* have suggested that "strength" has no real meaning for Lewis acids.[6] Nevertheless, attempts to correlate Lewis acid strength with various spectroscopic data have been successful. The closest to a method for the actual value of Lewis acidity involves the calculation or measurement of the enthalpy change accompanying the formation of a Lewis acid-base complex in the absence of solvation effects, i.e., the bond dissociation energy (BDE) in the vapor phase. This method, however, is not readily available for a wide range of compounds and so an alternative, more experimentally accessible, approach is required. The strength of $MX_3R_{3-n}(L)$ complexes have been studied in solution using NMR spectroscopy.[7,8,9,10,11,12] Additionally, bond distances as determined by X-ray diffraction have yielded sequences of Lewis acidity.[13] Interestingly, due to the importance

of Lewis acid sites in heterogeneous catalysis, precise measurement of Lewis acidity in solid systems has been attempted.[14,15]

In trying to define a simple qualitative scale for Lewis acidity, Lappert suggested that the IR spectroscopic shifts of the carbonyl stretching frequency for ethyl acetate were indicative of a Lewis acid's strength.[1] Perturbations in the $\nu_{C=O}$ were taken to reflect polarization of the C=O bond and thus the strength of the Lewis acid.[16] Based on this approach, a relative order for MX_3 was determined to be Br > Cl for B and Al, but Cl > Br for In, and the Group trend was determined to be B > Ga > Al > In.[1] Several other studies have developed similar trends.[17] Laszlo and Teston suggested that Lewis acidities be based upon the π^* energy level in the 1:1 complex formed between the Lewis acid and crotonaldehyde.[18,19] This approach predicted a trend similar to that found by Lappert.[1] It should be noted, however, that in these and other studies, a single parameter was employed as a measure of Lewis acidity. In an alternative approach, Carlson *et al.* suggested that the selection of Lewis acid catalysts for various organic reactions could be accomplished by a principle component analysis of measured Lewis acid properties.[20] While this computer-assisted strategy showed promise, the descriptors employed were not properties of a Lewis acid-base complex, but the uncomplexed Lewis acid (e.g., dielectric constant, ionization potential, and magnetic susceptibility). As part of our long standing interest in understanding Lewis acid-base interactions for the Group 13 metals, we have investigated a range of possible alternative parameters that may be used in determining the relative Lewis acidity for Group 13 compounds.

We have previously measured solution BDEs using variable temperature NMR spectroscopy. Though solution measurements do not take into account different solvation effects for reactants and products, they have been used as comparative values. Given that the predominant applications of Lewis acids as catalysts and reagents is in solution, these

are actually more relevant than vapor phase measurements and, as such, are appropriate values to consider. We have previously shown that, in addition to the $\nu_{C=O}$ for organic carbonyls, the ^{13}C NMR shift of the α-carbon is affected by coordination to a Lewis acid.[10,11] Thus, these parameters were also considered. In line with Laszlo's and Teston's work[18,19], we have shown that the reduction potential of a ketone is affected by complexation to a Lewis acid.[21] We have therefore investigated the UV spectroscopy as a measure of the relative π* energy level. Finally, X-ray crystallographic data have been used as an estimate of the strength of M-O bonds interactions in alkoxides[22] and of the relative Lewis acidity of a metal moiety. The comparison of structural data for a homologous series of $MX_3(L)$ complexes will be investigated.

In choosing a $MX_3(L)$ system for study, both the Lewis base (L) and ancillary ligands (X) must allow characterization by the methods described above. Based on Lappert's and our prior work,[1,10,11] an organic carbonyl is desirable to allow for IR measurements. Furthermore, the particular organic carbonyl must allow for ease of NMR characterization, promote crystallization, and provide a suitable absorption in the UV-visible. In order to limit any potential reactivity (e.g., reduction or alkylation) and obviate issues of complex formulation (e.g., the 1:2 complexes commonly formed with InX_3), we have limited the present study to the tri-halides MX_3, where M = B, Al, Ga and X = Cl, Br, I. There have been extensive studies of the organic carbonyl complexes of aluminum trihalides and, to a lesser extent, the other Group 13 metals.[23,24,25,26,27] Of the wide range of possible ligands, 9-fluorenone (**I**) offers a potential as a suitable ligand,[28] and the complex $AlCl_3$(9-fluorenone) has previously been characterized by X-ray crystallography.[29]

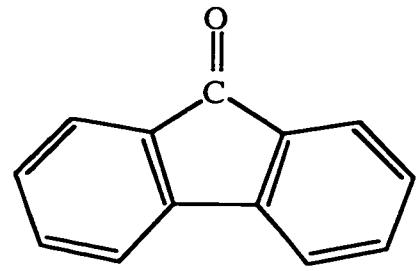

(I)

Results and Discussion

Characterization of 9-fluorenone complexes. The Lewis acid-base complexes MX_3(9-fluorenone) (M = B, Al, Ga; X = Cl, Br) were prepared in toluene solution and isolated as orange to red crystalline solids, where M = B; X = Cl (**1.1**), M = Al; X = Cl,[27] Br (**1.2**), M = Ga; X = Cl (**1.5**), Br (**1.6**) (see Experimental). Figure 1.1 shows several of the brightly colored compounds in benzene. During the synthesis of the aluminum tribromide complex, two different colored crystals were observed. In addition to the dark red product, $AlBr_3$(9-fluorenone) (**1.2**), a small quantity (<10%) light red crystals were isolated. These were determined to be due to the *bis*-9-fluorenone complex, $AlBr_3$(9-fluorenone)$_2$ (**1.3**). A mixture of compounds **1.2** and **1.3** were isolated irrespective of the Al:9-fluorenone ratio of the reaction mixture. Additionally, AlI_3 and GaI_3 formed *bis*-9-fluorenone complexes only.

Compounds **1.1** – **1.7** were characterized by IR, NMR and UV-visible spectroscopy (see Table 1.1 and Experimental). In addition, the molecular structures of compounds **1.1**, **1.2**, **1.3**, **1.5**, and **1.6** have been confirmed by X-ray crystallography.

We have previously demonstrated that the complexation of ketones to an aluminum Lewis acid results in an increase of the contribution of resonance form **II** over **III**, resulting in a decrease in the C=O bond order and placing a positive charge on the α-

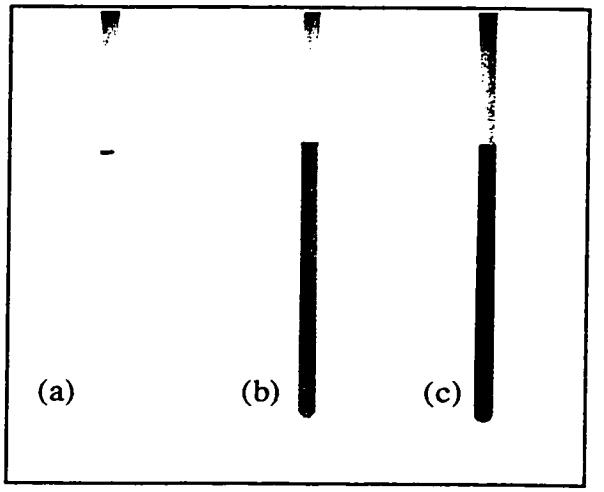

Figure 1.1. MX_3(9-fluorenone) complexes are brightly colored: (a) 9-fluorenone, (b) $GaCl_3$(9-fluorenone), and (c) $AlBr_3$(9-fluorenone).

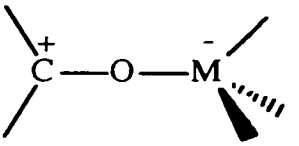

(II)

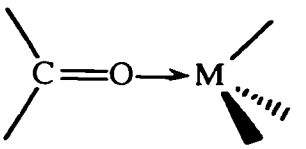

(III)

carbon.

The reduction of the C=O bond strength may be seen from the shift in the IR ($\Delta\nu$ = 50 – 130 cm^{-1}).[23] A similar effect is observed for MX_3(9-fluorenone), which is consistent with a weakening of the C=O bond (see Table 1.1). Furthermore, the $\nu_{C=O}$ stretch for $AlBr_3$(9-fluorenone)$_2$ (**1.3**) is significantly higher than in $AlBr_3$(9-fluorenone) (**1.2**), which agrees with the different C=O bond distances observed in the solid state (see below). IR spectra were also obtained for 9-fluorenone complexes of $MgCl_2$ (**1.8**), $HgCl_2$ (**1.9**), $ZrCl_4$ (**1.10**) and $SnCl_4$ (**1.11**) (see Table 1.1). If the solubility of the halides was

Table 1.1. Carbonyl stretching frequencies, ^{13}C NMR shifts, and λ_{max} for MX_n(9-fluorenone)$_n$.

Compound	$\nu_{C=O}$ (cm^{-1})	$\Delta\nu$ (cm^{-1})[a]	$^{13}C\ \delta_{(C=O)}$ (ppm)[b]	$\Delta\delta$ (ppm)[b,c]	λ_{max} (nm)[b]
BCl_3(9-fluorenone) (**1.1**)	1603	120	200.2	6.8	383
$AlCl_3$(9-fluorenone)	1637	86	205.2	11.8	376
$AlBr_3$(9-fluorenone) (**1.2**)	1634	89	205.0	11.6	380
$AlBr_3$(9-fluorenone)$_2$ (**1.3**)	1668	55	n/a	n/a	n/a
AlI_3(9-fluorenone)$_2$ (**1.4**)	1634	89	n/a	n/a	326
$GaCl_3$(9-fluorenone) (**1.5**)	1635	88	206.2	12.8	365
$GaBr_3$(9-fluorenone) (**1.6**)	1636	87	205.2	11.8	367
GaI_3(9-fluorenone)$_2$ (**1.7**)	1652	71	n/a	n/a	n/a
$MgCl_2$(9-fluorenone)$_n$ (**1.8**)	1653	70	n/a	n/a	309
$HgCl_2$(9-fluorenone)$_n$ (**1.9**)	1697	26	n/a	n/a	324
$ZrCl_4$(9-fluorenone)$_n$ (**1.10**)	1633	90	n/a	n/a	324
$SnCl_4$(9-fluorenone)$_n$ (**1.11**)	1635	88	n/a	n/a	297

[a] In comparison with free 9-fluorenone (1723 cm^{-1}).

[b] Determined in the presence of excess MX_3 to ensure complete coordination, see text.

[c] In comparison with free 9-fluorenone (δ = 193.4 ppm).

insufficient for reaction in toluene solution ($MgCl_2$, $HgCl_2$ and $ZrCl_4$), synthesis was carried out in the solid state. In the case of $ZrCl_4$, a color change (from 9-fluorenone's

yellow to a light brown) was observed.

We have shown that the effective increase in positive charge on the α-carbon of ketones, upon coordination to Lewis acids, is seen by a downfield shift of the resonance in the ^{13}C NMR spectrum ($\Delta\delta = 5 - 25$ ppm).[10] A similar effect is observed for MX_3(9-fluorenone), see Table 1.1. These shifts are consistent with **II** significantly contributing to the overall resonance structure.

The molecular structures of **1.1**, **1.2**, **1.5** and **1.6** are shown in Figures 1.2 – 1.5, respectively; selected bond lengths and angles, along with those for the previously reported $AlCl_3$(9-fluorenone),[27] are given in Table 1.2. As was reported for $AlCl_3$(9-fluorenone),[27] compounds **1.1**, **1.2**, **1.5** and **1.6** are monomeric in the solid state with no close intermolecular contacts. Compounds **1.1**, **1.2**, and **1.6** crystallize as toluene

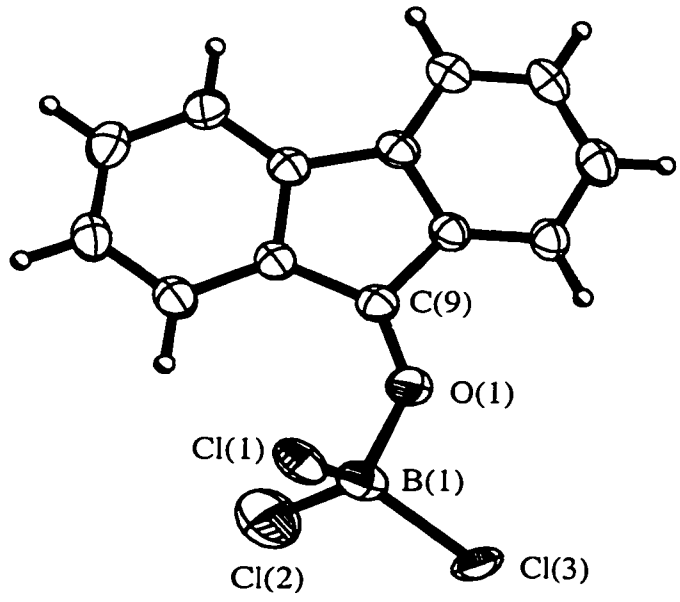

Figure 1.2. Molecular structure of BCl_3(9-fluorenone) (**1.1**). Thermal ellipsoids are shown at the 30% level.

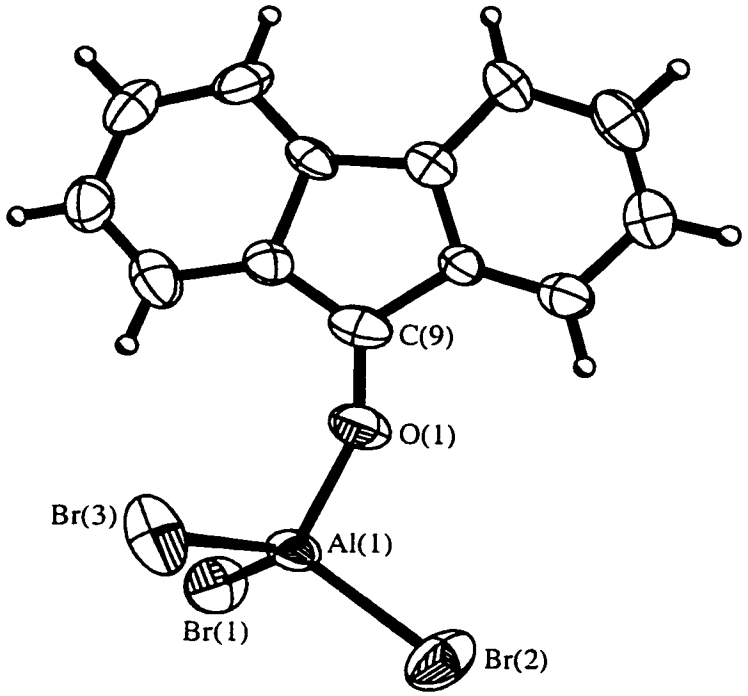

Figure 1.3. Molecular structure of $AlBr_3$(9-fluorenone) (**1.2**). Thermal ellipsoids are shown at the 30% level.

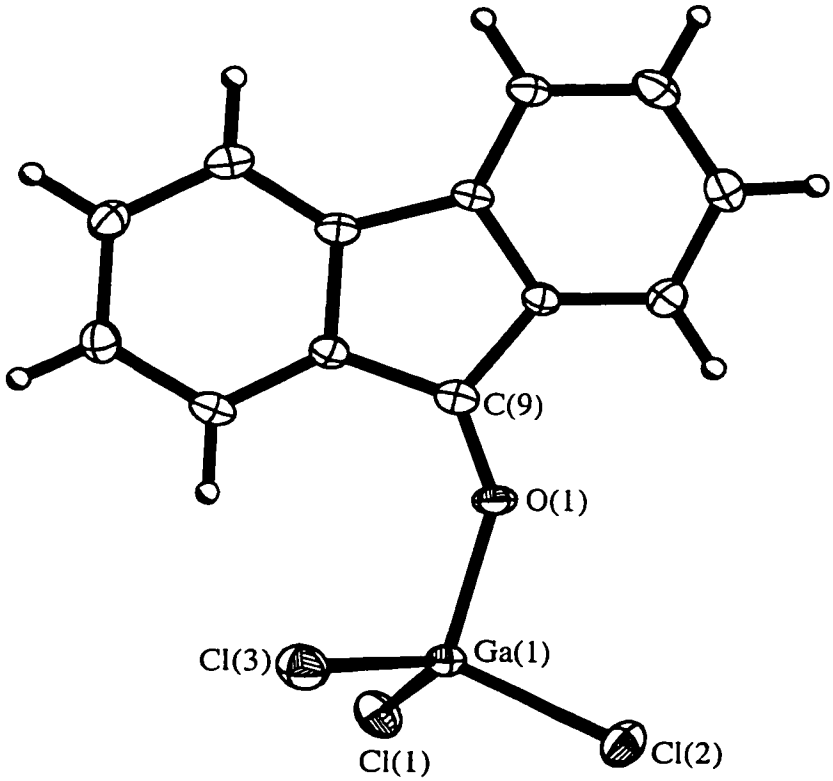

Figure 1.4. Molecular structure of $GaCl_3$(9-fluorenone) (**1.5**). Thermal ellipsoids are shown at the 30% level.

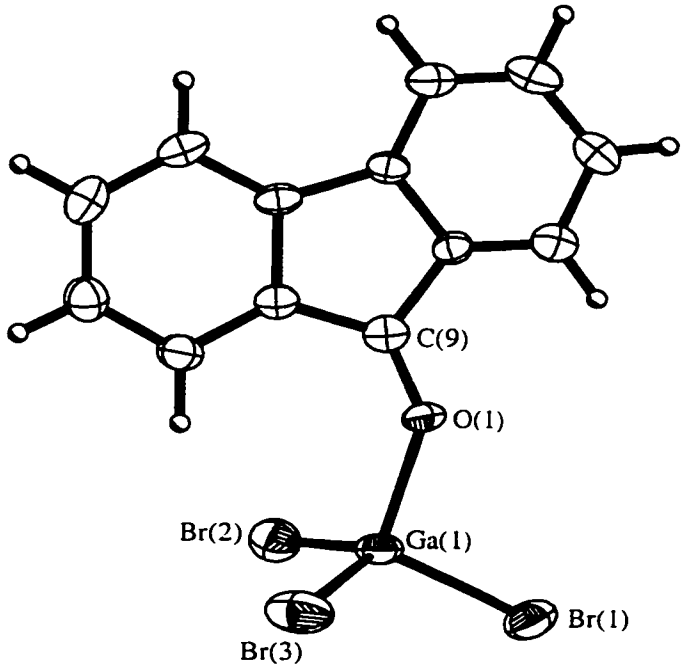

Figure 1.5. Molecular structure of $GaBr_3$(9-fluorenone) (**1.6**). Thermal ellipsoids are shown at the 30% level.

solvates, and the BCl_3 unit in compound **1.1** has a rotational disorder about the B-O bond. In common with other Lewis acid adducts of organic carbonyls,[30] the O=C bond lengths in compounds **1.1** – **1.3** and **1.6** are increased as compared to the free ligand (Table 1.2).[31]

The molecular structure of $AlBr_3$(9-fluorenone)$_2$ is shown in Figure 1.6; selected bond lengths and angles are given in Table 1.2. The structure consists of monomeric units, in which the aluminum is five coordinate trigonal bipyramidal with the two 9-fluorenone ligands occupying the axial positions. The O(1)-Al(1)-O(1A) angle is 174.3(3)°. The Al and Br atoms lie on a non-crystallographic mirror plane resulting in the 9-fluorenone ligands adopting an eclipsed orientation with each other, but staggered with respect to the equatorial bromides (see Figure 1.7).

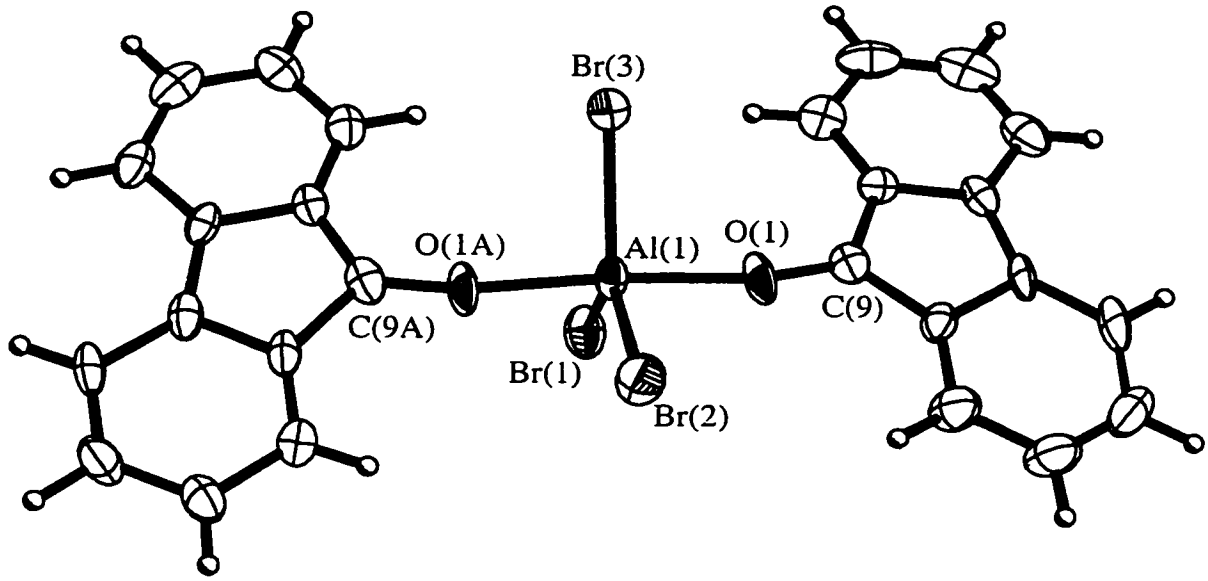

Figure 1.6. Molecular structure of $AlBr_3$(9-fluorenone)$_2$ (**1.3**). Thermal ellipsoids are shown at the 30% level.

The orientation of the two 9-fluorenone ligands can also explain the distortions away from an ideal trigonal bipyramidal (see Table 1.2).

During our studies we isolated the unusual mixed vanadium(IV,V) compound, VO(Cl)(9-fluorenone)$_2$(H_2O)(μ-O)($VOCl_2$) (**1.12**), by reaction of 9-fluorenone with partially hydrolyzed VCl_4. In the presence of water, VCl_4 is rapidly hydrolyzed to give solutions of oxovanadium(IV) chloride.[32] The molecular structure of compound **1.12** is shown in Figure 1.8; selected bond lengths and angles are given in Table 1.3. The core of the complex is an octahedral vanadium(IV) oxochloride [V(1)], to which are coordinated two 9-fluorenones and a water ligand. The coordination environment of V(1) is completed by a bridging oxo ligand from a $[VO_2Cl_2]^-$ anion. The terminal V=O bond distances (Table 1.3)

Table 1.2. Selected bond lengths (Å) and angles (°) for $MX_3(9\text{-fluorenone})_n$.

M	B	Al	Al	Al	Ga
X	Cl	Cl	Br	Br	Cl
n	1	1	1	2	1
	(1.1)	b	**(1.2)**	**(1.3)**	**(1.5)**
M-O	1.514(4)	1.787(3)	1.756(9)	1.907(6), 1.913(7)	1.915(2)
M-X	1.811(7)[a]	2.097(2)	2.239(4)	2.304(3)	2.134(1)
	1.833(5)[a]	2.109(2)	2.253(4)	2.312(3)	2.125(1)
	1.836(4)[a]	2.117(2)	2.256(4)	2.323(3)	2.143(1)
O-C	1.261(3)	1.266(5)	1.28(1)	1.25(1), 1.23(1)	1.258(4)
O-M-X	108.0(2)[a]	105.2(1)	102.9(4)	88.3(2), 87.4(2)	101.20(9)
	109.5(3)[a]	107.2(1)	105.7(3)	90.2(2), 89.2(2)	106.79(9)
	103.0(2)[a]	107.0(1)	108.2(3)	93.7(2), 91.7(2)	107.20(9)
X-M-X	112.1(3)	110.00(9)	112.6(2)	114.1(1)	114.20(5)
	111.8(2)	113.18(9)	113.1(2)	120.6(1)	111.21(5)
	111.9(3)	113.55(9)	113.4(2)	125.1(1)	115.01(5)
O-M-O	n/a	n/a	n/a	174.3(3)	n/a
M-O-C	135.3(2)	150.2(3)	153(1)	154.4(8), 167.5(7)	143.9(3)

[a] Major constiuent of rotational disorder.

[b] D. L. Boucher, M. A. Brown, B. R. McGarvey, and D. G. Tuck, *J. Chem. Soc., Dalton Trans.*, 1999, 3445.

are comparable to those reported for other vanadium oxohalides (1.55 – 1.60 Å),[33] and the V-O bonds associated with the 9-fluorenone ligands are within the range expected for V-O

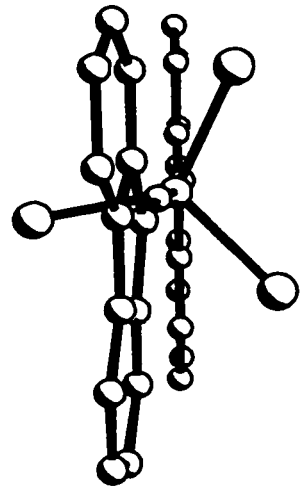

Figure 1.7. Coordination sphere of $AlBr_3$(9-fluorenone)$_2$ (**1.3**) viewed along the O(1)-Al(1)-O(1A) vector showing the orientation of the two 9-fluorenone with respect to each other an the $AlBr_3$ unit.

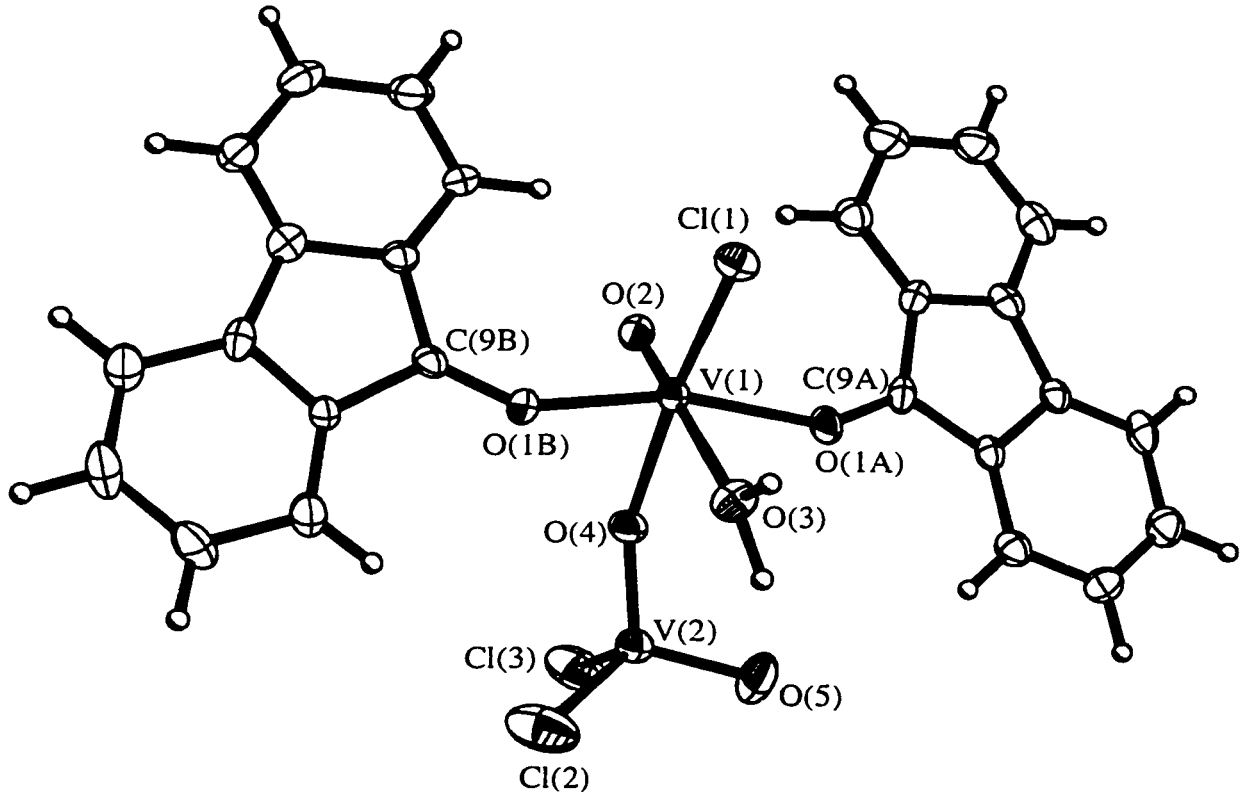

Figure 1.8. Molecular structure of VO(Cl)(9-fluorenone)$_2$(H_2O)(μ-O)($VOCl_2$) (**1.12**). Thermal ellipsoids are shown at the 30% level.

Table 1.3. Selected Bond Lengths (Å) and Angles (°) in $VO(Cl)(9\text{-fluorenone})_2(H_2O)(\mu\text{-}O)(VOCl_2)$ (**1.12**).

V(1)-O(2)	1.564(4)	V(1)-O(4)	2.014(4)
V(1)-O(1A)	2.013(4)	V(1)-O(1B)	2.031(4)
V(1)-O(3)	2.251(4)	V(1)-Cl(1)	2.336(2)
V(2)-O(5)	1.569(4)	V(2)-O(4)	1.640(4)
V(2)-Cl(2)	2.179(2)	V(2)-Cl(3)	2.187(3)
O(1A)-C(9A)	1.237(6)	O(1B)-C(9B)	1.241(6)
O(2)-V(1)-O(4)	96.2(2)	O(2)-V(1)-O(1A)	98.3(2)
O(4)-V(1)-O(1A)	87.3(2)	O(2)-V(1)-O(1B)	98.8(2)
O(4)-V(1)-O(1B)	83.1(2)	O(1A)-V(1)-O(1B)	161.2(2)
O(2)-V(1)-O(3)	176.2(2)	O(4)-V(1)-O(3)	80.6(2)
O(1A)-V(1)-O(3)	79.6(2)	O(1B)-V(1)-O(3)	82.9(2)
O(2)-V(1)-Cl(1)	100.8(2)	O(4)-V(1)-Cl(1)	162.7(1)
O(1A)-V(1)-Cl(1)	93.2(1)	O(1B)-V(1)-Cl(1)	91.1(1)
O(3)-V(1)-Cl(1)	82.5(1)	O(5)-V(2)-O(4)	108.8(2)
O(5)-V(2)-Cl(2)	107.9(2)	O(4)-V(2)-Cl(2)	106.9(2)
O(5)-V(2)-Cl(3)	110.2(2)	O(4)-V(2)-Cl(3)	108.8(8)
Cl(2)-V(2)-Cl(3)	114.06(9)	V(2)-O(4)-V(1)	155.6(2)

single bond interactions (1.91 – 2.20 Å).[34] The bridging oxo is asymmetrical, such that the V(1)-O(4) and V(2)-O(4) distances are consistent with V-O and V=O bonds, respectively.

Bond Dissociation Energies for MX_3(9-fluorenone). Given the common occurrence of Lewis acid-base complexes for the Group 13 elements, it is perhaps surprising that reports of thermodynamic data such as bond-dissociation energies (BDEs) are sparse. The majority of studies have been carried out on the complexes of AlR_3 and AlX_3 (X = Cl, Br),[10,23,35] but recently a wider range of derivatives have been studied.[36] Unfortunately, the dissociation process for the complex is complicated by the dimerization of AlR_3.[37]

The relative BDE's for such a series of complexes may be derived from the temperature dependence of the equilibrium constant, K_{eq} (Eq. 1.1).

$$MX_3(\text{9-fluorenone}) \overset{K_{eq}}{\rightleftharpoons} MX_3 + \text{9-fluorenone} \qquad (1.1)$$

where

$$\ln K_{eq} = \frac{-\Delta H_D}{R}\left(\frac{1}{T}\right) + \frac{\Delta S_D}{R} \qquad (1.2)$$

For the equilibrium between the complexes MX_3(9-fluorenone) and their constituents, (Eq. 1.1), the equilibrium constant, K_{eq}, can be described in terms of the mole fractions of 9-fluorenone present as free ligand, χ_{free}, and the total initial concentration, [total], Eq. 1.3.

$$K_{eq} = \frac{[\text{total}](\chi_{free})^2}{(1 - \chi_{free})} \qquad (1.3)$$

The ^1H NMR spectrum of 9-fluorenone is not simple, due to overlapping peaks, and is described as ABMX.[38] Complexation to MX_3, however, simplifies the spectrum somewhat. The deshielding of H(1) by the carbonyl group gives rise to a doublet downfield from the remainder of the spectrum, making this a suitable probe for equilibrium measurements. Unfortunately, the ^1H NMR spectra for MX_3(9-fluorenone) show a doublet arising from the 1-C<u>H</u> over the temperature ranges measured, indicating that the equilibria are rapid on the NMR time scale. In these situations, however, a common method is to derive the χ_{free} values, assuming the ^1H NMR chemical shift of the 1-CH proton is directly proportional to the mole fraction of the total species present as uncomplexed or "free" 9-fluorenone, χ_{free}. The ^1H NMR chemical shift of 1-C<u>H</u>, at a given temperature, may be used to calculate χ_{free} (Eq. 1.4).

$$\chi_{free} = \frac{\delta_{sample} - \delta_{coord}}{\delta_{free} - \delta_{coord}} \qquad (1.4)$$

The χ_{sample} value is measured directly from the sample under investigation, while χ_{free} is the ^1H NMR chemical shift of 9-fluorenone. χ_{coord} is the chemical shift of the fully complexed species, MX_3(9-fluorenone), determined by addition of a large excess of the Lewis acid, ensuring complete complexation.

The ^1H NMR for 9-fluorenone exhibits a slight concentration dependence of the ^1H NMR chemical shifts in C_6D_6 (Figure 1.9). Drake *et al.* reported a similar dependence using $CDCl_3$ as a solvent.[38] To correct for this effect, all solutions used to determine K_{eq} must have equal concentrations of fluorenone.

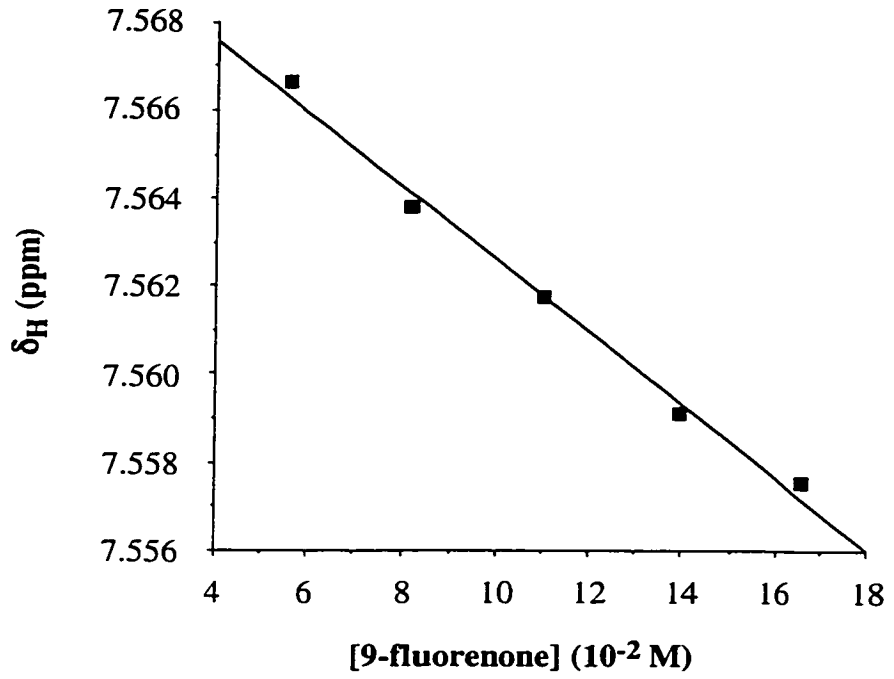

Figure 1.9. Concentration dependence of the ^{1}H NMR shift of the 1-C<u>H</u> in 9-fluorenone (R = 0.995).

In addition to a concentration dependence, the ^{1}H NMR chemical shifts of 9-fluorenone also exhibit some temperature dependence (Figure 1.10). Temperature-corrected shifts were subsequently employed for all calculations.

A data set for the representative $GaCl_3$(9-fluorenone) complex is given in Table 1.4. The associated $\ln(K_{eq})$ versus 1/T plot, from which the enthalpy (ΔH) and entropy (ΔS) were calculated, is shown in Figure 1.11. All calculated ΔH and ΔS values are given in Table 1.4. For all the compounds, ΔS_D is large and positive, as would be expected from a dissociative process. However, a direct comparison of the numbers is difficult due to potential complications with dimerization of the free MX_3.

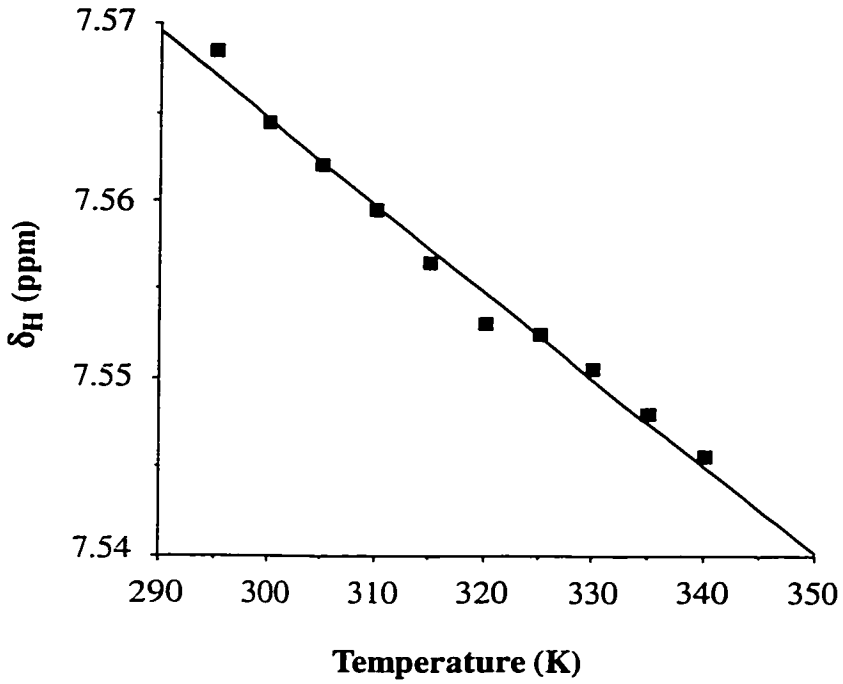

Figure 1.10. Temperature dependence of the ^1H NMR shift of the 1-CH in 9-fluorenone (R = 0.993).

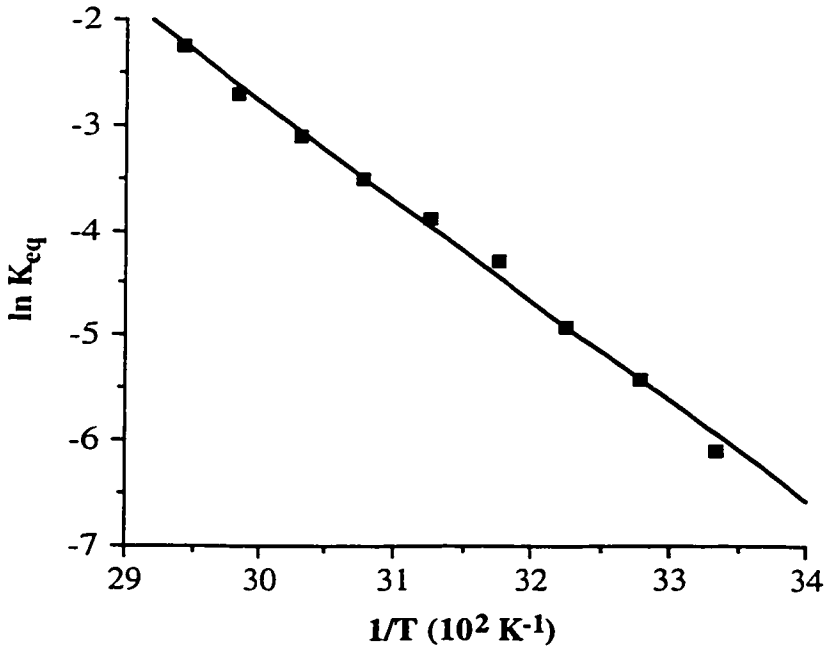

Figure 1.11. Temperature dependence of the equilibrium constant, K_{eq}, for the dissociation of $GaCl_3$(9-fluorenone) (R = 0.995).

Table 1.4. Determination of K_{eq} for the ligand dissociation of $GaCl_3$(9-fluorenone) from the ^1H NMR chemical shift of the 9-fluorenone's 1-C<u>H</u> proton.[a]

T (K)	δ_{sample} (ppm)	δ_{free} (ppm)	δ_{free}	K_{eq} (mol.dm^{-3})
300	7.425	7.564	0.192	2.28×10^{-3}
305	7.435	7.562	0.257	4.43×10^{-3}
310	7.445	7.559	0.317	7.36×10^{-3}
315	7.458	7.556	0.405	1.38×10^{-2}
320	7.467	7.553	0.468	2.06×10^{-2}
325	7.477	7.552	0.532	3.02×10^{-2}
330	7.486	7.550	0.598	4.45×10^{-2}
335	7.495	7.548	0.665	6.62×10^{-2}
340	7.505	7.545	0.740	1.05×10^{-1}

[a] Chemical shift of fully coordinated 9-fluorenone determined to be 7.392 ppm.

Is there a simple parameter for Lewis acidity? Before resorting to techniques such as principle component analysis using a number of spectroscopic and structural parameters,we have investigated if there is a consistent trend in the various parameters that will allow for easy prediction of Lewis acidity by a single measurement. In this regard, we have correlated the results for the five structurally characterized compounds MX_3(9-fluorenone) (M = B, X = Cl; M = Al, X = Cl, Br; M = Ga, X = Cl, Br). Table 1.6 provides a summary of the relative trends as measured by each technique. Those compounds where additional spectroscopic data is available are also discussed in context. It is readily apparent from Table 1.6 that the shift in the carbonyl IR stretching frequency (Δ

Table 1.5. Thermodynamic data for Group 13 halide complexes of 9-fluorenone.

Compound	K_{eq} @ 298 K (mol.dm^{-3})	ΔH (kJ.mol^{-1})	ΔS (J.K^{-1}.mol^{-1})	ΔG @ 298 K (kJ.mol^{-1})
BCl_3(9-fluorenone) (**1.1**)	2.78(1) x 10^{-6}	125(1)	313(2)	32(2)
$AlCl_3$(9-fluorenone)	6.34(3) x 10^{-4}	85.8(5)	227(3)	18(1)
$AlBr_3$(9-fluorenone) (**1.2**)	5.68(5) x 10^{-4}	92.4(9)	248(3)	19(1)
$GaCl_3$(9-fluorenone) (**1.5**)	2.117(5) x 10^{-3}	78.8(5)	214(2)	15(1)
$GaBr_3$(9-fluorenone) (**1.6**)	4.07(7) x 10^{-3}	152.0(3)	465(7)	13(2)

[a] Error is given in parentheses.

$\nu_{C=O}$) for MX_3(9- fluorenone) follows the same trends reported by Lappert.[1] If the largest shift in the stretching frequency is associated with increased Lewis acidity of MX_3, then, for the chlorides, the order follows B > Ga > Al. For AlX_3, the order of Br > Cl also follows the trend reported previously for Al and In.[1] Interestingly, the relative order for GaX_3 is the reverse (i.e., Cl > Br). This is the same result Lappert reported for boron, suggesting that the trends reverse between boron and aluminum, aluminum and gallium and then gallium and indium. We note, however, that inclusion of MI_3 (see Table 1.1) follows the appropriate trends, i.e., $AlI_3 \approx AlBr_3 > AlCl_3$ and $GaCl_3 > GaBr_3 > GaI_3$. The advantage of the IR parameter is that isolation of the compound is not required, and it should provide a suitable measurement for 1:2 complexes. Thus, IR would place $ZrCl_4$ between BCl_3 and $AlBr_3$, while $SnCl_4$ would be comparable to $GaCl_3$. Furthermore, the similarity of GaI_3 and $MgCl_2$ for which the 1:2 complexes are common,[39] suggests that GaI_3(9-fluorenone)$_2$ is the sole complex formed.

Table 1.6. Summary of spectroscopic and structural trends for MX_3(9-fluorenone).

Technique	Parameter[a]	Trend
IR	$\Delta \nu_{C=O}$	$BCl_3 > AlBr_3 > GaCl_3 > GaBr_3 > AlCl_3$
UV-visible	$\Delta \lambda_{max}$	$BCl_3 > AlBr_3 > AlCl_3 > GaBr_3 > GaCl_3$
^{13}C NMR	$\Delta \delta_{C=O}$	$GaCl_3 > GaBr_3 \approx AlCl_3 > AlBr_3 > BCl_3$
^{1}H NMR	K_{eq} @ 298 K	$BCl_3 > AlBr_3 > AlCl_3 > GaCl_3 > GaBr_3$
	ΔH	$GaBr_3 > BCl_3 > AlBr_3 > AlCl_3 > GaCl_3$
	ΔG	$BCl_3 > AlBr_3 > AlCl_3 > GaCl_3 > GaBr_3$
XRD	O(1)-C(9)	$AlBr_3 > AlCl_3 > BCl_3 > GaBr_3 > GaCl_3$
	Σ(X-M-X)	$AlBr_3 > AlCl_3 > BCl_3 > GaCl_3 > GaBr_3$
	$\Delta_{O,X}$	$AlBr_3 > AlCl_3 > BCl_3 > GaCl_3 > GaBr_3$

[a] See text for definitions.

The shift of the λ_{max} for MX_3(9-fluorenone) as compared to the free ligand ($\Delta \lambda_{max}$) follows B > Ga > Al, a different trend to that obtained from IR spectroscopy. Our data is in concert with the theoretically calculated values for π^* with regard to $BCl_3 > AlBr_3 > AlCl_3$.[17] These π^* values reported by Laszlo and Teston were not dependent on the transition, but rather the absolute energy of the level in eV. We have not determined the nature of the observed absorbtion, and if it is associated with a M-$X_\sigma \rightarrow$ L π^* transition, then the relative ordering is going to depend on the relative energies of the M-X_σ orbitals.

We have previously suggested that an increased downfield shift in the ^{13}C NMR

signal for the C=O carbon of an organic carbonyl as compared to the free ligand ($\Delta\delta_{C=O}$), correlates with the activation of the carbonyl towards nucleophilic attack. Furthermore, it would be assumed that the larger shifts are associated with stronger Lewis acid-base interactions. As may be seen from Table 1.6, the trend obtained from ^{13}C NMR ($\Delta\delta_{C=O}$) is essentially the reverse of the order found by any other parameter. There is even an almost inverse relationship between $\Delta\delta_{C=O}$ and ΔG, suggesting that while our proposal that $\Delta\delta_{C=O}$ can be correlated to reactivity, it clearly is not related to the strength of the Lewis acid-base interaction in MX_3(9-fluorenone).

Solution dissociation enthalpies have been assumed to represent the BDE for simple Lewis acid base complexes, and in the absence of potential dimerization (Eq. 5) they may be appropriate.[37]

$$2\ MX_3 \underset{}{\overset{K_{eq}}{\rightleftharpoons}} [X_2M(\mu\text{-}X)]_2 \qquad (1.5)$$

In the present study, however, it is clear that ΔH is not representative of Lewis acid strength. For example, the ΔH for $GaBr_3$ is the largest, but it has the highest dissociation constant (K_{eq}) at 298 K (see Table 1.5). This would suggest that the entropy term is very important in defining the extent of a Lewis acid-base interaction in solution. In contrast, the trend found for ΔG more closely matches that expected. Although ΔH defines the energy of the reaction between the Lewis acid and base, it does not take into account the extent of reaction at a given temperature. Thus, if the Lewis acid catalyzes a reaction that does not proceed in the absence of the Lewis acid, the "level of activation" rather than the "extent of reaction" may be more important. In contrast, if the reaction under consideration occurs in the absence of a Lewis acid, but the presence of the Lewis acid changes the site selectivity (e.g., alkylation of a 1,3-enone at the 2 or 4 positions[40]) then the extent of reaction will be

more important. In this regard, we propose that the value of K_{eq}, taken at a defined temperature (e.g., 298 K), may be a more useful parameter to determine the suitability of a Lewis acid as a catalyst. Unfortunately, neither of the simpler spectroscopic measurements (IR and UV) provide a positive correlation with either K_{eq} or ΔG.

Structural parameters are commonly employed in discussion of the strength of a Lewis acid interaction. As would be expected, the M-O distances in MX_3(9- fluorenone) are dependent on the ionic radii of the Group 13 element (Figure 1.12).

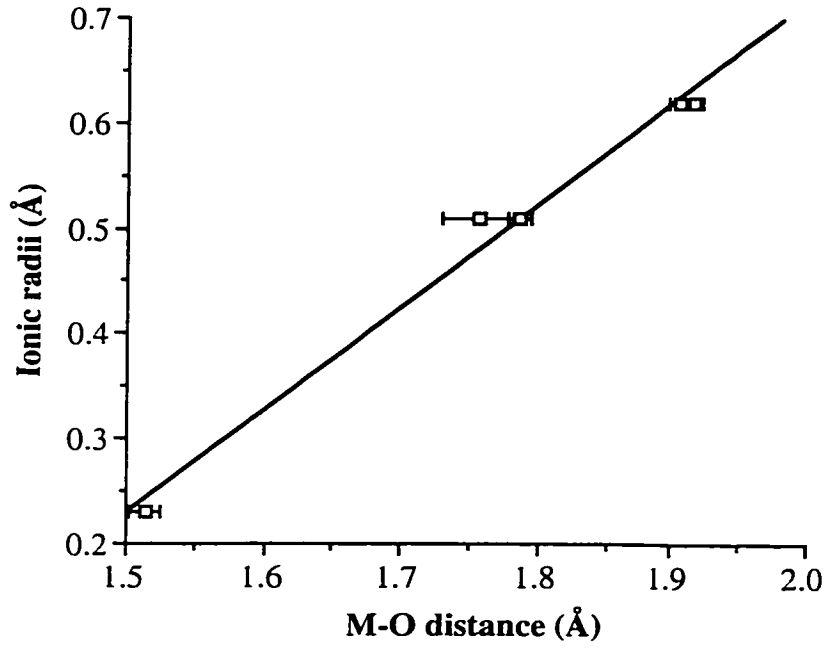

Figure 1.12. Plot showing the relationship between M-O bond distance in the complexes MX_3(9-fluorenone) (M = B, Al, Ga; X = Cl, Br) and the ionic radii for M (R = 0.986).

In fact, the experimental values for M-O and M-X are predicted with reasonable accurancy from the sum of the ionic radii (Figure 1.13). By comparison, the use of the covalent radii overestimates the M-O distances and underestimates the M-X distances (see Figure 1.13). Thus, the M-O distance cannot be used as a measure of relative Lewis acidity between complexes of dissimilar metals. Based upon the relative M-O distances, however, the

(a)

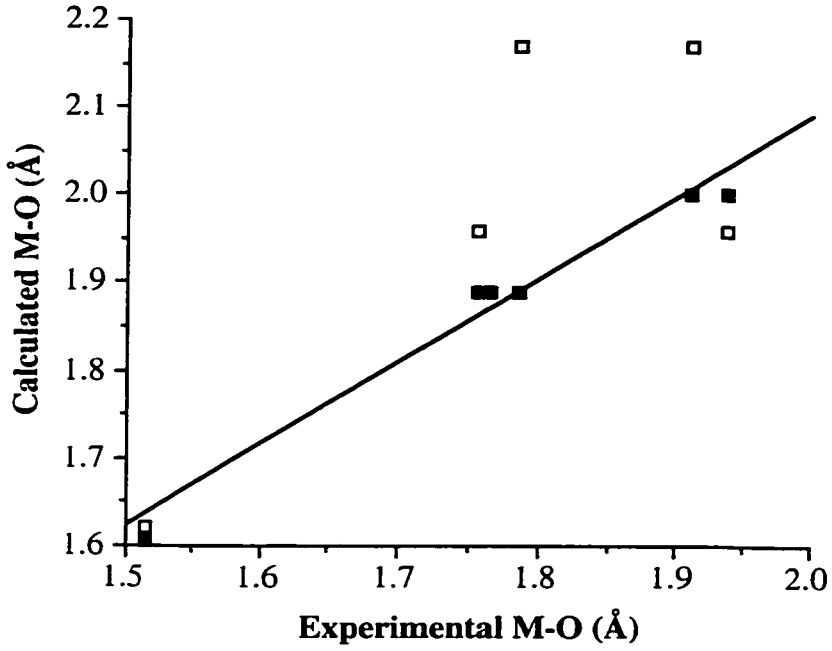

(b)

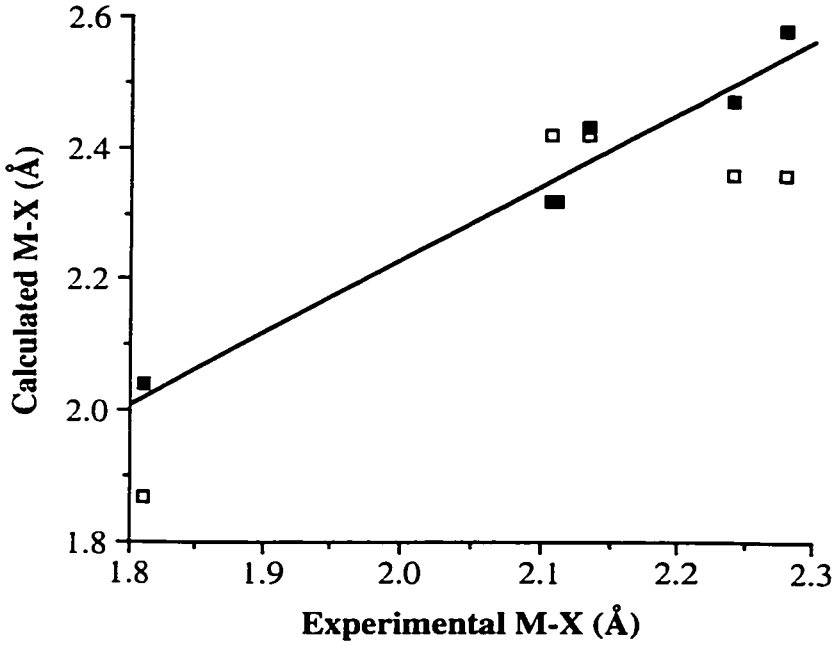

Figure 1.13. Plot showing the relationship between experimental M-O (a) and M-X (b) bond distance in the complexes MX_3(9-fluorenone) (M = B, Al, Ga; X = Cl, Br) and the sum of the ionic radii (■) and covalent radii (□) ($R_{(a)} = 0.979$; $R_{(b)} = 0.986$).

trends $AlBr_3 > AlCl_3$ and $GaCl_3 > GaBr_3$ would be expected, which agrees with the IR data.

The C=O bond distance should provide a comparison between complexes with different metals, and also should correlate with IR data measuring the change in the $\nu_{C=O}$ associated with weakening of the bond (rather than changes in the reduced mass). Despite the presence of a trend (see Table 1.1), the values are sufficiently close and the esds large enough, that no real comparison may be made.

It is generally assumed that (in the absence of overwhelming steric effects) the stronger a Lewis acid-base interaction, the greater the geometry about the Lewis acid will be distorted from an ideal planar structure associated with a monomeric structure. An alternative approach to measure Lewis acidity is to study the distortions from ideal tetrahedral. Within a series for an individual metal the distortion from planar, $AlBr_3 > AlCl_3$ and $GaCl_3 > GaBr_3$, both of which are consistent with IR data. As may be seen from Figure 1.14, however, the deviation from planarity is closely related to the M-O distance. This would suggest that intra-molecular repulsion is the controlling factor with regard to the geometry about the Group 13 center. We have previously shown that such a relationship is predominant in the phosphine complexes of $AlMe_3$.[41]

It has been noted that a consideration of the covalent radii and bond lengths reported for organic molecules would predict a metal alkoxide or aryloxide s-bond length to be 0.10 – 0.15 Å shorter than a metal-alkyl bond. Therefore, the parameter $\Delta_{O,C}$ was proposed (Eq. 1.6) as a qualitive probe for possible π-bonding between aryloxide, oxygen atoms, and electron-deficient metal centers.[4]

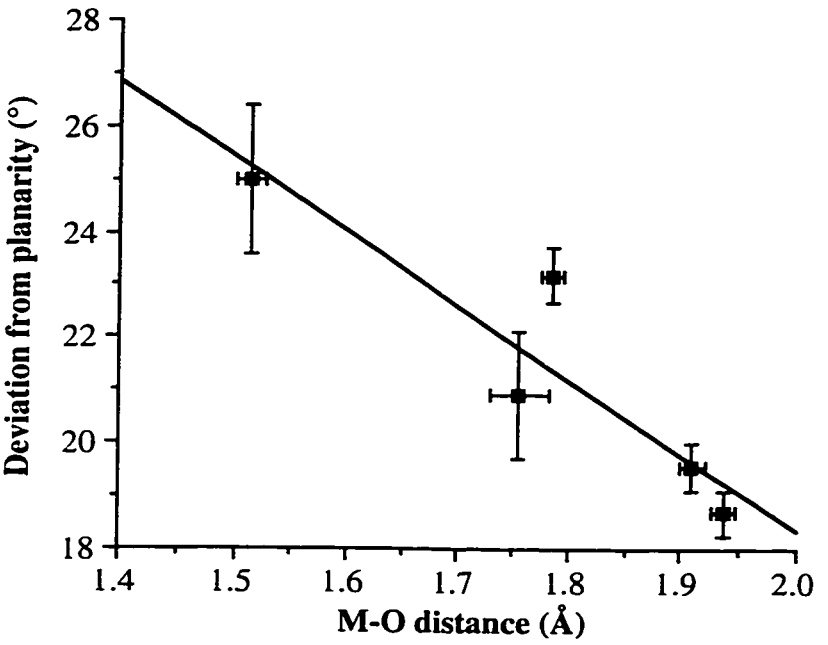

Figure 1.14. Plot of the deviation from planarity of the Group 13 element in MX_3(9-fluorenone) (M = B, Al, Ga; X = Cl, Br) as a function of the M-O bond distance (R = 0.851).

$$\Delta_{O,X} = d(M\text{-}O) - d(M\text{-}X) \tag{1.6}$$

Given the clear ionic character of the bonding in MX_3(9-fluorenone), we can propose a similar parameter, $\Delta_{O,X}$, using the ideal M-O and M-X bond lengths (see Figure 1.13). The difference between the $\Delta_{O,X}$ (Eq. 1.6) value calculated for each M/X combination and the experimentally determined M-O and M-X bond lengths allows for a measure of the shortening of the M-O bond over that expected. As is shown in Table 1.6, this order follows that of Σ(X-M-X). In addition, it suggest the trends $AlBr_3 > AlCl_3$ and $GaCl_3 > GaBr_3$, the order of which is observed from IR spectroscopy.

Conclusions

In an attempt to devise a simple test for Lewis acidity, we prepared the Lewis acid-base complexes MX_3(9-fluorenone) (M = B, Al, Ga; X = Cl, Br). Trends based on the correlation of thermodynamic and spectroscopic or structural parameters were observed, but, based on the forgoing, it is clear that none of the spectroscopic or structural parameters studied herein provides a consistent prediction of Lewis acid strength. We propose, however, that the parameters investigated above, in combination with a series of kinetic parameters, would provide the ideal basis for a principle component analysis of measured Lewis acid properties. In conclusion, it appears that, unlike Brønsted acidity (pK_a), Lewis acidity does not have a simple parameter that will allow for comparison of a range of compounds.

Experimental

Mass spectra were obtained on a Finnigan MAT 95 mass spectrometer operating with an electron beam energy of 70 eV for EI mass spectra. IR spectra (4000 - 400 cm^{-1}) were obtained using an Nicolet 760 FT-IR infrared spectrometer. NMR spectra were obtained on Bruker Avance 200, 400, and 500 spectrometers using (unless otherwise stated) d_6-benzene solutions. Chemical shifts are reported relative to internal solvent resonances (^1H and ^{13}C), and external $[Al(H_2O)_6]^{3+}$ (^{27}Al). Molecular weight measurements were made in C_6H_6 with the use of an instrument similar to that described by Clark.[42] $GaCl_3$ was obtained from Strem Chemicals. All other Lewis acids, as well as 9-fluorenone, were obtained from Aldrich. The Lewis acids were used without further purification; 9-fluorenone was recrystallized from toluene prior to use.

BCl_3(9-fluorenone) (1.1). 5.0 mL of a 1.0 M solution of BCl_3 (0.586 g, 5.0 mmol) in *o*-xylene was added to a 25 mL solution of 9-fluorenone (0.901 g, 5.0 mmol), resulting in a dark red solution. The reaction was allowed to stir at room temperature for two hours, then was cooled at –24 °C for several days, resulting in the formation of dark red crystalline blocks. Yield: 65%. Mp: (dec.) 150 °C. MS (EI, %): *m/z* 180 ($C_{13}H_8O$, 100). IR (cm^{-1}): 1611 (m), 1603 (s), 1583 (m), 1558 (s), 1310 (s), 1234 (w), 1206 (m), 1090 (w), 936 (m), 813 (s), 786 (m), 734 (s), 694 (m), 669 (w), 642 (w), 562 (m). ^1H NMR: δ 7.72 [2H, d, J(H-H) = 7.5 Hz, 1-CH], 6.56 [2H, dt, J(H-H) = 7.5 Hz, J(H-H) = 1.1 Hz, 3-CH], 6.31 [2H, dt, J(H-H) = 7.6 Hz, J(H-H) = 0.9 Hz, 2-CH], 6.25 [2H, d, J(H-H) = 7.3 Hz, 4-CH]. ^{13}C NMR: δ 200.2 (9-C), 146.7 (10-C), 139.6 (3-C), 133.2 (11-C), 130.2 (2-C), 126.0 (1-C), 121.5 (4-C).

$AlCl_3$(9-fluorenone). Prepared as previously described in the literature.[27] Yield: 75%. Mp: (dec.) 206 °C. MS (EI, %): *m/z* 277 (M^+ – Cl, 10), 241 (M^+ – Cl – H, 10), 180 ($C_{13}H_8O$, 100). IR (cm^{-1}): 1637 (s), 1602 (s), 1573 (s), 1313 (s), 1236 (w), 1210 (m), 1190 (w), 1163 (w), 1097 (m), 1007 (m), 1003 (w), 960 (w), 928 (m), 815 (w), 799 (m), 734 (s), 627 (w), 652 (m), 633 (s). ^1H NMR: δ 7.49 [2H, dd, J(H-H) = 7.5 Hz, J(H-H) = 0.4 Hz, 1-CH], 6.86 [2H, t, J(H-H) = 7.5 Hz, 3-CH], 6.79 [2H, d, J(H-H) = 6.8 Hz, 4-CH], 6.65 [2H, t, J(H-H) = 7.5 Hz, 2-CH]. ^{13}C NMR: δ 197.2 (9-C), 145.6 (10-C), 136.9 (3-C), 134.2 (11-C), 130.6 (2-C), 129.8 (1-C), 121.1 (4-C). ^{27}Al NMR (C_7H_8/C_6D_6): δ 93 ($W_{1/2}$ = 1800 Hz).

$AlBr_3$(9-fluorenone) (1.2). Toluene (30 mL) was added to 9-fluorenone (0.169 g, 0.94 mmol) and an excess of $AlBr_3$ (0.500 g, 1.88 mmol) at room temperature.

The resulting red solution was allowed to stir at room temperature for three hours. The solution was then filtered and cooled to –24 °C. Dark red crystalline needles formed overnight. Yield: 80%. Mp: (dec.) 179 °C. MS (EI, %): *m/z* 444 (M^+, 5), 365 (M^+ – Br, 10), 285 (M^+ – Br – H, 10), 265 ($AlBr_3$, 5), 185 ($AlBr_2$, 10), 180 ($C_{13}H_8O$, 100), 79 (Br, 5). IR (cm^{-1}): 1640 (s), 1603 (s), 1576 (s), 1312 (m), 1231 (w), 1207 (w), 1093 (m), 1030 (w), 1001 (w), 963 (w), 926 (w), 895 (w), 802 (m), 728 (s), 694 (w), 641 (m). ^1H NMR: δ 7.38 [2H, d, J(H-H) = 7.4 Hz, 1-CH], 6.54 [2H, dt, J(H-H) = 7.5 Hz, J(H-H) = 0.8 Hz, 2-CH], 6.22 [2H, t, 7.6 Hz, 3-CH], 6.20 [2H, d, J(H-H) = 7.3 Hz, 4-CH].^{13}C NMR: 204.5 (9-C), 147.3 (10-C), 141.7 (3-C), 132.7 (11-C), 132.2 (2-C), 130.7 (1-C), 122.3 (4-C). (^{27}Al NMR (C_7H_8/C_6D_6): δ 82 ($W_{1/2}$ = 3800 Hz).

$AlBr_3$(9-fluorenone)$_2$ (1.3). Prepared in the same manner as compound **1.2**, but using 9-fluorenone (0.169 g, 0.94 mmol) and $AlBr_3$ (0.250 g, 0.94 mmol). Upon cooling, a mixture of compounds **1.4** and **1.5** formed. Yield: 25%. Mp: (dec.) 179 °C. MS (EI, %): *m/z* 444 (M^+, 5), 365 (M^+ – Br, 10), 285 (M^+ – Br – H, 10), 265 ($AlBr_3$, 5), 185 ($AlBr_2$, 10), 180 ($C_{13}H_8O$, 100), 79 (Br, 5). IR (cm^{-1}): 1668 (s), 1607 (s), 1590 (s), 1307 (s), 1205 (s), 1158 (w), 1089 (m), 962 (w), 920 (s), 892 (m), 813 (m), 729 (s), 694 (m), 671 (m), 642 (m), 604 (s). ^1H NMR: δ 7.47 [2H, d, J(H-H) = 7.4 Hz, 1-CH], 6.79 [2H, t, J(H-H) = 7.5 Hz, 2-CH], 6.65 [2H, d, J(H-H) = 7.3 Hz, 4-CH], 6.55 [2H, J(H-H) = 7.5 Hz, 3-CH]. ^{13}C NMR: δ 197.9 (9-C), 145.8 (10-C), 137.5 (3-C), 134.0 (11-C), 129.9 (2-C), 127.7 (1-C), 121.3 (4-C). ^{27}Al NMR (C_7H_8/C_6D_6): δ 82 ($W_{1/2}$ = 3800 Hz).

AlI_3(9-fluorenone)$_2$ (1.4). Prepared in the same manner as **1.2**, but using 9-fluorenone (44 mg, 0.25 mmol) and AlI_3 (0.101 g, 0.25 mmol). AlI_3 is light-sensitive, so, though no decompostion was observed when leaving **1.4** exposed to light, compound **1.4** was protected from light by aluminum foil. Yield: 55%. Mp: (dec.) 174 °C. MS (EI, %): *m/z* 588 (M^+, 5), 461 (M^+ – I, 100), 333 (M^+ – 2 I – H, 30), 281 (AlI_2, 35), 207 (M^+ – 3 I, 10), 180 ($C_{13}H_8O$, 40), 152 ($C_{13}H_8O$ – CO, 50), 151 ($C_{13}H_8O$ – CO – H, 100). IR (cm^{-1}): 1634 (m), 1601 (m), 1572 (m), 1311 (w), 729 (s).

$GaCl_3$(9-fluorenone) (1.5). Prepared in the same manner as compound **1.1**, but using $GaCl_3$ (0.489 g, 2.77 mmol). Yield: 85%. Mp: (dec.) 171 °C. MS (EI, %): *m/z* 180 ($C_{13}H_8O$, 100), 152 ($C_{12}H_8$, 25), 76 (C_6H_4, 10). IR (cm^{-1}): 1635 (s), 1603 (s), 1573 (s), 1310 (s), 1237 (w), 1206 (m), 1188 (w), 1159 (w), 1098 (m), 1090 (m), 927 (m), 734 (s). ^1H NMR: δ 7.38 [2H, d, J(H-H) = 7.4 Hz, 1-CH], 6.63 [2H, dt, J(H-H) = 7.2 Hz, J(H-H) = 0.8 Hz, 3-CH], 6.33 [2H, t, J(H-H) = 7.9 Hz, 2-CH], 6.32 [2H, d, J(H-H) = 7.7 Hz, 4-CH]. ^{13}C NMR: δ 203.6 (9-C), 146.6 (10-C), 139.5 (3-C), 132.5 (11-C), 131.7 (2-C), 128.2 (1-C), 121.5 (4-C).

$GaBr_3$(9-fluorenone) (1.6). Prepared in the same manner as compound **1**, but using 9-fluorenone (0.146 g, 0.81 mmol) and $GaBr_3$ (0.250 g, 0.81 mmol). Yield: 80%. Mp: (dec.) 147 °C. MS (EI, %): *m/z* 306 ($GaBr_3$, 15), 227 ($GaBr_2$, 35), 180 ($C_{13}H_8O$, 100), 152 ($C_{12}H_8$, 35). IR (cm^{-1}): 1636 (m), 1605 (m), 1569 (m), 1495 (w), 1308 (m), 1204 (w), 1096 (w), 1030 (w), 956 (w), 924 (w), 812 (m), 783 (w), 727 (s), 694 (m), 670 (w), 648 (w), 602 (w), 439 (m). ^1H NMR: 7.51 [2H, d, J(H-H) = 7.5 Hz, 1-CH], 6.59 [2H, dt, J(H-H) = 7.5 Hz, J(H-H) = 1.0 Hz, 3-CH], 6.34 [2H, dt, J(H-H) = 7.6

Hz, J(H-H) = 0.8 Hz, 2-CH], 6.30 [2H, d, J(H-H) = 7.4 Hz, 4-CH]. ^{13}C NMR: 204.0 (9-C), 146.5 (10-C), 139.5 (3-C), 138.2 (11-C), 130.9 (2-C), 129.7 (1-C), 121.5 (4-C).

GaI_3(9-fluorenone)$_2$ (1.7). Prepared in the same manner as **1.1**, but with 9-fluorenone (40 mg, 0.22 mmol) and GaI_3 (0.2 g, 0.444 mmol). Yield: 70%. Mp: (dec.) 156 °C. MS (EI, %): *m/z* 450 (GaI_3, 25), 323 (GaI_2, 30), 198, 180 ($C_{13}H_8O$, 100), 152 ($C_{13}H_8O$ – CO, 40), 127 (I, 10). IR (cm^{-1}): 1652 (w), 1603 (w), 1558 (w), 1395 (m), 1153 (w), 919 (w), 728 (m).). ^{1}H NMR: 7.62 [2H, d, J(H-H) = 7.4 Hz, 1-CH], 6.58 [2H, dt, J(H-H) = 7.5 Hz, J(H-H) = 1.0 Hz, 2-CH], 6.36 [2H, dt, J(H-H) = 7.6 Hz, J(H-H) = 0.8 Hz, 3-CH], 6.29 [2H, d, J(H-H) = 7.4 Hz, 4-CH]. ^{13}C NMR: 205.2 (9-C), 146.8 (10-C), 140.8 (3-C), 132.3 (11-C), 131.3 (2-C), 130.4 (1-C), 122.2 (4-C).

$MgCl_2$(9-fluorenone)$_n$ (1.8). Prepared for IR characterization by grinding 9-fluorenone (10 mg, 55 μmol) and an excess of $MgCl_2$ (50 mg, 0.53 mmol) into a very fine mixture.

IR (cm^{-1}): 1653 (m), 1611 (s), 1297 (m), 1190 (m), 1149 (s), 1096 (m), 949 (w), 916 (m), 811 (w), 782 (w), 735 (s), (668 (m).

$HgCl_2$(9-fluorenone)$_n$ (1.9). Prepared for IR in the same manner as **1.8**, but using $HgCl_2$ (50 mg, 0.18 mmol).

IR (cm^{-1}): 1697 (s), 1612 (m), 1599 (m), 1300 (m), 735 (s), 728 (s).

$ZrCl_4$(9-fluorenone)$_n$ (1.10). Prepared for IR in the same manner as **1.8**, but using $ZrCl_4$ (50 mg, 0.21 mmol). As the two solids were ground together, a solid state reaction was observed, as evidenced by a color change from 9-fluorenone's yellow to

brown.

IR (cm^{-1}): 1632 (m), 1611 (m), 1601 (w), 1570 (m), 1299 (m), 1190 (m), 1150 (w), 916 (s), 735 (s).

$SnCl_4$(9-fluorenone)$_2$ (1.11). $SnCl_4$ (0.362 g, 1.39 mmol) was added by syringe to a tolune (60 mL) solution of 9-fluorenone (0.250 g, 1.39 mmol). The resulting orange-red solution was allowed to stir for several hours, then cooled to –24 °C. Red precipitate formed overnight. Yield: 75%. Mp: 156 °C. MS (EI, %): *m/z* 225 ($SnCl_3$, 15), 180 ($C_{13}H_8O$, 100), 152 ($C_{13}H_8O$ – CO, 35). IR (cm^{-1}): 1634 (s), 1607 (s), 1577 (s), 1310 (m), 1202 (m), 1097 (m), 1004 (w), 992 (w), 956 (m), 923 (m), 889 (m), 812 (m), 779 (m), 725 (s), 670 (m), 646 (w), 588 (s). ^1H NMR: δ 7.65 [2H, dt, J(H-H) = 7.3 Hz, J(H-H) = 1.0 Hz, 1-CH], 6.92 (4H, m, 3- and 4-CH), 6.74 (2H, m, 2-CH). ^{13}C NMR: 194.0 (9-C), 145.1 (10-C), 135.0 (3-C), 134.8 (11-C), 129.5 (2-C), 125.2 (1-C), 120.7 (4-C).

VO(Cl)(9-fluorenone)$_2$(H_2O)(μ-O)($VOCl_2$) (1.12). Prepared in the same manner as **1.9**, but using hydrolzyed VCl_4 (0.268 g, 1.39 mmol) and 9-fluorenone (0.25 g, 1.39 mmol) Yield: 75%. Mp: (dec.) 194 °C. IR (cm^{-1}): 1657 (s), 1608 (m), 1587 (s), 1310 (m), 1207 (w), 1158 (w), 1011 (w), 923 (w), 850 (w), 811 (w), 730 (s), 667 (m).

Crystallographic Studies. Crystals of **1** - **3**, **5**, **6**, and **12** were sealed in a glass capillary under argon and mounted on the goniometer of a Bruker CCD SMART system, equipped with graphite monochromated Mo-K_α radiation (λ = 0.71073 Å) and corrected for Lorentz and polarization effects. Data collection and unit cell and space group determination were all carried out in the usual manner.[43] Compounds **1.1**, **1.2**, and **1.6**

Table 1.7. Summary of X-ray diffraction data.

Compound	BCl_3(9-fluorenone).$^1/_2(C_6H_5Me)$ (**1.1**)	$AlBr_3$(9-fluorenone).$^1/_2(C_6H_5Me)$ (**1.2**)
empir. formula	$C_{16.5}H_{12}BCl_3O.^1/_2\ C_7H_8$	$C_{16.5}H_{12}AlBr_3O$
M_w	343.42	492.97
cryst system	triclinic	triclinic
space group	$P\bar{1}$	$P\bar{1}$
a, Å	9.472(2)	9.645(2)
b, Å	9.726(2)	10.020(2)
c, Å	9.973(2)	10.546(2)
α, °	79.92(3)	63.41(3)
β, °	62.55(3)	80.91(3)
γ, °	88.01(3)	88.23(3)
V, Å^3	801.6(3)	898.9(3)
Z	2	2
D(calcd), g/cm^3	1.423	1.821
μ, cm^{-1}	0.57	6.78
2θ range, deg	4.3 - 46.6	4.3 - 46.7
no. collected	3702	4165
no. ind	2284	2565
no. obsd	1830 ($\|F_o\| > 4.0\sigma\|F_o\|$)	1219 ($\|F_o\| > 4.0\sigma\|F_o\|$)
weighting scheme	SHELXTL 0.0709, 0	SHELXTL 0.0.05
R[a]	0.0399	0.0759
R_w[a]	0.1080	0.1617
Largest diff. peak	0.34	0.72

[a] $R = \sigma|F_o-F_c|/\sigma F_o$; $wR = \{\sigma[\{w(F_o^2-F_c^2)^2\}/\{w(F_o^2)^2\}]\}^{1/2}$.

Table 1.7, contd.

Compound	$AlBr_3$(9-fluorenone)$_2$	$GaCl_3$(9-fluorenone)
	(1.3)	**(1.5)**
empir. formula	$C_{26}H_{16}AlBr_3O_2$	$C_{13}H_9Cl_3GaO$
M_w	1254.20	357.27
cryst system	triclinic	orthorhombic
space group	$P\bar{1}$	Pbca
a, Å	7.248(1)	9.210(2)
b, Å	10.358(2)	17.153(3)
c, Å	16.214(3)	17.531(4)
α, °	86.47(3)	
β, °	83.29(3)	
γ, °	71.03(3)	
V, Å^3	1142.9(4)	2769.4(9)
Z	1	8
D(calcd), g/cm^3	1.822	1.709
μ, cm^{-1}	5.36	2.55
2θ range, deg	2.5 – 46.6	4.6 – 46.6
no. collected	5369	6468
no. ind	3296	1981
no. obsd	1802 ($\|F_o\| > 4.0\sigma\|F_o\|$)	1263 ($\|F_o\| > 4.0\sigma\|F_o\|$)
weighting scheme	SHELXTL, 0.0.04	SHELXTL, 0.015, 0
R[a]	0.0630	0.0315
R_w[a]	0.1303	0.0543
Largest diff. peak	0.95	0.34

[a] $R = \sigma|F_o-F_c|/\sigma F_o$; $wR = \{\sigma[\{w(F_o^2-F_c^2)^2\}/\{w(F_o^2)^2\}]\}^{1/2}$.

Table 1.7, contd.

Compound	$GaBr_3$(9-fluorenone).$^1/_2(C_6H_5Me)$ **(1.6)**	$VO(Cl)$(9-fluorenone)$_2(H_2O)(\mu$-$O)(VOCl_2)$ **(1.12)**
empir. formula	$C_{16.5}H_{12}Br_3GaO$	$C_{26}H_{18}Cl_3O_6V_2$
M_w	535.71	634.63
cryst system	monoclinic	triclinic
space group	$P2_1/n$	$P\bar{1}$
a, Å	7.598(2)	9.806(2)
b, Å	11.619(2)	10.259(2)
c, Å	20.321(4)	14.098(3)
α, °		107.79(3)
β, °	96.71(3)	101.79(3)
γ, °		95.55(3)
V, Å^3	1781.7(6)	1302.5(5)
Z	4	2
D(calcd), g/cm^3	1.997	1.618
μ, cm^{-1}	8.27	1.07
2θ range, deg	4.0 - 46.6	3.14 - 46.58
no. collected	7944	6035
no. ind	2568	3748
no. obsd	1616 ($\|F_o\| > 4.0\sigma\|F_o\|$)	1894 ($\|F_o\| > 4.0\sigma\|F_o\|$)
weighting scheme	SHELXTL, 0.04, 0	SHELXTL, 0.02, 0
R[a]	0.0383	0.0514
R_w[a]	0.0810	0.0835
Largest diff. peak	0.48	0.44

[a] $R = \sigma|F_o-F_c|/\sigma F_o$; $wR = \{\sigma[\{w(F_o^2-F_c^2)^2\}/\{w(F_o^2)^2\}]\}^{1/2}$

crystallize as toluene solvates. Table 1.7 lists a summary of X-ray diffraction data.

References

1 M. F. Lappert, *J. Chem. Soc.*, **1962**, 542.

2 C. A. Tolman, *J. Am. Chem. Soc.*, 1970, **92**, 2953.

3 C. A. Tolman, *Chem. Rev.*, 1977, **77**, 616.

4 See for example, A. R. Barron, *J. Chem. Soc., Dalton Trans.*, **1988**, 3047.

5 D. Farcasiu and A. Ghenciu, *Prog. NMR Spectroscopy*, 1996, **29**, 129, and references therein.

6 G. A. Olah, G. K. Surya Prakash, and J. Sommer, *Superacids*, Wiley-Interscience, New York, 1985, pp. 24 – 25.

7 D. Farcasiu and M. Stan, *J. Chem. Soc., Perkin Trans.*, **1998**, 1219.

8 R. J. Gillespie and J. S. Hartman, *Can. J. Chem.*, 1968, **46**, 2147.

9 D. P. N. Satchell and R. S. Satchell, *Chem. Rev.*, 1969, **69**, 251.

10 M. B. Power, J. R. Nash, M. D. Healy, and A. R. Barron, *Organometallics*, 1992, **11**, 1830.

11 J. A. Francis, C. N. McMahon, S. G. Bott, and A. R. Barron, *Organometallics*, 1999, **18**, 4399.

12 See, for example, (a) H. Jacobsen, H. Burke, S. Döring, G. Kehr, G. Erker, R. Fröhlich, and O. Meyer, *Organometallics*, 1999, **18**, 1724.

(b) S. Shambayati, W. E. Crowe, and S. L. Schreiber, *Angew. Chem. Int. Ed. Engl.*, 1990, **29**, 256.

13 S. Shambayti, W. E. Crowe, and S. L. Schreiber, *Angew. Chem. Int. Ed. Engl.*, 1990, **29**, 256.

14 (a) B. H. Davis, R. A. Keogh, S. Alerasool, D. J. Zalewski, D. E. Day, and P. K.

Doolin, *J. Catal.*, 1999, **183**, 45.

(b) G. Berhault, M. Lacroix, M. Breysse, F. Maugé, J.-C. Lavalley, H. Nie, and L. Qu, *J. Catal.*, 1998, **178**, 555.

(c) C. Morterra, G. Cerrato, V. Bolis, S. Di Ciero, and M. Signoretto, *J. Chem. Soc., Faraday Trans.*, 1997, **93**, 1179.

(d) G. Catana, D. Baetens, T. Nommaerts, R. A. Schoonheydt, and B. M. Weckhuysen, *J. Phys. Chem. B*, 2001, **105**, 4904.

15 B. Hu and I. D. Gay, *J. Phys. Chem. B*, 2001, **105**, 217.

16 M. F. Lappert, *J. Chem. Soc.*, **1961**, 817.

17 R. F. Childs, D. L. Mulholland, and A. Nixon, *Can. J. Chem.*, 1982, **60**, 801.

18 P. Laszlo and M. Teston, *J. Am. Chem. Soc.*, 1990, **112**, 8750.

19 P. Laszlo and M. Teston-Henry, *Tetrahedron Lett.*, 1991, **32**, 3837.

20 R. Carlson, T. Lundstedt, A. Nordahl, and M. Prochazka, *Acta Chem. Scand.*, 1986, **B40**, 522.

21 M. B. Power, S. G. Bott, J. L. Atwood, and A. R. Barron. *J. Am. Chem. Soc.*, 1990, **112**, 3446.

22 G. D. Smith, P. E. Fanwick, and I. P. Rothwell, *Inorg, Chem.*, 1990, **29**, 3221.

23 M. B. Power, S. G. Bott, D. L. Clark, J. L. Atwood, and A. R. Barron., *Organometallics*, 1990, **9**, 3086.

24 M. Akakura, H. Yamamoto, S. G. Bott, and A. R. Barron, *Polyhedron*, 1997, **16**, 4389.

25 (a) V. Sharma, M. Simard, and J. D. Wuest, *J. Am. Chem. Soc.*, 1992, **114**, 7931.

(b) G. Quinkert, H. Becker, M. Del Grosso, G. Dambacher, J. W. Bats, and G. Dürner, *Tetrahedron Lett.*, 1993, **34**, 6885.

(c) A. P. Shreve, R. Mulhaupt, W. Fultz, J. Calabrese, W. Robbins, and S. D. Ittel, *Organometallics,* 1988, **7**, 409.

(d) G. Sartori, F. Bigi, X. Tao, C. Porta, R. Maggi, G. Predieri, M. Lanfranchi, and M. A. Pellinghelli, *J. Org. Chem.*, 1995, **60**, 6588.

(e) B. Chevrier, J.-M. Le Carpentier, and R. Weiss, *Acta Cryst.*, 1972, **B28**, 2659.

(f) A. Bittner, D. Mannig, and H. Z. Noth, *Naturforsch., Tiel B*, 1986, **41**, 587.

(g) S. E. Rasmussen and N. C. Broch, *Acta Chem. Scand.*, 1966, **20**, 1351.

(h) J. Utko, M. Wróblewska, T. Lis, and P. Sobota, *J. Organomet. Chem.*, 1993, **447**, 159.

(i) F. Bigi, G. Sartori, R. Maggi, C. Valerio-Papa, E. Marzi, M. Lanfranchi, and M. A. Pellinghelli, *J. Chem. Soc., Perkin Trans. 1*, **1996**, 1815.

(j) P. Sobota, S. Szafert, and T. Glowiak, *J. Organometal. Chem.*, 1996, **526**, 329.

26 D. L. Boucher, M. A. Brown, B. R. McGarvey, and D. G. Tuck, *J. Chem. Soc., Dalton Trans.*, **1999**, 3445.

27 (a) R. L. Beddoes, D. Collison, F. E. Mabbs, and J. Temperley, *Acta Cryst.*, 1991, **C47**, 58.

(b) S. Jin, V. McKee, M. Nieuwenhuyzen, W. T. Robinson, and C. J. Wilkins, *J.* Chem. Soc., Dalton Trans., **1993**, 3111.

28 H. Kuroda and T. L. Kunii, *Theoret. Chim. Acta* 1967, **9**, 51.

29 D. L. Boucher, M. A. Brown, B. R. McGarvey, and D. G. Tuck, *J. Chem. Soc., Dalton Trans.*, **1999**, 3445.

30 See, for example, (a) H. Barucki, S. J. Coles, J. F. Costello, T. Gelrich, and M. B. Hursthouse, *Dalton*, 2000, **14**, 2319.

(b) O. Saied, M. Simard, and J. D. Wuest, *Inorg. Chem.*, 1998, **37**, 2620.

(c) D. J. Parks, W. E. Piers, P. Masood, R. Atencio, and M. J. Zaworotko, *Organometallics*, 1998, **17**, 1369.

(d) J. W. Faller, Y. Ma, C. J. Smart, and M. J. DiVerdi, *J. Organomet. Chem*, 1991, **2**, 237.

(e) T. Laube, A. Weidenhaupt, and R. Hunziker, *J. Am. Chem. Soc.*, 1991, **117**, 2561.

31 H. R. Luss and D. L. Smith, *Acta Cryst.*, 1972, **B28**, 884.

32 N. N. Greenwood and A. Earnshaw, *Chemistry of the Elements, Second Edition*, Butterworth-Heineman, Oxford, 1998, Chapter 22.

33 F. A. Cotton, G. Wilkinson, C. A. Murillo, and M. Bochmann, *Advanced Inorganic Chemistry, Sixth Edition*, Wiley-Interscience, New York, 1999, 17-B.

34 See, for example, (a) F. Avecilla, C. F. G. C. Geraldes, and M. M. C. A. Castro, *Eur. J. Inorg. Chem.*, 2001, 3135.

(b) Y. Sun, M. Melchior, D. A. Summers, R. C. Thompson, S. J. Rettig, and C. Orvig, *Inorg. Chem.*, 1998, **37**, 3119.

(c) K. Isobe, S. I. Ooi, Y. Nakamura, S. Kawaguchi, and H. Kuroya, *Chem. Lett.*, 1975, 35.

(d) C. R. Cornman, J. Kampf, M. S. Lah, and V. L. Pecoraro, *Inorg. Chem.*, 1992, **31**, 2035.

(e) X. Li, M. S. Lah, and V. L. Pecoraro, *Inorg. Chem.*, 1988, **27**, 4657.

(f) M. R. Caira, J. M. Haigh, and L. R. Nassimbeni, *J. Inorg. Nucl. Chem.*, 1972, **24**, 3171.

35 M. D. Healy, J. W. Ziller, and A. R. Barron, *Organometallics*, 1991, **10**, 597.

36 See, for example, (a) R. Amunugama and M. T. Rodgers, *J. Phys. Chem. A*,

2001, **105**, 9883.

(b) M. Czerw, A. S. Goldman, and K. Krogh-Jesperson, *Inorg. Chem.*, 200, **39**, 363.

37 (a) M. B. Smith, *J. Phys. Chem.*, 1967, **71**, 364.

(b) M. B. Smith, *J. Organomet. Chem.*, 1970, **22**, 273.

(c) M. B. Smith, *J. Organomet. Chem.*, 1972, **46**, 31.

(d) M. B. Smith, *J. Organomet. Chem.*, 1972, **46**, 211.

(e) M. B. Smith, *J. Organomet. Chem.*, 1974, **70**, 13.

38 J. A. G. Drake and D. W. Jones, *Spectrochim. Acta*, 1980, **36A**, 23.

39 See, for example, (a) H. Kageyama, K. Miki, Y. Kai, N. Kasai, Y. Okamoto, and H. Yuki, *Bull. Chem. Soc. Jpn.*, 1983, **56**, 2411.

(b) X. Shijing, Q. Minxie, Z. Naijue, and T. Youqi, *Sci. Sin., Ser. B (Engl. Ed.)*, 1987, **30**, 1247.

(c) C. Dohmeier, D. Loos, C. Robl, H. Schnockel, and D. Fenske, *J. Organomet. Chem.*, 1993, **448**, 5.

(d) D. E. Hibbs, C. Jones, and A. F. Richards, *J. Chem. Soc., Dalton Trans.*, **1999**, 3531.

40 D. Liotta and G. Zima, *J. Org. Chem.*, 1980, **45**, 2551.

41 A. R. Barron, *J. Chem. Soc., Dalton Trans.*, **1988**, 3047.

42 E. P. Clark, *Ind. Eng. Chem. Anal. Ed.*, 1941, **13**, 820.

43 M. R. Mason, J. M. Smith, S. G. Bott, and A. R. Barron, *J. Am. Chem. Soc.*, 1993, **115**, 4971.

Chapter 2

Aluminum and Gallium Compounds of Salicylic and Anthranilic Acids: Examples of Weak Intra-Molecular Hydrogen Bonding

Introduction

A recent study from the Barron group involves the observation of strong intra-molecular hydrogen bonding of alcohol-amines (**I**) and diamines (**II**) upon coordination to a Group 13 Lewis acid.[1] The increase in the hydrogen bond strength in comparison to the "free" compounds is due to a dramatic increase in the acidity of the alcohol or amine proton. This "enhanced" hydrogen bonding strength has been used to create compounds possessing desirable crystallographic architectures.[2]

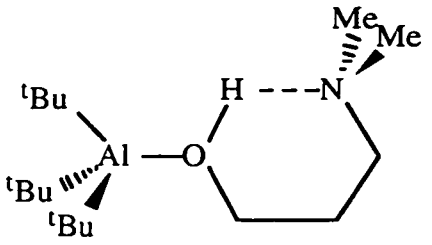

(**I**)

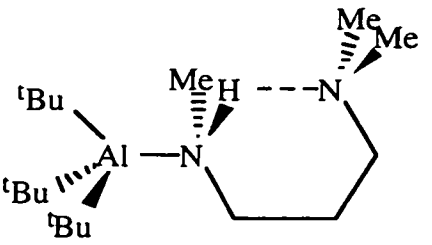

(**II**)

Based on these results, we are interested in determining if hydrogen bonding strength may be increased through activation of the Lewis base termini of the hydrogen bond (i.e., X-H...X'), rather than the Brønsted acidic termini (i.e., X-H...X'). In this regard, salicylic acid (**III**) and anthranilic acid (**IV**), both of which have intra-molecular hydrogen bonds in the solid state,[3,4] should offer a suitable system of study.

We have previously reported that the reaction of salicylic acid with AlR_3 (R = Me, Et) yields the tetra-aluminum compound, **V**, due to the reaction of the hydroxide

with additional aluminum alkyl.[5,6] We now report the synthesis and characterization of the sterically more demanding *tert*-butyl aluminum and gallium derivatives.

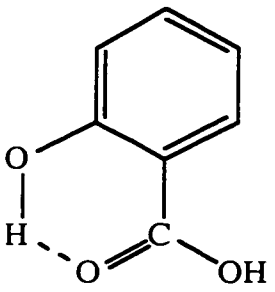

(III)

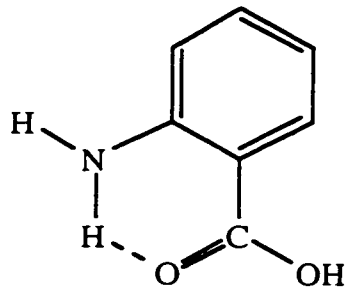

(IV)

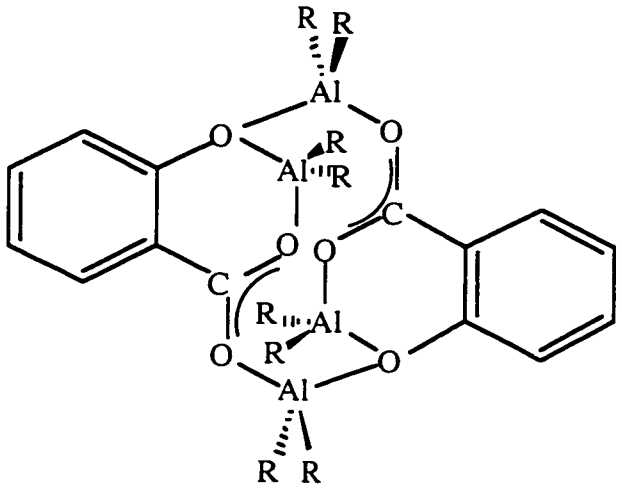

(V)

Results and Discussion

The reaction of $M(^tBu)_3$ (M = Al, Ga) with one molar equivalent of the *ortho*-substituted carboxylic acids, $HO_2CC_6H_4$-2-X, yields the dimeric carboxylates, $[(^tBu)_2M(\mu\text{-}O_2CC_6H_4\text{-}2\text{-}X)]_2$, in moderate to high yield, where X = NH_2, M = Al (**2.1**), Ga (**2.2**) and X = OH, Ga (**2.3**) (Eq. 2.1). Attempts to prepare the aluminum analog of compound **2.3** were unsuccessful, resulting in a complex mixture of products.

$$M(^tBu)_3 + HO_2CC_6H_4\text{-}2\text{-}X \longrightarrow [(^tBu)_2M(\mu\text{-}O_2CC_6H_4\text{-}2\text{-}X)]_2 \quad (2.1)$$

Compounds **2.1** – **2.3** have been characterized by IR and NMR spectroscopy, and the spectra are consistent with the solid state structures as determined by X-ray crystallography. The molecular structures of compounds **2.2** and **2.3** are shown in Figures 2.1 and 2.2, respectively; compound **2.1** is isostructural to compound **2.2**. Selected bond lengths and angles for compounds **2.1** – **2.3** are given in Table 2.1.

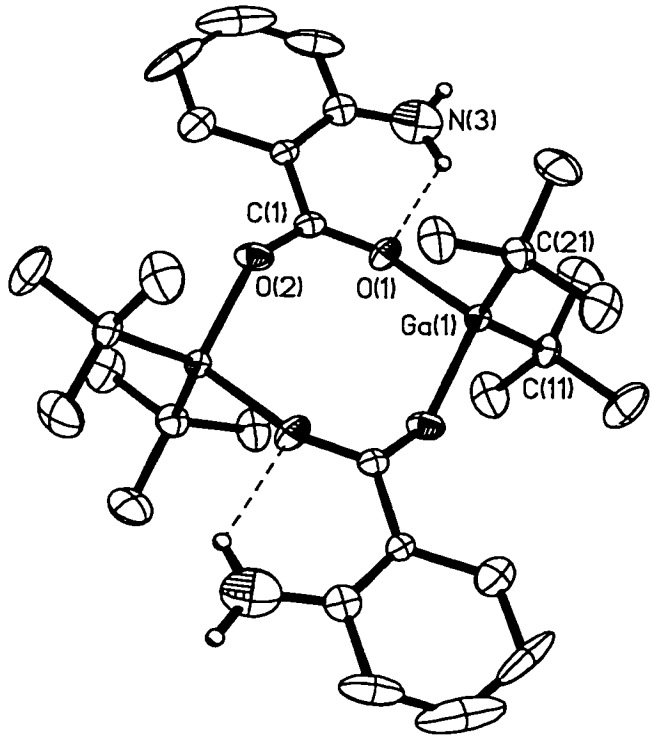

Figure 2.1. Molecular structure of $[(^tBu)_2Ga(\mu\text{-}O_2CC_6H_4\text{-}2\text{-}NH_2)]_2$ (**2.2**). Thermal ellipsoids are shown at the 20% level, and hydrogen atoms bound to carbon are omitted for clarity. Hydrogen bonding interactions are denoted by a dashed line.

The structures of compounds **2.1** – **2.3** consist of centro-symmetric dimers of two $(^tBu)_2M$ units bridged by two carboxylate groups. This is consistent with previous reports of alkylaluminum and alkylgallium carboxylates.[7,8,9,10] The M-O bond lengths to the

Table 2.1. Selected Bond Lengths (Å) and Angles (°) in $[(^tBu_2M)_2(\mu\text{-}O_2CC_6H_4\text{-}2\text{-}X)]_2$.

M	Al	Ga	Ga	Ga
X	NH_2	NH_2	OH	Me
	(2.1)	**(2.2)**	**(2.3)**	**(2.4)**
M(1)-O(1)	1.801(2)	1.946(3)	1.963(3)	1.966(2)
M(1)-O(2')	1.817(2)	1.941(3)	1.938(3)	1.954(2)
M(1)-C(11)	1.991(3)	1.988(5)	1.975(4)	1.987(3)
M(1)-C(21)	1.977(3)	1.972(5)	1.968(4)	1.988(3)
O(1)-C(1)	1.261(3)	1.262(5)	1.253(5)	1.262(3)
O(2)-C(1)	1.268(3)	1.255(5)	1.244(4)	1.256(3)
O(1)-M(1)-O(2')	109.4(1)	107.5(2)	105.2(1)	102.6(1)
O(1)-M(1)-C(11)	105.6(1)	102.1(2)	102.3(2)	102.6(1)
O(1)-M(1)-C(21)	107.2(1)	106.8(2)	105.0(2)	109.0(1)
O(2')-M(1)-C(11)	104.0(1)	101.8(2)	102.6(2)	103.0(1)
O(2')-M(1)-C(21)	106.0(1)	106.8(2)	107.5(2)	107.4(1)
C(11)-M(1)-C(21)	124.0(1)	130.3(2)	131.7(2)	129.3(1)

carboxylate ligands in these dimeric systems (Table 2.1) are within the range expected for aluminum [1.767(7) – 1.837(6) Å][8] and gallium [1.956(7) – 1.967(8) Å] carboxylates.[8,9,10,11] The carboxylate's O-C bond lengths in each compound are similar [Δ(O-C) ≈ 0.01 Å], indicating a symmetrically bound acid group that is unaffected by the carboxylate organic substituents. The bond lengths and angles within the carboxylate unit are typical of such moieties. The ligand bite distances [M(1)···M(1a) = 4.20 Å (**2.1**), 4.26

Å (**2.2**), 4.39 Å (**2.3**)] are comparable to the ranges previously observed for alkylaluminum (3.26 – 4.18 Å)[12,13] and alkylgallium (4.35 – 4.68 Å)[10] carboxylates.

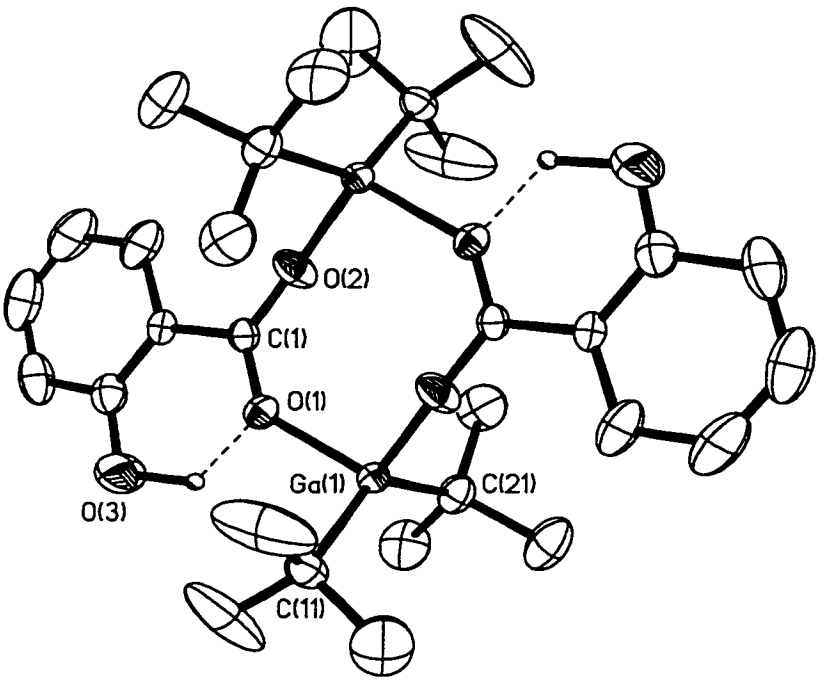

Figure 2.2. Molecular structure of $[(^tBu)_2Ga(\mu\text{-}O_2CC_6H_4\text{-}2\text{-}OH)]_2$ (**2.3**). Thermal ellipsoids are shown at the 30% level, and hydrogen atoms bound to carbon are omitted for clarity. Hydrogen bonding interactions are denoted by a dashed line.

As may be seen from Figures 2.1 and 2.2, the NH_2 in **2.2** and OH in **2.3** are oriented such that hydrogen bonding interaction is possible with one of the carboxylate oxygens, O(1). The N(3)···O(1) distance in compounds **2.1** and **2.2** (2.73 and 2.72 Å, respectively) are longer than observed in the free ligand [2.688(4) and 2.682(7) Å[4]], but shorter than reported for N-H···O=C interactions (*ca.* 2.85 Å).[14] The O(3)···O(1) distance in compound **2.3** (2.627 Å) is the same as in the free ligand (2.620 Å).[3] Thus, based upon these distances it appears that, although the intra-molecular H-bond remains intact, it is not enhanced by the presence of the Group 13 metal as compared to the free ligand.

It has been previously shown that the intra-molecular hydrogen bonding in anthranilic and salicylic acids results in a near-planar geometry of the arene and carboxylate groups (e.g., the maximum deviation from planarity in salicylic acid is 0.028 Å).[3] Similarly, the phenyl substituents on the anthranilate and salicylate ligands in compounds **2.1** - **2.3** are almost coplanar with the carboxylate moiety; O(1)-C(1)-C(2)-C(3) = 2.8° (**2.1**), 9.2° (**2.2**) and 2.9° (**2.3**). We have previously reported the molecular structures of $[(^tBu)_2M(\mu\text{-}O_2CPh)]_2$ in which the equivalent torsion angles are 5.9° and 0.12° for M = Al[8] and Ga,[9] respectively. Clearly, the presence of coplanarity within the anthranilate and salicylate ligands is not in itself an indication of the presence of intra-molecular hydrogen bonding and could be an artifact of intra-molecular steric interactions.

In an effort to ascertain the magnitude of such steric effects, the molecular structure was determined for the *ortho*-toluic acid derivative, $[(^tBu)_2Ga(\mu\text{-}O_2CC_6H_4\text{-}2\text{-}Me)]_2$ (**2.4**) (Eq 2.2) (see Experimental and Table 2.1). As may be seen from Figure 2.3, the aromatic ring is twisted away from co-planarity with the carboxylate group, i.e., O(1)-C(1)-C(2)-C(3) = 42.6°. Thus, if steric factors were dominating in compounds **2.1** - **2.3**, a similar twist would be expected due to the comparable steric bulk of CH_3, NH_2 and OH groups.[15] The planarity of the anthranilate and salicylate ligands is, therefore, a further indication that the orientations of the ligands are due to intra-molecular hydrogen bonding.

$$(^tBu)_3Ga + HO_2CC_6H_4\text{-}2\text{-}Me \longrightarrow [(^tBu)_2Ga(\mu\text{-}O_2CC_6H_4\text{-}2\text{-}Me)]_2 \qquad (2.2)$$

The IR spectra for compounds **2.1** and **2.2**, both in toluene solution and solid state, show the presence of two bands associated with the amine's $\nu_{N\text{-}H}$ stretch (e.g.,

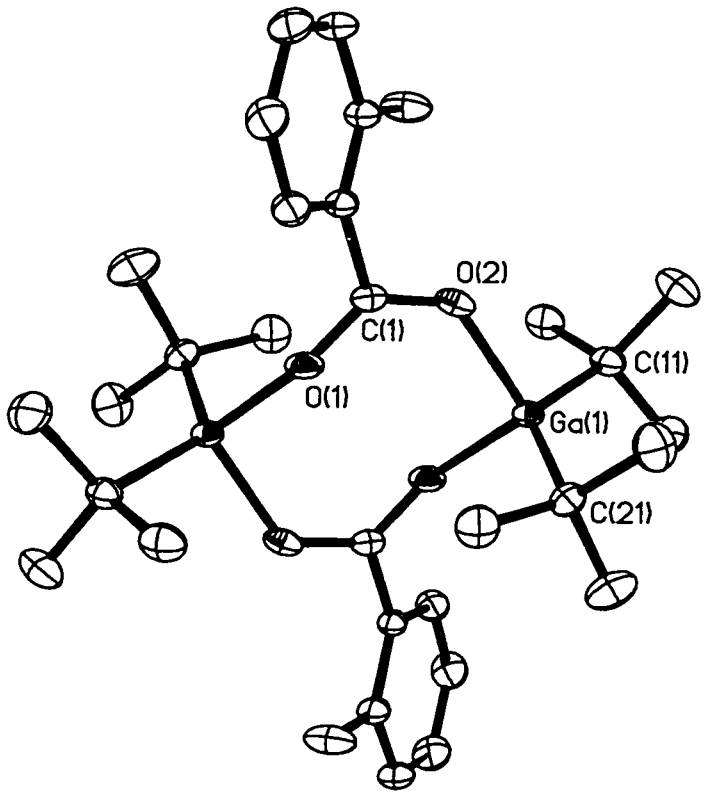

Figure 2.3. Molecular structure of $[(^tBu)_2Ga(\mu\text{-}O_2CC_6H_4\text{-}2\text{-}Me)]_2$ (**2.4**). Thermal ellipsoids are shown at the 30% level, and hydrogen atoms are omitted for clarity.

Figure 2.4a), which is consistent with the retention of N-H···O bonding on the IR time scale. Variable temperature solution ^1H NMR, however, show single broad resonances [δ 5.02 (**2.1**) and 5.11 (**2.2**)], down to -115 °C, indicating facile rotation about the C(3)-N(3) bond. Thus, we can estimate that the lifetime of the intra-molecular N-H···O bonds in compounds **2.1** and **2.2** is between 10^{-5} and 10^{-12} s. In addition, it is worth noting that in the solid state IR spectrum of compound **2.2**, solid state splitting of the $\nu_{N\text{-}H}$ resonances is observed (see Figure 2.4b) with a ν_L of 8 cm^{-1}.

The position of the O-H band in the IR spectra of compound **2.3** (solid and solution) shows intra-molecular hydrogen bonding to be present in both solid state (3298

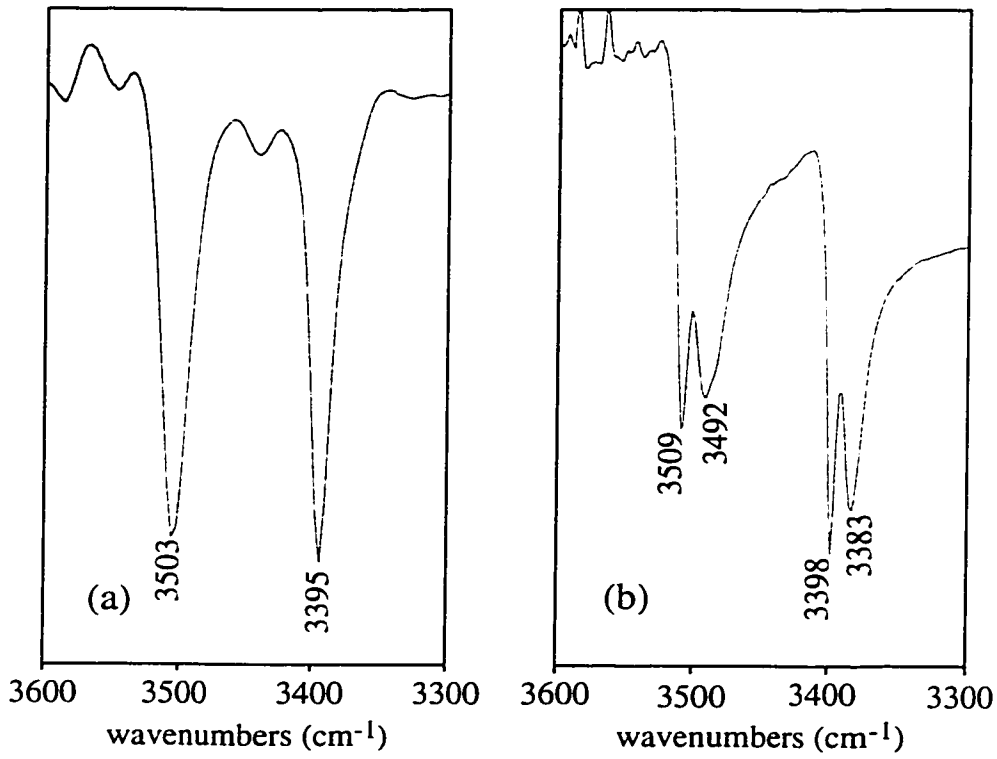

Figure 2.4. IR spectra of $[(^tBu)_2Ga(\mu\text{-}O_2CC_6H_4\text{-}2\text{-}NH_2)]_2$ (**2.2**) in toluene solution (a) and solid state (b), showing the presence of discrete hydrogen bonded and non-hydrogen bonded N-H groups.

cm^{-1}) and solution (3298 cm^{-1}). The ^1H NMR chemical shift of the O-H peak is found to be temperature dependent, suggesting fluxionality on the NMR time scale. However, no asymptote was reached down to -115 °C.

In conclusion, we have found that the intra-molecular hydrogen bonds in the anthranilate and salicylate ligands remain present in the Group 13 compounds. However, complexation of a Group 13 metal to the donor (i.e., O-H···X-M; where X = N, O) does not appear to enhance the strength of the hydrogen bond as it does when complexed to the acceptor (i.e., M-O-H···X). We note, however, that the presence of hydrogen bonding

in the anthranilate complex $[Me_2In(O_2CC_6H_4\text{-}2\text{-}NH_2)]_\infty$,[16] leads to a decrease in the indium coordination number as compared to the acetate complex.[17]

Reaction of $Al(^tBu)_3$ with anthranilic acid in a 2:1 ratio yields the dialuminum compound, $(^tBu)_2Al(\mu\text{-}O_2CC_6H_4\text{-}2\text{-}NH_2)Al(^tBu)_3$ (**2.5**) (Eq. 2.3). The molecular structure of compound **2.5** has been determined by X-ray crystallography (Figure 2.5); selected bond lengths and angles are given in Table 2.2. The Al(2)-O(2) [1.896(2) Å] is slightly longer than Al(1)-O(1) [1.822(2) Å], which is consistent with the difference in bonding to a neutral $Al(^tBu)_3$ versus a cationic $Al(^tBu)_2$ moiety. The Al(1)-N(1) distance [2.003(3) Å] is within the range expected for amine complexes of aluminum (1.94 – 2.10 Å).[18]

$$2\ Al(^tBu)_3 + HO_2CC_6H_4\text{-}2\text{-}NH_2 \longrightarrow (^tBu)_2Al(\mu\text{-}O_2CC_6H_4\text{-}2\text{-}NH_2)Al(^tBu)_3 \quad (2.3)$$

Based upon the isolation of compound **2.5** and its conversion to compound **2.1** during physical grinding (see Experimental), we propose that the formation of compounds **2.1** and **2.2** (and possibly **2.3**) occurs *via* a chelate species, $(^tBu)_2M(O_2CC_6H_4\text{-}2\text{-}X)$ (**VI**).

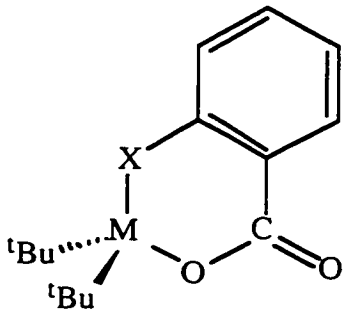

M = Al, X = NH_2; M = Ga, X = OH, NH_2

(VI)

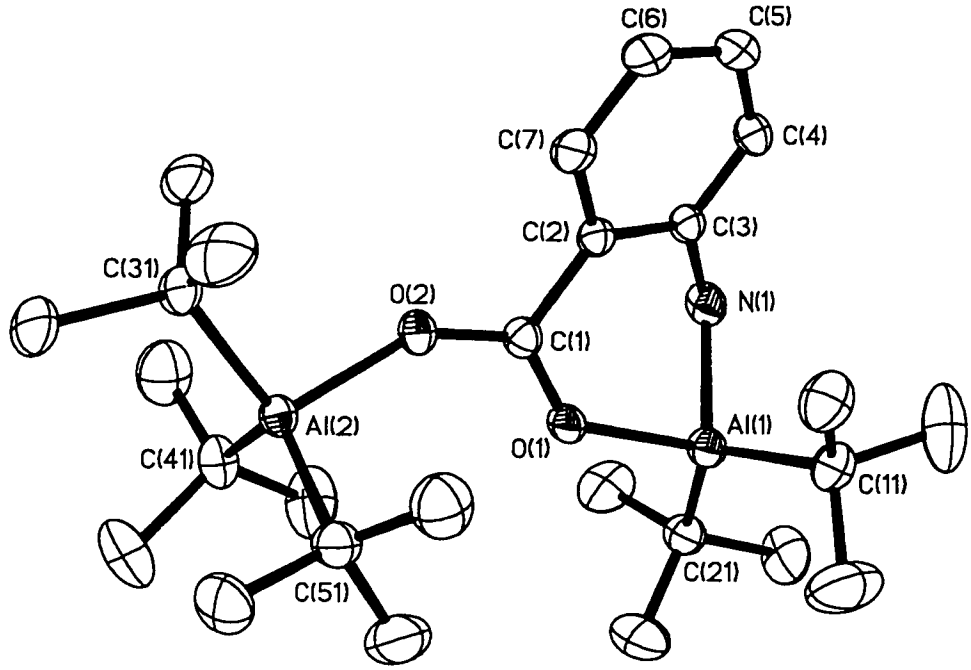

Figure 2.5. Molecular structure of $(^tBu)_2Al(\mu\text{-}O_2CC_6H_4\text{-}2\text{-}NH_2)Al(^tBu)_3$ (**2.5**). Thermal ellipsoids are shown at the 30% level, and hydrogen atoms are omitted for clarity.

The related chelate complexes **VII**[19] and **VIII**[20] have been reported in which the **VI**-like structure is stabilized by an extended hydrogen bond network rather than Lewis acid-base interaction, as we observe in compound **2.5**.

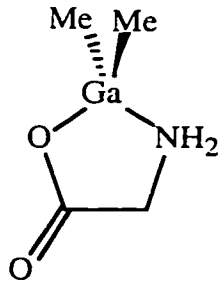

(VII)

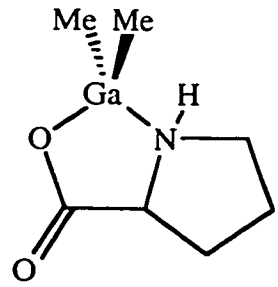

(VIII)

Table 2.2. Selected bond lengths (Å) and angles (°) for $(^tBu)_2Al(\mu\text{-}O_2CC_6H_4\text{-}2\text{-}NH_2)Al(^tBu)_3$ (**2.5**).

Al(1)-O(1)	1.822(2)	Al(1)-N(1)	2.003(3)
Al(1)-C(11)	1.960(4)	Al(1)-C(21)	1.958(3)
Al(2)-O(2)	1.896(2)	Al(2)-C(31)	2.021(3)
Al(2)-C(41)	2.005(4)	Al(2)-C(51)	2.001(3)
O(1)-C(1)	1.270(3)	O(2)-C(1)	1.250(3)
O(1)-Al(1)-N(1)	89.1(1)	O(1)-Al(1)-C(11)	113.1(1)
O(1)-Al(1)-C(21)	108.9(1)	N(1)-Al(1)-C(11)	108.6(1)
N(1)-Al(1)-C(21)	107.8(1)	C(11)-Al(1)-C(21)	123.7(2)
O(2)-Al(2)-C(31)	98.3(1)	O(2)-Al(2)-C(41)	106.0(1)
O(2)-Al(2)-C(51)	104.6(1)	C(31)-Al(2)-C(41)	115.0(2)
C(31)-Al(2)-C(51)	114.9(2)	C(41)-Al(2)-C(51)	115.4(2)

We have previously demonstrated that, although the chelate binding (**IX**) of a carboxylate to aluminum (or gallium) is highly disfavored (*ca.* 130 $kJ.mol^{-1}$) as compared to bridging (**X**), it is favored (*ca.* 75 $kJ.mol^{-1}$) over the monodentate modes [i.e., *eclipsed* and *staggered* (**XI**)].[8] In the present case, the Lewis base substituents (OH or NH_2) in the *ortho* position on the phenyl ring provide an alternative stabilization to the monomeric derivatives. The stability of **VI** will be dependent on the strength of the M-X interaction. Based upon known Lewis acid-base bond strength for aluminum alkyls, the interaction is expected to be *ca.* 80 $kJ.mol^{-1}$ for X = OH and *ca.* 125 $kJ.mol^{-1}$ for X = NH_2. The greater stability of the anthranilate complex (**VI** where X = NH_2) presumably is such to allow **VI** to be"trapped" by the presence of an excess of $Al(^tBu)_3$ and thus forming compound **2.5**. In contrast, the similarity in stabilization for salicilate between

the chelate carboxylate (**IX**) and chelation *via* the hydroxide (**VI** where X = OH), as well as the greater acidity of the hydroxide, may explain the observation that a complex mixture of products is obtained with the reaction of salicylic acid with either an equimolar equivalent or excess of $Al(^tBu)_3$.

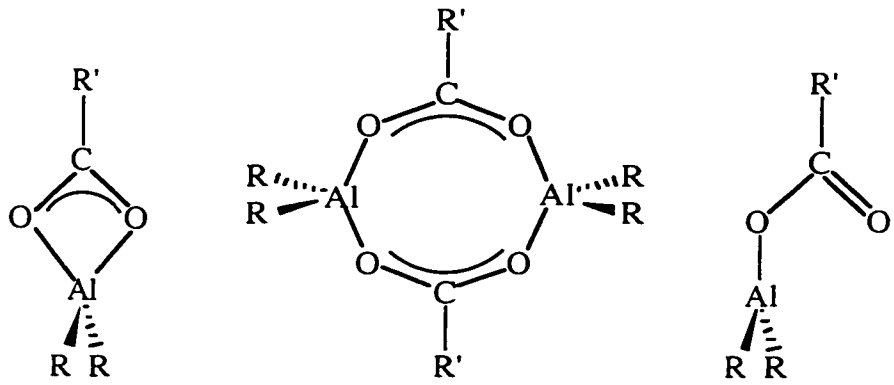

(IX) **(X)** **(XI)**

Conclusions

Reaction of $M(^tBu)_3$ with anthranilic, salicylic, and *ortho*-toluic acids yields $[(^tBu)_2M(\mu\text{-}O_2CC_6H_4\text{-}2\text{-}NH_2)]_2$, M = Al (**2.1**), Ga (**2.2**), $[(^tBu)_2Ga(\mu\text{-}O_2CC_6H_4\text{-}2\text{-}OH)]_2$ (**2.3**), and $[(^tBu)_2Ga(\mu\text{-}O_2CC_6H_4\text{-}2\text{-}Me)]_2$ (**2.4**), respectively. Reaction of anthranilic acid with two equivalents of $Al(^tBu)_3$ allows for the isolation of $(^tBu)_2Al(\mu\text{-}O_2CC_6H_4\text{-}2\text{-}NH_2)Al(^tBu)_3$ (**2.5**). Compounds **2.1** – **2.5** have been characterized by NMR and IR spectroscopy, mass spectrometry, and X-ray crystallography. Intra-molecular hydrogen bonding, found in the anthranilate and salicylate ligands, remains present in the Group 13 compounds but is not enhanced.

Experimental Section

General experimental procedures were carried out as described in Chapter 1. Due to the partial conversion of compound **2.5** to compound **2.1** upon mechanical grinding

required for KBr sample preparation, the IR spectrum of compound **2.5** was determined by a computer subtraction of a reference spectrum of compound **2.1**. NMR spectra were obtained on Bruker AM-250 and Avance 400 spectrometers using d_8-toluene solutions. The synthesis of $Al(^tBu)_3$ and $Ga(^tBu)_3$ were performed according to literature methods.[21,22] Salicylic, anthranilic, and *ortho*-toluic acids were obtained from Aldrich and used without further purification.

$[(^tBu)_2Al(\mu\text{-}O_2CC_6H_4\text{-}2\text{-}NH_2)]_2$ (2.1). To a toluene (40 mL) slurry of anthranilic acid (0.693 g, 5.05 mmol) at –78 °C was added $Al(^tBu)_3$ (1.0 g, 5.05 mmol). The yellow reaction mixture was allowed to warm to room temperature and then to stir for three hours. The solution was filtered and placed in a freezer, yielding yellow crystals. Yield: 70%. Mp: 170 °C (dec.). Anal. (%, calc.): C, 64.9 (64.9); H, 8.58 (8.72); N, 4.29 (5.05). MS (EI, %): *m/z* 497 ($2\ M^+ - {}^tBu$, 35), 439 ($2\ M^+ - 2\ {}^tBu - H$, 52), 277 (M^+, 10), 220 ($M^+ - {}^tBu$, 35), 120 ($O_2CC_6H_4$, 30). IR (cm^{-1}): 3513 (w), 3411 (w), 1629 (m), 1577 (m), 1545 (m), 1419 (w), 1301 (w), 1163 (w), 1010 (w), 973 (w), 722 (w), 543 (s). ^1H NMR: δ 8.19 [2H, dd, J(H-H) = 9.1 Hz, J(H-H) = 1.7 Hz, 6-CH], 6.92 [2H, ddd, J(H-H) = 8.4 Hz, J(H-H) = 7.2 Hz, J(H-H) = 1.5 Hz, 4-CH], 6.44 [2H, ddd, J(H-H) = 8.2 Hz, J(H-H) = 7.0 Hz, J(H-H) = 1.1 Hz, 5-CH], 6.03 [2H, dd, J(H-H) = 8.6 Hz, J(H-H) = 0.9 Hz, 3-CH], 5.02 (2H, s, NH_2), 1.20 [36H, s, $C(CH_3)_3$]. ^{13}C NMR: δ 175.4 (O_2C), 152.5 (1-C), 133.6 (2-C), 121.5 (6-CH), 117.8 (4-CH), 117.2 (5-CH), 109.8 (3-CH), 30.3 [$C(CH_3)_3$].

$[(^tBu)_2Ga(\mu\text{-}O_2CC_6H_4\text{-}2\text{-}NH_2)]_2$ (2.2). Prepared in the same manner as **2.1**, but using anthranilic acid (1.93 g, 7.03 mmol) and $Ga(^tBu)_3$ (3.40 g, 7.03 mmol). Yield: 60%. Mp: 243 °C (dc). Anal. (%, calc.): C, 55.8 (56.3); H, 7.53 (7.56); N, 3.67 (4.38).

MS (EI): *m/z* 319 (M^+, 10), 262 ($M^+ - {}^tBu$, 50), 205 ($M^+ - 2\ {}^tBu$, 12), 120 ($O_2CC_6H_4$, 100), 92 ($C_6H_4NH_2$, 15), 69 (Ga, 25), 57 (^tBu, 85). IR (cm^{-1}): 3509 (m), 3492 (m), 3398 (m), 3383 (m), 1623 (s), 1580 (s), 1536 (s), 1305 (s), 1255 (s), 1163 (m), 1020 (w), 985 (w), 825 (w), 499 (s). ^1H NMR: δ 8.25 [2H, dd, J(H-H) = 8.1 Hz, J(H-H) = 1.5 Hz, 6-CH], 6.99 [2H, ddd, J(H-H) = 8.4 Hz, J(H-H) = 6.9 Hz, J(H-H) = 1.6 Hz, 4-CH], 6.54 [2H, ddd, J(H-H) = 8.1 Hz, J(H-H) = 7.1 Hz, J(H-H) = 1.0 Hz, 5-CH], 6.15 [2H, dd, J(H-H) = 8.3 Hz, J(H-H) = 0.7 Hz, 3-CH], 5.11 (4H, s, NH_2), 1.27 [36H, s, $C(CH_3)_3$]. ^{13}C NMR: δ 179.7 (O_2C), 151.3 (1-C), 135.3 (2-C), 133.3 (6-CH), 117.4 (4-CH), 116.8 (5-CH), 113.2 (3-CH), 30.3 (CH_3), 25.0 [$C(CH_3)_3$].

$[(^tBu)_2Ga(\mu\text{-}O_2CC_6H_4\text{-}2\text{-}OH)]_2$ (2.3). Prepared in the same manner as **2.1**, but using salicylic acid (1.12 g, 4.04 mmol) and $Ga(^tBu)_3$ (1.95 g, 4.04 mmol). Yield: 50%. Mp: 150 °C (dec). Anal. (%, calc.): C, 55.6 (56.1); H, 6.96 (7.22). MS (EI): *m/z* 320 (M^+, 10), 263 ($M^+ - {}^tBu$, 38), 206 ($M^+ - 2\ {}^tBu$, 10), 189 [$Ga(O_2CC_6H_4)$, 72], 69 (Ga, 28), 57 (^tBu, 100). IR (cm^{-1}): 3324 (w), 3180 (w), 3078 (w), 1613 (s), 1567 (w), 1526 (w), 1398 (s), 1250 (s), 1165 (w), 1147 (m), 1034 (w), 896 (w), 866 (w), 850 (w), 825 (w), 758 (m), 712 (w), 681 (w), 543 (s). ^1H NMR: δ 10.26 (2H, s, OH), 8.04 [2H, d, J(H-H) = 6.6 Hz, 6-CH], 7.03 [2H, t, J(H-H) = 8.4 Hz, 4-CH], 6.90 [2H, d, J(H-H) = 8.2 Hz, 3-CH], 6.60 [2H, t, J(H-H) = 6.5 Hz, 5-CH], 1.19 [36H, s, $C(CH_3)_3$]. ^{13}C NMR: δ 178.2 (O_2C), 168.3 (1-C), 138.0 (2-C), 133.5 (6-CH), 123.1 (4-CH), 118.1 (3-CH), 112.9 (5-CH), 24.8 [$C(CH_3)_3$], 21.0 [$C(CH_3)_3$].

$[(^tBu)_2Ga(\mu\text{-}O_2CC_6H_4\text{-}2\text{-}Me)]_2$ (2.4). To a hexane (30 mL) slurry of *o*-toluic acid (0.565 g, 4.15 mmol) at –78 °C was added $Ga(^tBu)_3$ (1.0 g, 4.15 mmol). The clear reaction mixture was allowed to warm to room temperature and then to stir for three hours. The solution was filtered and placed in a freezer, yielding colorless crystals. Yield: 75%. Mp: 160 °C. Anal. (%, calc.): C, 60.2 (60.2); H, 7.69 (7.90). MS (EI, %): *m/z* 205 ($M^+ - 2\ ^tBu + H$, 30), 91 (C_6H_4Me, 10), 69 (Ga, 40), 57 (^tBu, 100). IR (cm^{-1}): 3336 (w), 3168 (w), 3075 (w), 2730 (w), 2350 (w), 1605 (w), 1585 (m), 1561 (m), 1457 (s), 1413 (m), 1373 (m), 1299 (w), 1166 (w), 1102 (w), 1018 (w), 939 (w), 855 (w), 821 (w), 747 (w), 668 (w). ^1H NMR: δ 8.27 [2H, dd, J(H-H) = 7.6 Hz, J(H-H) = 1.5 Hz, 6-CH], 7.03 [2H, ddd, J(H-H) = 7.4 Hz, J(H-H) = 7.4 Hz, J(H-H) = 1.6 Hz, 4-CH], 6.98 [2H, ddd, J(H-H) = 7.6 Hz, J(H-H) = 7.4 Hz, J(H-H) = 1.7 Hz, 5-CH], 6.91 [2H, dd, J(H-H) = 7.4 Hz, J(H-H) = 0.9 Hz, 3-CH], 2.67 (6H, s, CH_3), 1.26 [36H, s, $C(CH_3)_3$]. ^{13}C NMR: δ 179.7 (O_2C), 140.6 (2-C), 132.9 (4-CH), 132.4 (1-C), 132.1 (6-CH), 128.0 (3-CH), 126.2 (5-CH), 30.2 [$C(CH_3)_3$], 24.9[$C(CH_3)_3$], 23.2 (CH_3).

$(^tBu)_2Al(\mu\text{-}O_2CC_6H_4\text{-}2\text{-}NH_2)Al(^tBu)_3$ (2.5). To a toluene (40 mL) solution of anthranilic acid (0.277 g, 2.0 mmol) at –78 °C was added $Al(^tBu)_3$ (0.8 g, 4.0 mmol). The orange reaction mixture was allowed to warm to room temperature and then to stir for three hours. The solution was filtered and placed in a freezer, yielding yellow crystals. Mechanical grinding of a sample resulted in its slow conversion to compound **2.1** and $Al(^tBu)_3$ as confirmed by ^1H NMR spectroscopy. Yield: 65%. Mp: 80 °C. MS (EI): *m/z* 475 (M^+, 35), 418 ($M^+ - {}^tBu$, 55), 361 ($M^+ - 2\ ^tBu$, 100), 277 [$M^+ - Al(^tBu)_3$, 10]. IR (cm^{-1}): 3513 (w), 3416 (w), 2724 (w), 2366 (w), 2325 (w), 1629 (m), 1577 (m), 1552 (m), 1470 (s), 1413 (m), 1378 (s), 1306 (m), 1255 (m), 1163 (w), 825 (w), 753 (w), 676

Table 2.3. Summary of X-ray diffraction data.

Compound	$[(^tBu)_2Al(\mu\text{-}O_2CC_6H_4\text{-}2\text{-}NH_2)]_2$ (**2.1**)	$[(^tBu)_2Ga(\mu\text{-}O_2CC_6H_4\text{-}2\text{-}NH_2)]_2$ (**2.2**)
empir. formula	$C_{30}H_{48}Al_2N_2O_4$	$C_{30}H_{48}Ga_2N_2O_4$
Formula weight	554.68	640.17
cryst system	monoclinic	monoclinic
space group	$P2_1/c$	$P2_1/c$
a, Å	9.411(2)	8.927(2)
b, Å	16.601(3)	12.645(3)
c, Å	10.923(2)	14.662(3)
α, deg		
β, deg	106.58(3)	101.17(3)
γ, deg		
V, Å^3	1635.6(5)	1623.7(6)
Z	2	2
μ, cm^{-1}	1.22	1.693
temp, K	293	298
no. collected	7257	7171
no. ind	3717	2321
no. obsd	3717	1833 ($\|Fo\| > 4.0\sigma\|Fo\|$)
weighting scheme SHELXTL		0.1017, 0.0834
R	0.0816	0.0496
R_w	0.2280	0.136
largest diff peak, eÅ^{-3}	0.78	1.80

Table 2.3, contd.

Compound	$[(^tBu)_2Ga(\mu\text{-}O_2CC_6H_4\text{-}2\text{-}OH)]_2$ (**2.3**)	$[(^tBu)_2Ga(\mu\text{-}O_2CC_6H_4\text{-}2\text{-}Me)]_2$ (**2.4**)
empir. formula	$C_{30}H_{46}Ga_2O_6$	$C_{32}H_{50}Ga_2O_4$
Formula weight	642.14	638.19
cryst system	monoclinic	triclinic
space group	$P2_1/c$	$P\bar{1}$
a, Å	8.984(2)	8.601(2)
b, Å	17.028(3)	10.433(2)
c, Å	11.064(2)	11.225(2)
α, deg		101.40(3)
β, deg	103.35(3)	110.76(3)
γ, deg		108.61(3)
V, $Å^3$	1646.8(6)	835.9(3)
Z	2	1
μ, cm^{-1}	1.67	1.64
temp, K	298	298
no. collected	7307	3821
no. ind	2372	2392
no. obsd	1806 ($\|Fo\| > 6.0\sigma\|Fo\|$)	2194 ($\|Fo\| > 6.0\sigma\|Fo\|$)
weighting scheme SHELXTL	0.067, 0	0.0625, 0
R	0.0397	0.0348
R_w	0.1032	0.0918
largest diff peak, $eÅ^{-3}$	0.50	0.87

Table 2.3, contd.

Compound	$(^tBu)_2Al(\mu\text{-}O_2CC_6H_4\text{-}2\text{-}NH_2)Al(^tBu)_3$ (**2.5**).
empir. formula	$C_{34}H_{59}Al_2NO_2$
Formula weight	567.81
cryst system	monoclinic
space group	$P2_1/n$
a, Å	9.008(2)
b, Å	19.590(4)
c, Å	21.077(4)
α, deg	
β, deg	93.33(3)
γ, deg	
V, Å3	3713.0(1)
Z	4
μ, cm-1	1.10
temp, K	298
no. collected	16880
no. ind	5321
no. obsd	3006 ($\|Fo\| > 6.0\sigma\|Fo\|$)
weighting scheme SHELXTL	0.10, 0
R	0.0591
R_w	0.1496
largest diff peak, eÅ^{-3}	0.24

(w). ^{1}H NMR: δ 8.33 (1H, m, 3-C<u>H</u>), 6.64 (2H, m, 6-C<u>H</u> and 4-C<u>H</u>), 5.61 (1H, m, 5-C<u>H</u>), 1.60 [27H, s, C(C<u>H</u>$_3$)$_3$], 0.84 [18H, s, C(C<u>H</u>$_3$)$_3$]. ^{13}C NMR: δ 170.2 (O_2<u>C</u>), 135.8 (1-<u>C</u>), 134.9 (2-<u>C</u>), 134.6 (4-<u>C</u>H), 133.9 (6-<u>C</u>H), 126.2 (3-<u>C</u>H), 124.4 (5-<u>C</u>H), 34.0 [<u>C</u>(CH$_3$)$_3$], 30.8 [<u>C</u>(CH$_3$)$_3$] 29.8 [C(<u>C</u>H$_3$)$_3$], 24.9 [C(<u>C</u>H$_3$)$_3$].

Crystallographic Studies. Crystals of all compounds were sealed in glass capillaries under argon. A summary of cell parameters, data collections, and structure solutions is given in Table 2.3. Data were collected on either a NONIUS KappaCCD system (Institute of Physical Chemistry of the Polish Academy of Sciences) or a Bruker CCD SMART system, equipped with graphite monochromated Mo-K_α radiation (λ = 0.71073 Å).[23]

References

1 C. N. McMahon, S. G. Bott, and A. R. Barron, *J. Chem. Soc., Dalton Trans.*, 1997, 3129.

2 A. Keys, T. Barbarich, S. G. Bott, and A. R. Barron, *J. Chem. Soc., Dalton Trans.*, 2000, 577.

3 M. Sundaralingam and L. H. Jensen, *Acta Cryst.* 1965, **18**, 1053.

4 (a) C. D. G. Boone, J. L. Derissen, and J. C. Schoone, *Acta Cryst.* 1977, **B33**, 3205.

(b) H. Takazawa, S. Ohba, and Y. Saito, *Acta Cryst.* 1986, **C42**, 1880.

5 J. Lewinski, J. Zachara, and I. Justyniak, *Inorg. Chem.*, 1998, **37**, 2575.

6 J. Lewinski, J. Zachara, and I. Justyniak, *Organometallics*, 1997, **16**, 3859.

7 (a) J. Weidlein, *Z.Anorg. Allgem. Chem.*, 1970, **378**, 245.

(b) A. Pietrzykowski, S. Pasynkiewicz, and J. Poplawska, *Main Group Metal Chem.*, 1996, **18**, 651.

(c) G. S. Kolesnikov, S. L. Davidova, M. A. Yampolskaya, and N. V. Klimentova, *Bull. Acad. Sci. USSR Engl. Transl.*, 1962, 783.

(d) L. J. Zakharkin, G. S. Kolesnikov, S. L. Davidova, V. V. Gavrilenko, A. A. Kamyshova, *Bull. Acad. Sci. USSR Engl. Transl.*, 1961, 336.

(e) G. V. Zenina, N. I. Sheverdina, and K. A., Kocheskov, *Proc. Acad. Sci. USSR Engl. Trans.* 1970, **195**, 786.

8 C. E. Bethley, C. L. Aitken, Y. Koide, C. J. Harlan, S. G. Bott, and A. R. Barron, *Organometallics*, 1997, **16**, 329.

9 A. Keys, S. G. Bott, and A. R. Barron, *Polyhedron*, 1998, **17**, 3121.

10 H. D. Hausen, K. Sille, J. Weidlein, and W. Schwarz, *J. Organomet. Chem.*, 1978, **160**, 411.

11 M. J. Zaworotko, R. D. Rogers, and J. L. Atwood, *Organometallics*, 1982, **1**, 1179.

12 Y. Koide, S. G. Bott, and A. R. Barron, *Organometallics*, 1996, **15**, 2213.

13 P. Sobota, M. O. Mustafa, J. Utko, and T. Lis, *J. Chem. Soc., Dalton Trans.*, 1990, 1809.

14 R. Taylor and O. Kennard, *Acta Crystallogr., Sect. B*, 1983, **B39**, 133.

15 L. E. Manzer and C. A. Tolman, *J. Am. Chem. Soc.*, 1975, **97**, 1955.

16 J. Lewinski, I. Justyniak, and J. Lipkowski, *Inorg. Chem. Commun.*, in press.

17 (a) H. D. Hausen, *J. Organomet. Chem.*, 1972, **39**, C37.

(b) F. W. B. Einstein, M. M. Gilbert, and D. G. Tuck, *J. Chem. Soc. A*, 1973, 248.

(c) S. J. Lin, T. N. Hong, J. Y. Tung, and J. H. Chen, *Inorg. Chem.*, 1998, **37**,

2575.

18 See, for example, (a) K. M. Nykerk and D. P. Eyman, *Inorg. Chem.*, 1967, **6**, 1461.

(b) G. H. Robinson, H. Zhang and J. L. Atwood, *J. Organomet. Chem.*, 1987, **331**, 153.

(c) D. W. Goebel, J. L. Hencher, and J. P.Oliver, *Organometallics,* 1983, **2**, 746.

(d) A. Almennigen, G. Gundersen, T. Haugen, and A. Haaland, *Acta Chem. Scand.*, 1972, **26**, 3928.

(e) J. L. Atwood, S. K. Seale, and D. H. Roberts, *J. Organomet. Chem.*, 1973, **51**, 105.

19 S. J. Rettig, A. Storr, and J. Trotter, *Can. J. Chem.*, 1987, **65**, 1349.

20 K. R. Breakell, S. J. Rettig, A. Storr, and J. Trotter, *Can. J. Chem.*, 1977, **55**, 4174.

21 (a) R. A. Kovar, H. Derr, D. Brandau, and J. O. Callaway, *Inorg. Chem.*, 1975, **14**, 2809.

(b) H. -U. Schwering, E. Jungk, and J. Weidlein, *J. Organomet. Chem.*, 1975, **91**, C47.

22 (a) W. Uhl, *Z. Anorg. Allg. Chem.*, 1989, **570**, 37.

(b) H. Lehmkuhl, O. Olbrysch, and H. Nehl, *Liebigs Ann. Chem.*, 1973, 708.

(c) H. Lehmkuhl and O. Olbrysch, *Liebigs Ann. Chem.*, 1973, 715.

23 C. S. Branch, J. Lewinski, I. Justyniak, S. G. Bott, J. Lipkowski, and A. R. Barron, *J. Chem. Soc., Dalton Trans.*, 2001, 1253.

Chapter 3

Arene-Mercury Complexes Stabilized by Gallium Chloride: Relative Rates of H/D and Arene Exchange

Introduction

Recent work in the Barron group has reported that the reaction of $HgCl_2$ with two equivalents of MCl_3 (M = Al, Ga) in an aromatic solvent yields $Hg(arene)_2(MCl_4)_2$ where arene = C_6H_5Me, C_6H_5Et, *o*-$C_6H_4Me_2$, and C_6H_3-1,2,3-Me_3.[1,2] In the solid state, these compounds exist as either neutral complexes in which two arenes are bound to the mercury and the MCl_3 groups are bound through bridging chlorides to the mercury (**I**) or as a cation-anion pair (**II**). In solution, however, all the complexes exist in their neutral form.[2]

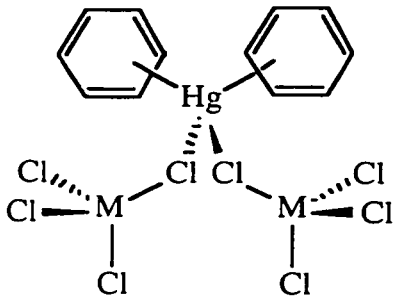

(**I**)

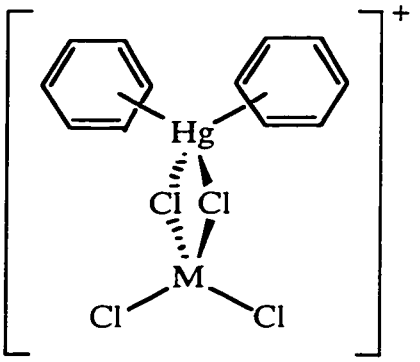

(**II**)

Dissolution of $Hg(arene)_2(MCl_4)_2$ in C_6D_6 results in a rapid H/D exchange and the formation of the appropriate d_n-arene and C_6D_5H.[3] The H/D exchange reaction was found to be catalytic with respect to $Hg(arene)_2(MCl_4)_2$ and independent of the initial

arene ligand. The rate of these exchange reactions is unexpectedly fast, given that they are carried out *in an aprotic solvent and without a Brönsted acid.*[4]

The majority of H/D exchange reactions are carried out under acid catalyzed conditions. The addition of water or a mineral acid can significantly enhance the rate of exchange between C_6D_6 and HO_2CCF_3,[5] whereas the addition of an aprotic Lewis acid reduces the rate of exchange.[6] H/D exchange reactions for aromatic compounds are also known to occur in the presence of transition metal catalysts. For example, H/D exchange between heavy water and aromatic hydrocarbons is homogeneously catalyzed by $[PtCl_4]^{2-}$ salts.[7] Recently Calderazzo *et al.*[8] have reported H/D exchange of the ring protons between C_6D_6 and $C_6H_{6-n}Me_n$ promoted by titanium(IV)–arene complexes. Gaseous deuterium can be exchanged with C_6H_6 if tantalum (Cp_2TaH_3) or iridium [$(PhEt_2P)_2IrH_5$] hydrides are used as catalysts.[9]

Based upon DFT calculations,[10] we have proposed that the reaction pathway for arene H/D exchange involves the protonation of benzene by $Hg(C_6H_6)_2(MCl_4)_2$ and the formation of a Wheland intermediate, Eq. 3.1.

$$Hg(C_6H_6)_2(MCl_4)_2 + C_6D_6 \longrightarrow [HgPh(C_6H_6)(MCl_4)_2]^- + [C_6D_6H]^+ \quad (3.1)$$

Furthermore, we proposed that the coordination of the arene to the mercury/Group 13 complex results in a significant increase in the acidity of the aromatic hydrogens,[11] sufficient to cause the coordinated arene to act as the acid in a typical electrophilic aromatic substitution reaction.

In order to confirm that the mechanism of H/D exchange catalyzed by $Hg(arene)_2(MCl_4)_2$ involves an electrophilic aromatic substitution reaction, we have investigated the kinetics of the H/D exchange reaction. In particular, we are interested in

comparing the site preference of the reaction in comparison with a well characterized electrophilic aromatic substitution reaction.[12]

Naphthalene undergoes a number of usual electrophilic aromatic substitution reactions such as nitration, halogenation, sulfonation and Friedel-Crafts acylation. Although the exact ratio of products is dependent on the reactants and the reaction conditions, the 1-position is the more reactive (e.g., Eq. 3.2).[13,14] If arene H/D exchange catalyzed by $Hg(C_6H_6)_2(MCl_4)_2$ involves an electrophilic aromatic substitution reaction, a similar site preference should be observed for the H/D exchange between C_6D_6 and naphthalene. The results of this study are presented herein.

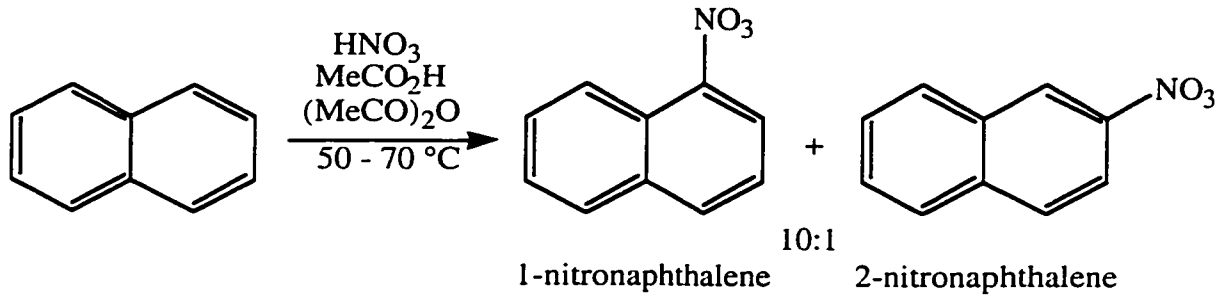

(3.2)

Results and Discussion

Reaction of naphthalene ($C_{10}H_8$) with excess C_6D_6 in the presence of a catalytic quantity of $Hg(C_6H_5Me)_2(GaCl_4)_2$ results in the formation of $C_{10}D_8$ and C_6D_5H. The presence of octadeuterionaphthalene ($C_{10}D_8$) is confirmed by ^{13}C NMR spectroscopy and MS (see Experimental).

We have studied the kinetics of the $Hg(C_6H_5Me)_2(GaCl_4)_2$ catalyzed reaction of C_6D_6 with naphthalene. Even though the catalytic exchange involves C_6D_6 and $C_{10}H_8$, we employed $Hg(C_6H_5Me)_2(GaCl_4)_2$ as a source of $Hg(C_6H_6)_2(GaCl_4)_2$, rather than $Hg(C_6H_6)_2(GaCl_4)_2$ directly. This is because the toluene complex may be isolated as a

solid, while the benzene complex forms a liquid clathrate. We have previously shown that the identity of the initial arene complex is unimportant with regard to the product distribution of the H/D exchange. We proposed that this was due to the facile ligand exchange between toluene and benzene, resulting in the formation of $Hg(C_6H_6)_2(GaCl_4)_2$ *in situ*. This assumption is confirmed by the present study (see below).

In a typical experiment 0.78 mmol of naphthalene is dissolved in 1 mL of C_6D_6. To this is added *ca.* 3 μmol of $Hg(C_6H_5Me)_2(GaCl_4)_2$. These quantities enable ^1H NMR measurements to be made over *ca.* 3 - 12 hours for runs between 20 and 65 °C, and allow us to overcome the errors that occur when initial rates are measured at temperatures different from ambient. We note that only H/D exchange reactions may be followed by ^1H NMR spectroscopy: degenerate H/H and D/D exchanges are not observed. Furthermore, retrogressive H/D exchanges (i.e., between two naphthalene molecules) should not be significant during the early stages of the reaction and in the presence of a large excess of C_6D_6. The rate of loss of naphthalene C-H groups (and thus concurrent formation of naphthalene C-D groups) may be followed by ^1H NMR.

Separate first order observed rate constants, k_{obs} (Eq. 3.3), were calculated from the corresponding plot of $-\ln[C\text{-}H_n]$ versus time for the 1- and 2-positions on naphthalene (e.g., Figure 3.1) where $[C\text{-}H_n]$ is the concentration of the hydrogen atoms at the n-position on naphthalene (**III**).

$$-d[C\text{-}H_n]/dt = k_{obs}[C\text{-}H_n] \qquad (3.3)$$

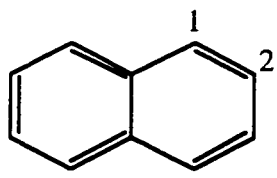

(III)

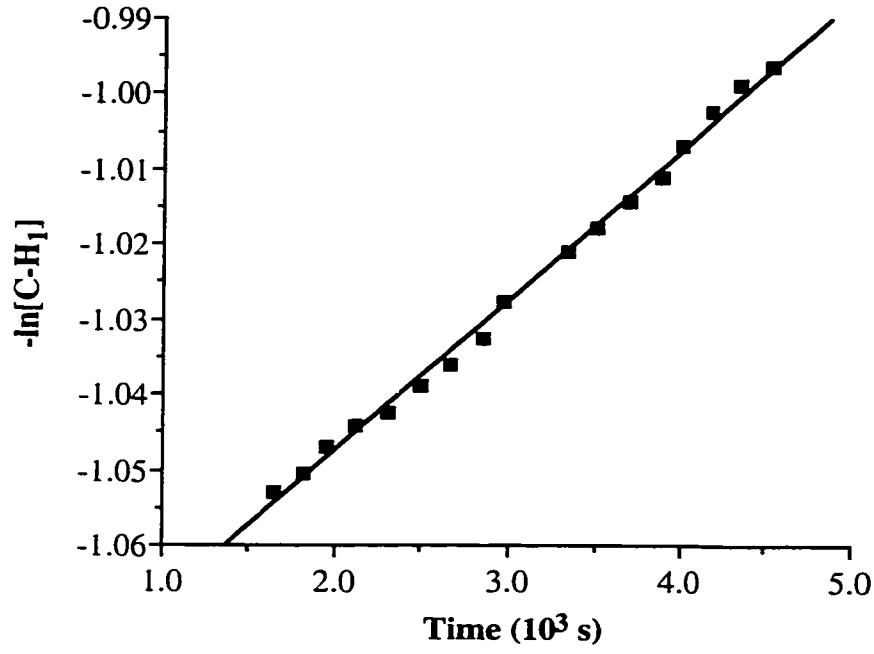

Figure 3.1. Representative plot of $-\ln[C\text{-}H_1]$ versus time (s) for the $Hg(arene)_2(GaCl_4)_2$ catalyzed H/D exchange between C_6D_6 and $C_{10}H_8$ at 308 K ($R = 0.991$).

A plot of k_{obs} versus the concentration of the catalyst, $[Hg(C_6H_5Me)_2(GaCl_4)_2]$, shows a linear dependence (e.g., Figure 3.2), indicating that the rate of H/D exchange is first order with respect to the substrate and catalyst. An overall rate equation may be described for the initial phase of the H/D exchanges (Eq. 3.4).[15,16,17]

$$\text{rate H/D exchange} = k_{1i}[Hg][C\text{-}H_1] + k_{2i}[Hg][C\text{-}H_2] \qquad (3.4)$$

Measurement of the temperature dependence for k_{1i} and k_{2i} (Figure 3.3) allows for the determination of $\Delta H^{\ddagger}$ and $\Delta S^{\ddagger}$, see Table 3.1. The large positive value of $\Delta S^{\ddagger}$ at each position is indicative of a dissociative reaction.[18]

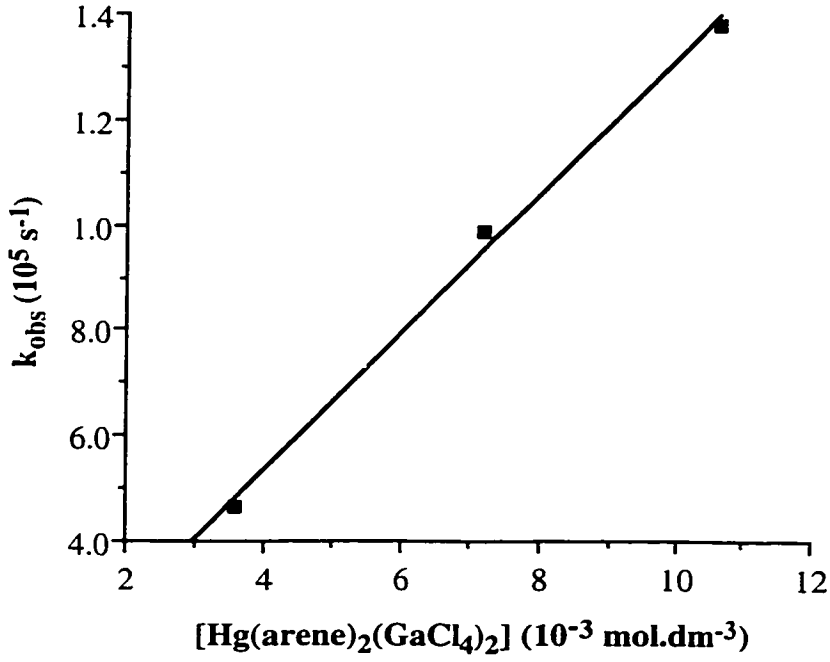

Figure 3.2. Plot of k_{obs} versus catalyst concentration for the $Hg(arene)_2(GaCl_4)_2$ catalyzed H/D exchange between C_6D_6 and $C_{10}H_8$ at 298 K (R = 0.997).

Table 3.1. Summary of activation enthalpy and entropy for the $Hg(C_6H_5Me)_2(GaCl_4)_2$ catalyzed H/D exchange reaction.[a]

	Naphthalene substituent	k_n @ 338 K (10^{-2} mol^{-1}dm^{3}s^{-1})	$\Delta H^{\ddagger}$ (kJ.mol^{-1})	$\Delta S^{\ddagger}$ (J.K^{-1}mol^{-1})
Initial reaction	1	7.5(3)	77(1)	158(5)
	2	2.9(1)	110(10)	250(20)
Final reaction	1	9.5(4)	61(2)	114(6)
	2	8.7(3)	63(5)	120(10)

[a] Esd's given in parentheses.

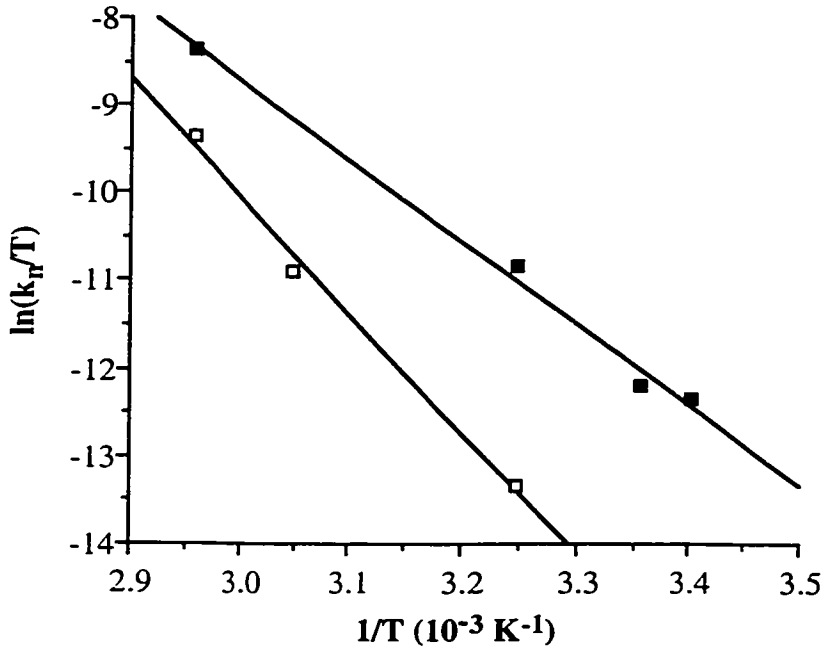

Figure 3.3. An Eyring plot of $\ln(k_1/T)$ versus 1/T for the initial $Hg(arene)_2(GaCl_4)_2$ catalyzed H/D exchange between C_6D_6 and $C_{10}H_8$: 1-position (■, R = 0.993) and the 2-position (□, R = 0.993).

The initial H/D exchange with the 2-position is sufficiently slow at 25 °C under the conditions studied that it is not possible to measure the rate. Above 35 °C, however, the relative rates may be determined and show a preferential reaction with the 1-position (e.g., Eq. 3.5). The ratio of k_{1i}/k_{2i} ranges from 11 to 2.5 over the temperature range studied (35 - 65 °C). This agrees with previous proton affinity studies,[14] and suggests that protonation of the naphthalene is occurring during the H/D exchange. The site selectivity for the $Hg(C_6H_5Me)_2(GaCl_4)_2$ catalyzed H/D exchange reaction is consistent with an electrophilic aromatic substitution reaction. In addition, the rate equation is consistent with the protonation of naphthalene by the coordinated benzene in $Hg(C_6D_6)_2(GaCl_4)_2$ (Eq. 3.6).

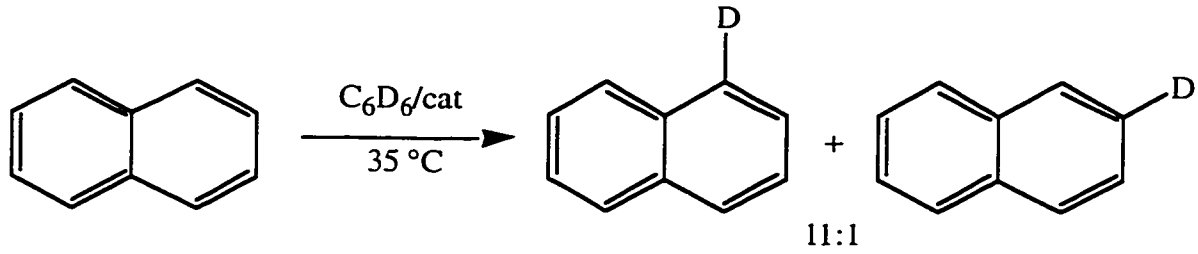

11:1

1-deuterionaphthalene 2-deuterionaphthalene

(3.5)

$$Hg(C_6D_6)_2(GaCl_4)_2 + C_{10}H_8 \longrightarrow$$

$$[Hg(C_6D_5)(C_6D_6)(GaCl_4)_2]^- + [C_{10}H_8D]^+ \qquad (3.6)$$

Although the rates for H/D exchange follow first order kinetics during the first hour, observation of the reactions over an extended time period shows that the rates change with time. After an initial period, the reaction rates increase until they once again reach a new first order kinetics regime. The final rates do not change throughout the rest of the observed reaction (e.g., Figure 3.4). The overall form of the rate equation is unchanged (Eq. 3.7), though the rate constants (k_{1f} and k_{2f}) both increase significantly.

$$\text{final rate of H/D exchange} = k_{1f}[Hg][C\text{-}H_1] + k_{2f}[Hg][C\text{-}H_2] \qquad (3.7)$$

As may be seen from Table 3.1, the value for k_{2f} is closer to that of k_{1f} than during the initial reaction period (i.e., $k_{1i} > k_{2i}$ while $k_{1f} \approx k_{2f}$). The $\Delta H^{\ddagger}$ and $\Delta S^{\ddagger}$ for these reactions may be determined from the temperature dependence for k_{1f} and k_{2f} (see Table 3.1). As with the initial reactions, the positive values of $\Delta S^{\ddagger}$ are indicative of a dissociative

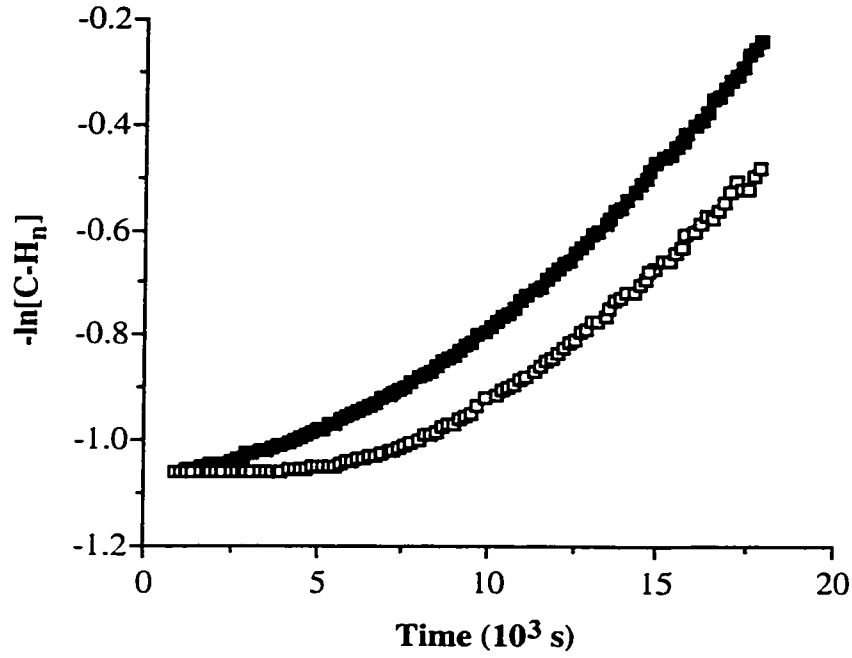

Figure 3.4. Representative plot of -ln[C-H_1] (■) and -ln[C-H_2] (□) versus time (s) for the Hg(arene)$_2$($GaCl_4$)$_2$ catalyzed H/D exchange between C_6D_6 and $C_{10}H_8$ at 308 K.

reaction.[17]

The $\Delta H^{\ddagger}$ for the H/D exchange at the 1-position is only slightly decreased between the two reaction regimes. In contrast, the $\Delta H^{\ddagger}$ for the H/D exchange at the 2-position decreases significantly such that it becomes comparable to that for exchange at the 1-position. This is in direct contrast to the trend expected for an electrophilic aromatic substitution reaction on naphthalene. It would therefore appear that the reaction pathway changes with time. Two questions are raised from these observations. *What is the change in reaction pathway, and why does the site selectivity of the H/D exchange change?*

We have observed that, during the NMR experiments, small quantities of a dark orange solid precipitate is observed once the H/D exchange has concluded. MS of this material shows that naphthalene is the only arene present, while ^{13}C CPMAS NMR

spectroscopy and analysis indicates the composition to be $Hg(C_{10}H_8)_2(GaCl_4)_2$ (**3.1**) (see Figure 3.5).

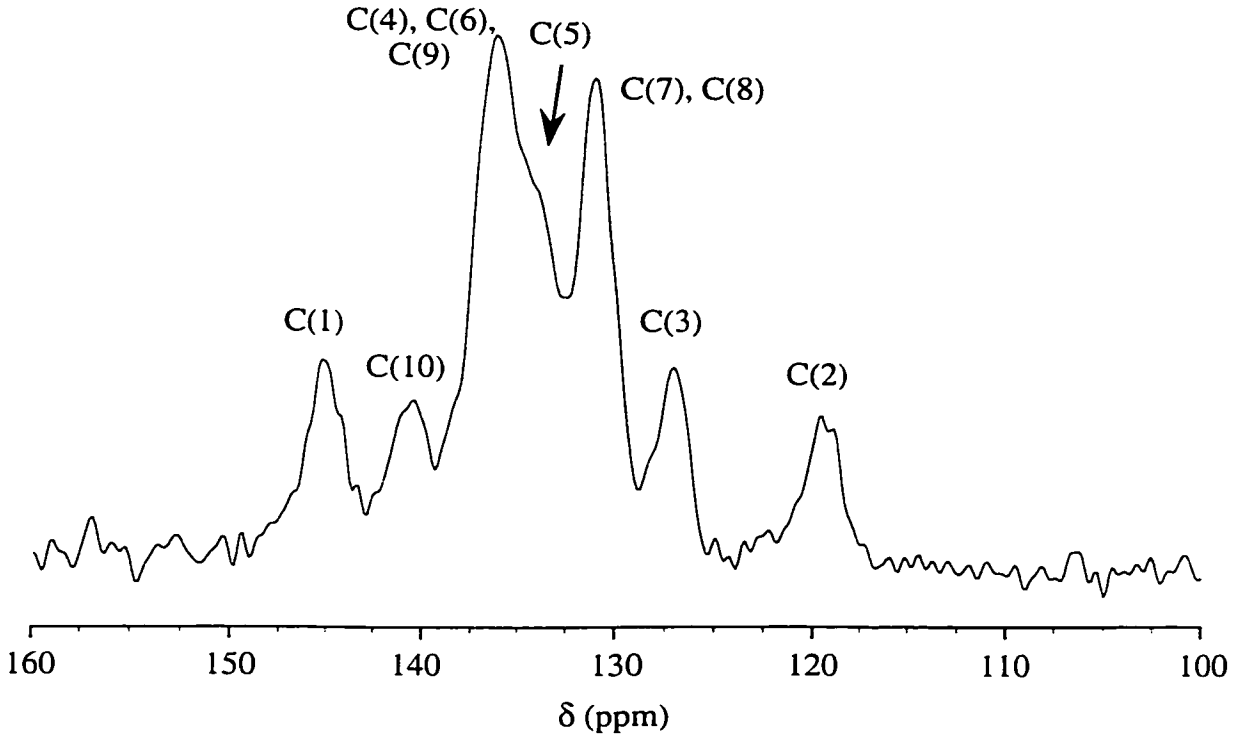

Figure 3.5. ^{13}C CPMAS NMR spectra of $Hg(C_{10}H_8)_2(GaCl_4)_2$ (**3.1**).

^{13}C CPMAS NMR spectroscopic peak assignments were obtained by a combination of dipolar dephasing experiments[19] and comparison with calculated (DFT) chemical shifts (see Experimental). Figure 3.6 shows the calculated structure for $Hg(C_{10}H_8)_2(GaCl_4)_2$. Table 3.2 gives a comparison of the calculated and experimental ^{13}C NMR shifts for compound **3.1**.

We have previously noted that, even without X-ray crystallographic data, the ^{13}C CPMAS NMR spectrum of $Hg(arene)_2(MCl_4)_2$ (M = Al, Ga) is able to provide limited

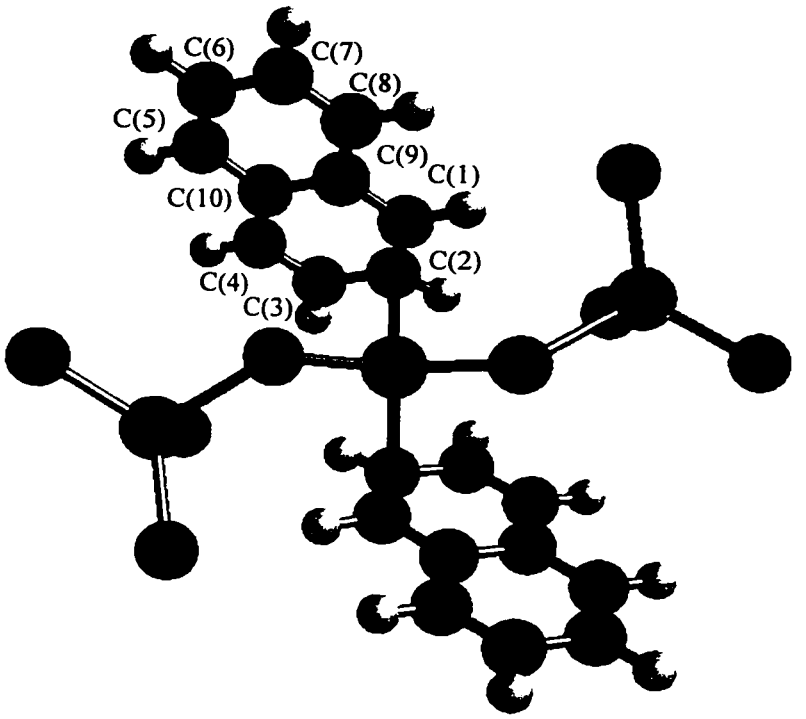

Figure 3.6. Calculated structure for $Hg(C_{10}H_8)_2(GaCl_4)_2$.

structural information. First, the number of aromatic resonances observed in the ^{13}C CPMAS NMR spectrum correlates well with the crystallographic symmetry. Thus, the observation of a single set of resonances in the ^{13}C CPMAS NMR spectrum (including the dipolar dephasing experiment) indicates that $Hg(C_{10}H_8)_2(GaCl_4)_2$ crystallizes with C_2 symmetry. Second, there is a strong correlation between Hg···C distance and the ^{13}C chemical shift.[10] Thus, based upon the observed ^{13}C chemical shifts for C(1) and C(2) (see Table 3.2) and using the previously reported relationship, the Hg-C(2) and Hg···C(1) distances are predicted to be 2.38 Å and 2.86 Å, respectively. Table 3.3 gives the calculated (DFT) bond lengths and angles for $Hg(C_{10}H_8)_2(GaCl_4)_2$ and $Hg(C_6H_6)_2(GaCl_4)_2$ (shown in Figure 3.7), along with X-ray crystallographic data for $Hg(C_6H_5R)_2(GaCl_4)_2$ (R = Me, Et). As may be seen from Table 3.3, the calculated Hg-C(2) and Hg···C(1) distances are slightly shorter (*ca.* 2%) than predicted from ^{13}C NMR

Table 3.2. Experimental and calculated (DFT) ^{13}C NMR spectra for $Hg(C_{10}H_8)_2(GaCl_4)_2$.

Atom[a]	Calculated shift δ (ppm)	Experimental shift δ (ppm)
C(1)	138.6	145
C(2)	108.0	119
C(3)	126.1	127
C(4)	134.6	136
C(5)	127.0	134
C(6)	131.7	136
C(7)	128.0	130
C(8)	128.4	130
C(9)	131.3	136
C(10)	136.2	140

[a] See Figure 3.6 for atom numbering scheme.

spectroscopy. We have previously observed, however, a similar underestimation of the Hg-C distance by DFT calculations.[10]

The UV-visible spectrum for compound **3.1** (λ = 313 nm) is distinct from that of the toluene (λ = 305 nm) or benzene (λ = 279 nm) complexes. The UV-visible spectrum for a solution of $Hg(C_6H_5Me)_2(GaCl_4)_2$ in toluene shows a change with the addition of naphthalene consistent with the formation of $Hg(C_{10}H_8)_2(GaCl_4)_2$ (**3.1**) (i.e., Eq. 3.8).

Table 3.3. Calculated bond lengths (Å) and angles (°) in $Hg(arene)_2(GaCl_4)_2$

	Calcd.		Exp.[a]
	$C_{10}H_8$	C_6H_6	C_6H_5R (R = Me, Et)
Hg-C	2.410	2.411	2.33(1) - 2.249(9)
Hg···C	2.690	2.830	2.71(1) - 2.75(1)
Hg-Cl	2.470	2.450	2.634(4) - 2.652(2)
$Ga-Cl_{br}$	2.429	2.448	2.239(2) - 2.230(4)
$Ga-Cl_{ter}$	2.220 - 2.260	2.225 - 2.272	2.128(4) - 2.166(3)
Cl-Hg-Cl	103.63	102.86	84.5(6) - 85.6(2)
C-Hg-C	101.89	108.54	126(1) - 131.3(6)
Hg-Cl-Ga	116.63	119.33	110.6(1) - 111.4(2)

[a] A. Borovik, S. G. Bott, and A. R. Barron, *J. Am. Chem. Soc.*, 2001, **123**, 11219.

$$Hg(C_6H_6)_2(GaCl_4)_2 + 2\,C_{10}H_8 \longrightarrow Hg(C_{10}H_8)_2(GaCl_4)_2 + 2\,C_6H_6 \quad (3.8)$$

(3.1)

The time at which compound **3.1** is dominant coincides with the point at which the H/D exchange kinetics alter from the initial to final rates. We propose, therefore, that the change in the reaction rates observed by ^1H NMR accompanies ligand exchange. Since the naphthalene complex is the dominant species during the later H/D exchange reaction, we propose that the rate equation is consistent with the protonation of d_6-benzene by the coordinated naphthalene in $Hg(C_{10}H_8)_2(GaCl_4)_2$ (Eq. 3.9).

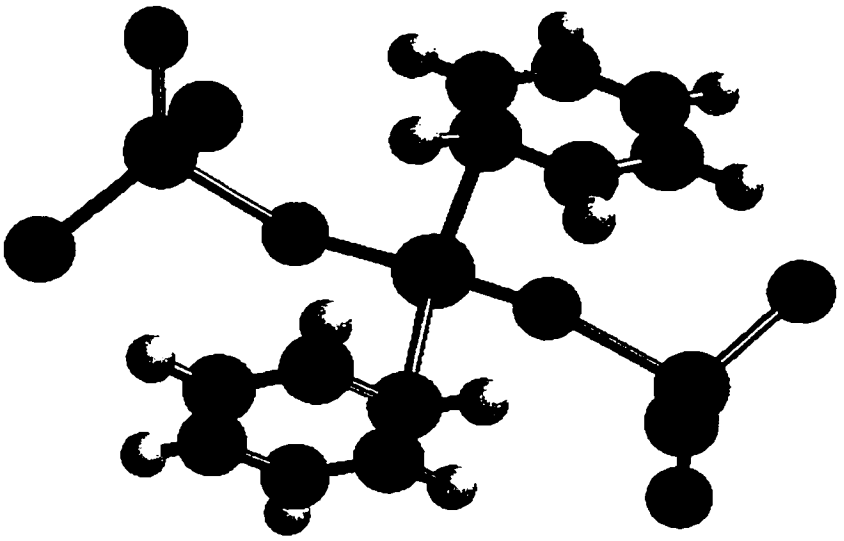

Figure 3.7. Calculated structure for $Hg(C_6H_6)_2(GaCl_4)_2$.

$$Hg(C_{10}H_8)_2(GaCl_4)_2 + C_6D_6 \longrightarrow$$

$$[Hg(C_{10}H_7)(C_{10}H_8)(GaCl_4)_2]^- + [C_6D_6H]^+ \qquad (3.9)$$

Based upon the assumption that the initial phase of the reaction is dominated by Eq. 3.6 and that the final reaction is dominated by Eq. 3.9, the rate for H/D exchange at the n-position of the naphthalene is defined as a combined rate equation (Eq. 3.10).

$$\text{H/D exchange for n-position} = k_{ni}[Hg][C\text{-}H_n] + k_{nf}[Hg][C\text{-}H_n] \qquad (3.10)$$

Given the above, and using the ^1H NMR data over the whole reaction, the concentration of $Hg(C_6H_6)_2(GaCl_4)_2$ at time (t) may be determined. The rate of ligand exchange (Eq. 3.8) is determined to be first order with respect to the concentration of $Hg(C_6H_6)_2(GaCl_4)_2$ (Eq. 3.11).

$$\text{rate of ligand exchange} = k_{ex}[Hg(C_6H_6)_2(GaCl_4)_2] \quad (3.11)$$

First order rate constants, k_{ex}, were calculated from the corresponding plot of $-\ln[Hg(C_6H_6)_2(GaCl_4)_2]$ versus time (e.g., Figure 3.8). Measurement of the temperature dependence for k_{ex} (Figure 3.9) allows for the determination of $\Delta H^{\ddagger}$ and $\Delta S^{\ddagger}$ to be 63(1) kJ.mol^{-1} and 86(7) J.K^{-1}mol^{-1}, respectively.

$$Hg(C_6H_6)_2(GaCl_4)_2 \longrightarrow Hg(C_6H_6)(GaCl_4)_2 + C_6H_6 \quad (3.12)$$

The positive values of $\Delta S^{\ddagger}$ are indicative of a dissociative reaction (Eq. 3.12),[17] while the value for $\Delta H^{\ddagger}$ [63(1) kJ.mol^{-1}] is consistent with our previously calculated bond dissociation energy (ΔH = 60 kJ.mol^{-1}) for $Hg(C_6H_6)_2(AlCl_4)_2$.[10]

Based upon the forgoing, the initial $Hg(arene)_2(GaCl_4)_2$ catalyzed reaction of naphthalene with d_6-benzene involves the deuteration of naphthalene by coordinated C_6D_6 (*cf.*, Eq. 3.6). As ligand exchange progresses, the pathway for H/D exchange changes to where the protonation of C_6D_6 by coordinated naphthalene dominates (Eq. 3.9). We propose that it is this change in the reaction pathway that is responsible for the apparent loss in site selectivity for the H/D exchange.

Based upon the ^{13}C CPMAS NMR spectrum for $Hg(C_{10}H_8)_2(GaCl_4)_2$ and the calculated structure (Figure 3.6), it appears that there is a preference for coordination of the mercury to the 2-position of the naphthalene. Such a preferential coordination to the 2-position is predicted on steric and electronic grounds. We have previously also observed by X-ray crystallographic analysis of $Hg(C_6H_{6-n}Me_n)_2(MCl_4)_2$ that there is a

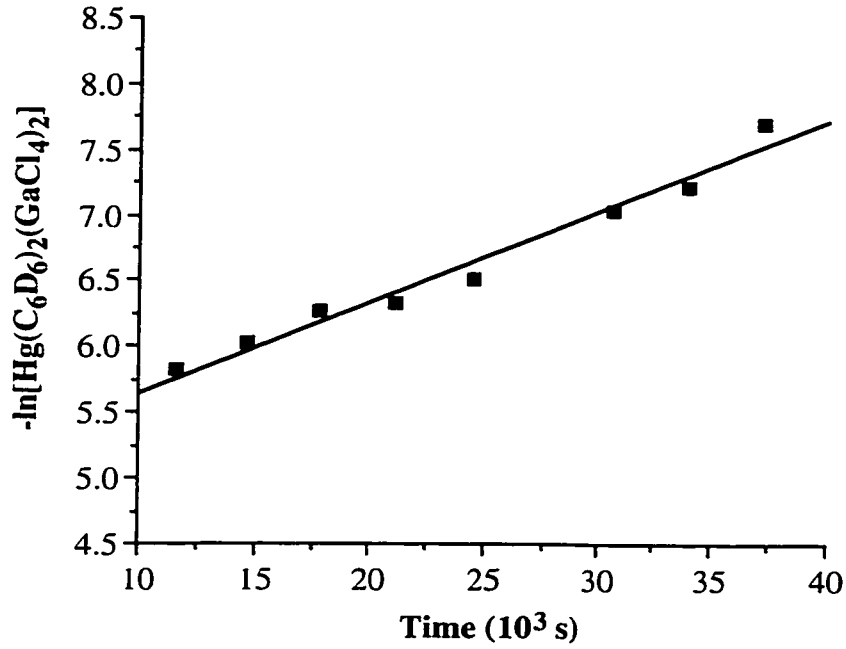

Figure 3.8. Representative plot of $-\ln[Hg(C_6D_6)_2(GaCl_4)_2]$ versus time (s) at 298 K (R = 0.956).

similar preference for the coordination of the mercury to the carbon *para* to the arene's substituents.[10] Based upon ^{13}C CPMAS NMR chemical shifts[10] and DFT calculations,[10] the charge on the proton and carbon associated with the shortest Hg···C interaction is significantly higher than that on the free arene. The effect is also present, albeit reduced, on the C and H atoms *ortho* to the short Hg···C interaction. Thus, the C-H bond on the carbon associated with mercury is the most highly activated (Figure 3.9). This is confirmed by observation of the calculated charge distribution on the aromatic C and H atoms for $Hg(C_{10}H_8)_2(GaCl_4)_2$ (Figure 3.10).

The relative rate for the H/D exchange between naphthalene and $Hg(C_6D_6)_2(GaCl_4)_2$ (Eq. 3.9) is controlled in the same way as any related electrophilic

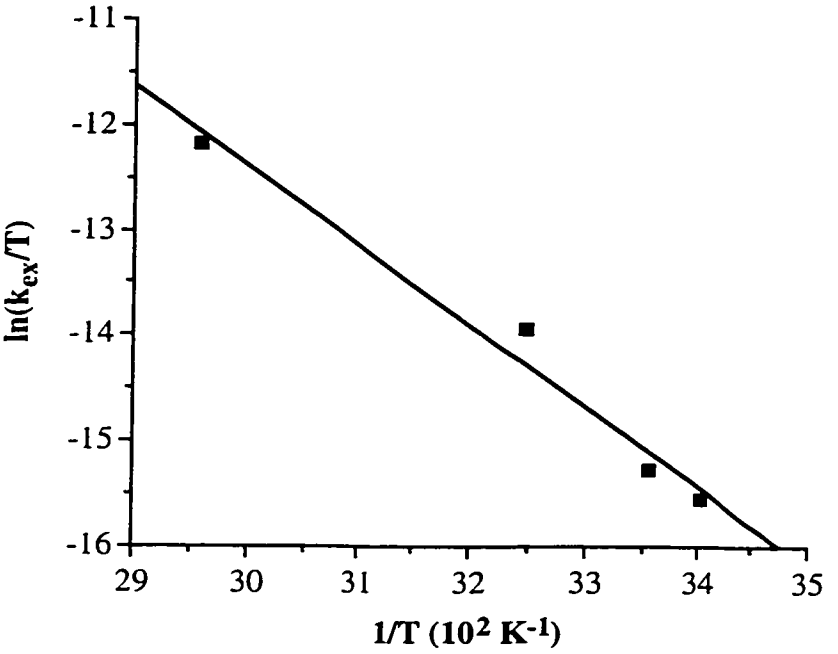

Figure 3.9. An Eyring plot of the $\ln(k_{ex}/T)$ versus 1/T for the $C_6D_6/C_{10}H_8$ ligand exchange reaction (R = 0.976).

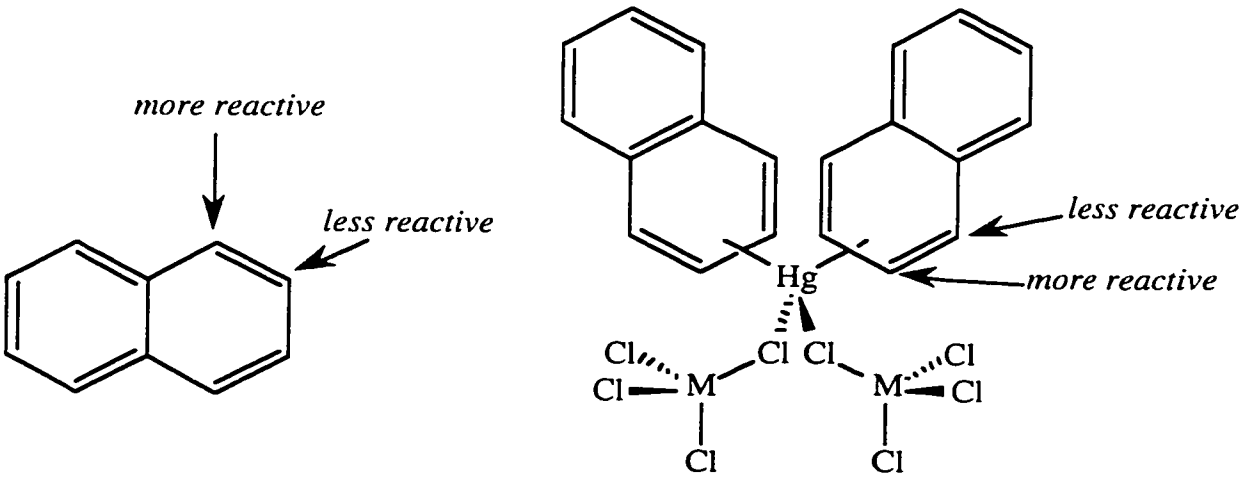

Figure 3.10. Schematic representation of relative reactivity of the hydrogens in the 1- and 2-position of naphthalene towards H/D exchange.

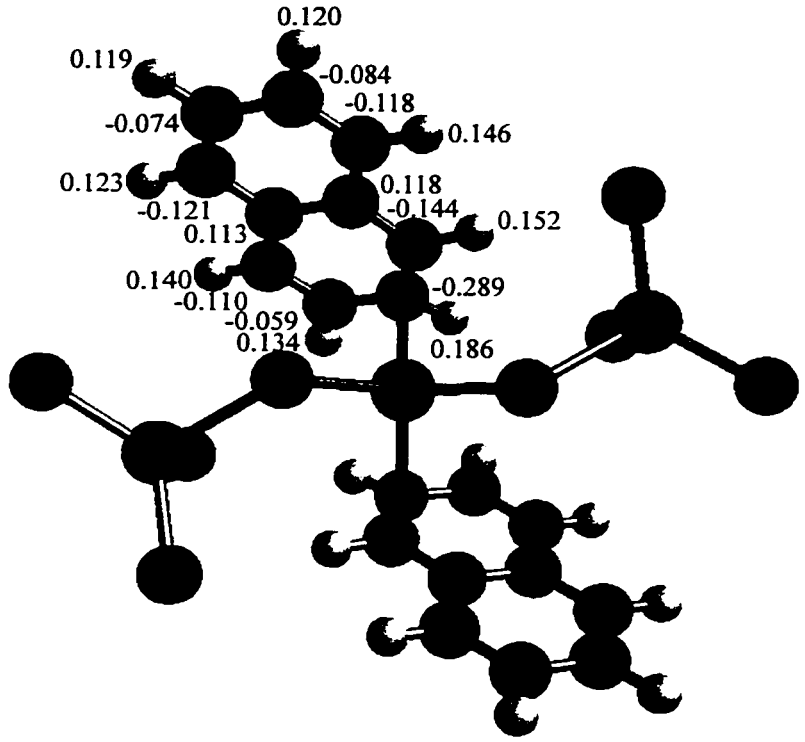

Figure 3.11. Calculated charge distribution on the aromatic C and H atoms in $Hg(C_{10}H_8)_2(GaCl_4)_2$.

aromatic substitution reaction of naphthalene. In contrast, the relative rate for the H/D exchange between benzene and $Hg(C_{10}H_8)_2(GaCl_4)_2$ (Eq. 3.6) is controlled by the relative activation of the naphthalene C-H bonds. Since the mercury will preferentially bind to the carbon at the 2-position, this C-H bond will be activated significantly more that the C-H associated with the 1-position (see Figures 3.10 and 3.11).

The change in site selectivity upon ligand exchange is unfortunate in that it precludes the easy site specific H/D exchange for many arenes, however, the presence of a ligand exchange in favor of the most substituted arene does allow for the isolation of complexes previously unobtainable by direct synthesis.

The reaction of $Hg(C_6H_5Me)_2(GaCl_4)_2$ with two equivalents of C_6Me_6 in toluene yields a liquid clathrate (Figure 3.12).

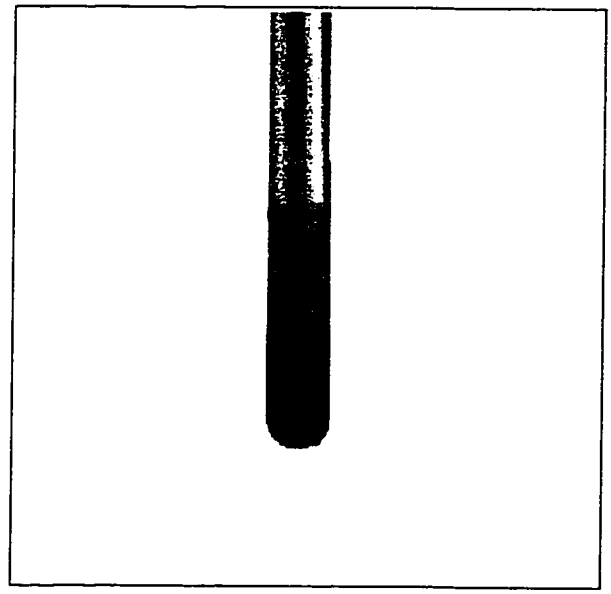

Figure 3.12. Liquid clathrate formed from the reaction of $Hg(C_6H_5Me)_2(GaCl_4)_2$ with C_6Me_6 in toluene.

The formation of the clathrate is concentration dependent; below 0.08 M (Hg) a homogeneous solution is formed. The homogeneous solution is spectroscopically identical to the upper layer of the clathrate. The arene:Hg ratio for the lower layer was determined to be *ca.* 13.5. The ^1H and ^{13}C NMR spectra for the upper layer shows a single set of resonances, while the UV-visible spectrum exhibits a band at 323 nm. Both spectroscopies are consistent with the upper layer containing $Hg(C_6Me_6)_2(GaCl_4)_2$.

The presence of ligand exchange to the more stable substituted arene, also helps explain why the use of $Hg(C_6H_5Me)_2(GaCl_4)_2$ as a Friedel-Crafts catalyst (e.g., alkylation of toluene by ethylene) does not allow for complete conversion of all the toluene.[20] Presumably, preferential coordination of the polyalkylated toluene occurs such that ligand exchange with toluene to provide fresh substrate cannot occur.

Conclusions

We have confirmed that the H/D exchange between naphthalene and C_6D_6 occurs by electrophilic substitution. In this regard, we have studied the kinetics ofH/D exchange. We found that there are two distinct first order regimes, separated by a non-first order regime. In the first regime, $Hg(C_6D_6)_2(GaCl_4)_2$ deuterates free naphthalene. As the reaction progresses, a ligand exchange occurs between C_6D_6 and naphthalene, resulting in the protonation of C_6D_6 by $Hg(C_{10}H_8)_2(GaCl_4)_2$. Ths ligand exchange has been confirmed by ^{13}C CPMAS NMR of $Hg(C_{10}H_8)_2(GaCl_4)_2$, as well as by DFT calculations, UV-visible spectroscopy, and MS.

Experimental

NMR spectra were obtained on Bruker Avance 200, 400 and 500 spectrometers. Chemical shifts are reported relative to internal solvent resonances. NMR tubes are cleaned in basic solution, followed by acetone wash. The tubes are dried and stored in an oven prior to use, from which they are taken directly to the port on the dry box which is immediately evacuated. The C_6D_6 is pre-dried and stored in the dry box over molecular sieves. ^{13}C MAS spectra were obtained at 50.32 MHz using Bruker Avance 200 spectrometer. A 7 mm zirconium dioxide rotor was used for all spectra, with the spin rates up to 5 kHz. UV-visible spectral data were recorded on a Varian Cary 4 spectrometer. MS analyses were carried out using a Finnigan MAT 95 mass spectrometer operating with an electron beam energy of 70 eV for EI mass spectra. The synthesis of $Hg(C_6H_5Me)_2(GaCl_4)_2$ was as reported previously.[1,2] Solvents and all arenes were distilled and degassed prior to use.

Reaction of $Hg(C_6H_5Me)_2(MCl_4)_2$ with $C_{10}H_8$ in C_6D_6. To a yellow solution of $Hg(C_6H_5Me)_2(GaCl_4)_2$ (0.128 g, 0.158 mmol) in C_6D_6 (35 g, 416 mmol) was added

naphthalene (2.50 g, 19.5 mmol). The resulting orange solution was allowed to stir for 12 hours. After the reaction was complete, water (5 mL) was added to kill the catalyst. The aromatic and aqueous layers were allowed to separate, and the aromatic layer was isolated by decanting. Solid was isolated by removing the volatiles in the aromatic layer, and its identity was confirmed by MS and ^{13}C NMR.

$C_{10}D_8$. MS (EI, %): *m/z* 136 (M^+, 100), 134 (M^+ - H, 24), 132 (M^+ - 2 H, 5). ^{13}C NMR (C_6D_6): δ 134.2 (s, 9-C), 128.2 [t, J(C-D) = 24 Hz, 1-CD], 125.8 [t, J(C-D) = 24 Hz, 2-CD].

Catalytic H/D Exchange. In at typical experiment, naphthalene (0.100 g, 0.78 mmol) was dissolved in C_6D_6 (*ca.* 1 mL) in a 5 mm NMR tube. To this was added $Hg(C_6H_5Me)_2(GaCl_4)_2$ (3.00 mg, 3.71 μmol), turning the clear solution light yellow. The sample was protected from light by a sleeve of aluminum foil because $Hg(C_6H_5Me)_2(GaCl_4)_2$ is light-sensitive. At temperatures other than 294 K, the NMR was equilibrated before the sample was inserted. Each NMR measurement yielded a spectrum consisting of two sets of naphthalene peaks and a peak due to C_6D_5H. The peaks were integrated over consistent ranges. From these integrations, the concentrations of C-H at both the 1- and 2-positions, as well as the growing C_6D_5H concentration, were determined.

$Hg(C_{10}H_8)_2(GaCl_4)_2$ (3.1). $Hg(C_6H_5Me)_2(GaCl_4)_2$ (0.50 g, 0.062 mmol) was dissolved in toluene (20 mL) and heated slightly to ensure complete dissolution. A large excess of naphthalene (7.93 g, 0.062 mol) was added to the warm yellow solution, resulting in a red solution. The reaction flask was covered in aluminum foil to prevent decomposition of the light-sensitive mercury complexes and was allowed to cool to room temperature. The solution was stirred for 12 hours to ensure that the ligand exchange

between C_6H_5Me and naphthalene went to completion. Upon to cooling to –24 °C, orange precipitate formed. Yield: 80%. MS (EI, %): *m/z* (M^+, 100). ^{13}C CPMAS NMR (50.32 MHz): δ 145 (1C, 1-C), 140 (1C, 10-C), 136 (3C, 4-C,6-C, 9-C), 134 (1C, 5-C), 130 (2C, 7-C, 8-C) 127 (1C, 3-C), 119 (1C, Hg···CH).

$Hg(C_6Me_6)_2(GaCl_4)_2$ (3.2). Toluene (10 mL) was added to a solid mixture of $HgCl_2$ (1.00 g, 3.68 mmol) and $GaCl_4$ (1.30 g, 7.36 mmol). The resulting yellow solution was heated to 60 °C and stirred vigorously until all the $HgCl_2$ dissolved. To this solution was added hexamethylbenzene (1.19 g, 7.68 mmol). In approximately 30 minutes, stirring was halted, and, within another five minutes, the reaction mixture was separated into two layers. The bottom layer has the formula $Hg(arene)_{13.5}(GaCl_4)_2$. The concentration of the top layer permitted characterization by ^1H and ^{13}C NMR. ^1H NMR: δ 2.06 (18 H). ^{13}C NMR: δ 133.4 (C-CH_3), 17.4 (C-CH_3).

Computational Methods. All density functional calculations were carried out using a Gaussian-98 suite.[21] Complete geometry optimizations were performed at B3LYP[22] level using the 6-31G** basis set for C and H only and Stuttgart RLC ECP basis set for Hg, Cl, and Ga. C_2 symmetry was imposed. Vibrational frequencies were then evaluated for naphthalene complexes to verify the existence of the true potential minimum and to determine zero-point energies. ^{13}C NMR chemical shifts for $Hg(C_{10}H_8)_2(GaCl_4)_2$ were calculated at the same level of theory.

References

1 A. S. Borovik, S. G. Bott, and A. R. Barron, *Angew. Chem. Int. Ed.*, 2000, **39**, 4117.

2 A. Borovik, S. G. Bott, and A. R. Barron, *J. Am. Chem. Soc.*, 2001, **123**, 11219.

3 A. Borovik and A. R. Barron, *J. Am. Chem. Soc.*, 2002, **124**, 3743.

4 Although $AlCl_3$ will catalyze the H/D exchange between C_6D_6 and toluene, traces of dissolved water are involved in the proton transfer, see (a) J. L. Garrett, M. A. Long, and R. F. W. Vining, *J. Chem. Soc., Chem. Commun.*, 1972, 1172. (b) D. F. Gaines and H. Beall, *Inorg. Chem.*, 2000, **39**, 1812.

5 E. L. Mackor, P. J. Smit, and J. H. van der Waals, *Trans. Faraday Soc.*, 1957, **53**, 1309.

6 R. Taylor, *Comprehensive Chemical Kinetics*, Elsevier, Amsterdam, Vol. 13, 1972, pp. 194 - 277.

7 R. J. Hodges and J. L. Garnett, *J. Catal.*, 1969, **13**, 83.

8 F. Calderazzo, G. Pampaloni, and A. Vallieri, *Inorg. Chim. Acta*, 1995, **229**, 179.

9 E. K. Barefield, G. W. Parshall, and F. N. Tebbe, *J. Am. Chem. Soc.*, 1970, **92**, 5234.

10 A. Borovik, Ph.D. Thesis, Rice University, 2001.

11 It has previously been shown that Group 13 Lewis acids, such as AlR_3, can increase the proton acidity of coordinated alcohols, as measured by a decrease in the pK_a, by at least 7 units, C. N. McMahon, S. G. Bott, and A. R. Barron, *J. Chem. Soc., Dalton Trans.*,1997, 3129.

12 R. Taylor, *Electrophilic Aromatic Substitution*, Wiley, New York, 1990, Chapter 3.

13 E. L. Makor, A. Hofstra, and J. H. van der Waals, *Trans. Faraday Soc.*, 1958, **54**, 66.

14 P. Fischer and R. Taylor, *J. Chem. Soc., Perkin Trans.*, 1980, 781.

15 We have defined k_{1i} and k_{2i} as the rate constants for the initial H/D exchange reaction.

16 It should be noted that the major source of error in the calculation of the individual second order rate constants involves the measurment of the mass of catalyst.

17 The two active sites can be treated independently of each other. Both the electronic and steric effects on site reactivity by a deuterium versus a proton is negligible.

18 J. D. Atwood, *Inorganic and Organometallic Reaction Mechanisms*, VCH, New York, 1997, p. 14.

19 L. B. Alemany, D. M. Grant, T. D. Alger, and R. J. Pugmire, *J. Am. Chem. Soc.*, 1983, **105**, 6697.

20 A. Borovik and A. R. Barron, *J. Am. Chem. Soc.*, 2002, **124**, 3743.

21 M. J. Frisch, G. W. Trucks, H. B. Schlegel, G. E. Scuseria, M. A. Robb, J. R. Cheeseman, V. G. Zakrzewski, J. A. Montgomery, Jr., R. E. Stratmann, J. C. Burant, S. Dapprich, J. M. Millam, A. D. Daniels, K. N. Kudin, M. C. Strain, O. Farkas, J. Tomasi, V. Barone, M. Cossi, R. Cammi, B. Mennucci, C. Pomelli, C. Adamo, S. Clifford, J. Ochterski, G. A. Petersson, P. Y. Ayala, Q. Cui, K. Morokuma, D. K. Malick, A. D. Rabuck, K. Raghavachari, J. B. Foresman, J. Cioslowski, J. V. Ortiz, A. G. Baboul, B. B. Stefanov, G. Liu, A. Liashenko, P. Piskorz, I. Komaromi, R. Gomperts, R. L. Martin, D. J. Fox, T. Keith, M. A. Al-Laham, C. Y. Peng, A. Nanayakkara, M. Challacombe, P. M. W. Gill, B. Johnson, W. Chen, M. W. Wong, J. L. Andres, C. Gonzalez, M. Head-Gordon, E. S. Replogle, and J. A. Pople, *Gaussian 98, Revision A.9*; Gaussian, Inc., Pittsburgh PA, 1998.

22 (a) A. D. Becke, *J. Chem. Phys.*, 1993, **98**, 5648.

(b) P. J. Stephens, C. F. Devlin, C. F. Chabalowski, and M. J. Frisch, *J. Phys. Chem.* 1994, **98**, 11623.

(c) C. Lee, W. Yang, and R. G. Parr, *Phys. Rev.*, 1988, **B37**, 785.

Appendix for

Chemistry of Group 13 Lewis Acids

by

Catherine S. Branch

BCl_3(9-fluorenone) (**1.1**)

Atomic coordinates [x 10^4] and equivalent isotropic displacement parameters [$Å^2$ x 10^3]. U(eq) is defined as one third of the trace of the orthogonalized Uij tensor.

	x	y	z	U(eq)
O	3975(2)	2256(2)	7637(2)	59(1)
C(1)	4068(3)	2023(2)	6394(3)	47(1)
C(2)	5288(3)	2782(2)	4945(3)	49(1)
C(3)	6434(3)	3777(3)	4686(3)	58(1)
C(4)	7445(3)	4366(3)	3179(3)	66(1)
C(5)	7278(3)	3975(3)	1996(3)	65(1)
C(6)	6122(3)	2975(3)	2254(3)	58(1)
C(7)	5132(3)	2370(2)	3752(3)	48(1)
C(8)	3803(3)	1292(2)	4442(3)	47(1)
C(9)	3208(3)	533(3)	3767(3)	58(1)
C(10)	1945(3)	-438(3)	4718(3)	64(1)
C(11)	1299(3)	-642(3)	6290(3)	64(1)
C(12)	1889(3)	117(3)	6990(3)	57(1)
C(13)	3152(3)	1089(2)	6051(3)	47(1)
B(1)	2800(4)	1844(3)	9321(3)	63(1)
Cl(1)	817(4)	2319(4)	9561(4)	54(1)
Cl(1A)	806(8)	2300(7)	9599(7)	118(2)
Cl(2)	2874(9)	-10(6)	9940(7)	118(2)
Cl(2A)	2879(5)	-25(3)	9980(4)	53(1)
Cl(3)	3521(5)	2909(4)	10252(4)	64(1)
Cl(3A)	3447(10)	2886(7)	10266(7)	134(3)
C(1S)	9735(25)	6360(17)	4539(30)	357(17)
C(2S)	9008(19)	5836(15)	5646(26)	264(10)
C(3S)	9020(10)	4442(9)	6408(12)	176(3)
C(4S)	8227(14)	3828(14)	7588(11)	121(4)

Bond lengths [Å] and angles [°]

O-C(1)	1.261(3)	O-B(1)	1.514(4)
C(1)-C(2)	1.454(3)	C(1)-C(13)	1.460(3)
C(2)-C(3)	1.382(3)	C(2)-C(7)	1.390(3)
C(3)-C(4)	1.384(4)	C(4)-C(5)	1.376(4)
C(5)-C(6)	1.391(4)	C(6)-C(7)	1.377(3)
C(7)-C(8)	1.482(3)	C(8)-C(9)	1.366(3)
C(8)-C(13)	1.407(3)	C(9)-C(10)	1.394(4)
C(10)-C(11)	1.374(4)	C(11)-C(12)	1.383(4)
C(12)-C(13)	1.392(3)	B(1)-Cl(3A)	1.790(7)
B(1)-Cl(2)	1.811(7)	B(1)-Cl(1A)	1.828(8)
B(1)-Cl(1)	1.833(5)	B(1)-Cl(2A)	1.833(4)
B(1)-Cl(3)	1.836(4)	C(1S)-C(2S)	1.04(4)
C(1S)-C(3S)'	1.43(2)	C(2S)-C(3S)	1.44(2)
C(3S)-C(4S)	1.130(10)		
C(1)-O-B(1)	135.3(2)	O-C(1)-C(2)	119.3(2)
O-C(1)-C(13)	132.7(2)	C(2)-C(1)-C(13)	108.0(2)
C(3)-C(2)-C(7)	122.2(2)	C(3)-C(2)-C(1)	129.2(2)
C(7)-C(2)-C(1)	108.6(2)	C(2)-C(3)-C(4)	117.7(2)
C(5)-C(4)-C(3)	120.2(2)	C(4)-C(5)-C(6)	122.2(2)
C(7)-C(6)-C(5)	117.8(2)	C(6)-C(7)-C(2)	120.0(2)
C(6)-C(7)-C(8)	132.4(2)	C(2)-C(7)-C(8)	107.6(2)
C(9)-C(8)-C(13)	120.5(2)	C(9)-C(8)-C(7)	130.6(2)
C(13)-C(8)-C(7)	108.9(2)	C(8)-C(9)-C(10)	118.1(2)
C(11)-C(10)-C(9)	121.9(2)	C(10)-C(11)-C(12)	120.7(2)
C(11)-C(12)-C(13)	117.9(2)	C(12)-C(13)-C(8)	120.9(2)
C(12)-C(13)-C(1)	132.2(2)	C(8)-C(13)-C(1)	106.9(2)
O-B(1)-Cl(3A)	104.3(3)	O-B(1)-Cl(2)	109.5(3)
O-B(1)-Cl(1A)	109.1(3)	Cl(3A)-B(1)-Cl(1A)	110.1(4)
O-B(1)-Cl(1)	108.0(2)	Cl(2)-B(1)-Cl(1)	112.1(3)
O-B(1)-Cl(2A)	110.2(2)	Cl(3A)-B(1)-Cl(2A)	111.1(3)
Cl(1A)-B(1)-Cl(2A)	111.8(3)	O-B(1)-Cl(3)	103.0(2)
Cl(2)-B(1)-Cl(3)	111.9(3)	Cl(1)-B(1)-Cl(3)	111.8(2)
C(2S)-C(1S)-C(3S)'	115(2)	C(1S)-C(2S)-C(3S)	131.5(13)
C(4S)-C(3S)-C(2S)	133.4(13)	C(4S)-C(3S)-C(1S)'	113(2)
C(2S)-C(3S)-C(1S)'	114(2)		

Symmetry transformations used to generate equivalent atoms:'

' (x,y,z) → (2-x,1-y,1-z)

Anisotropic displacement parameters [$Å^2 \times 10^3$].

	U11	U22	U33	U23	U13	U12
O	56(1)	72(1)	47(1)	-5(1)	-23(1)	-7(1)
C(1)	44(1)	52(1)	46(1)	-4(1)	-23(1)	4(1)
C(2)	42(1)	51(1)	49(1)	-3(1)	-20(1)	0(1)
C(3)	53(2)	58(2)	61(2)	-4(1)	-27(1)	-5(1)
C(4)	51(2)	62(2)	73(2)	2(1)	-23(1)	-11(1)
C(5)	55(2)	58(2)	59(2)	5(1)	-12(1)	-4(1)
C(6)	58(2)	58(2)	50(1)	-1(1)	-21(1)	2(1)
C(7)	43(1)	48(1)	47(1)	-1(1)	-20(1)	5(1)
C(8)	43(1)	48(1)	51(1)	-3(1)	-24(1)	5(1)
C(9)	60(2)	59(2)	61(2)	-7(1)	-34(1)	3(1)
C(10)	60(2)	62(2)	82(2)	-13(1)	-42(2)	1(1)
C(11)	53(2)	58(2)	77(2)	0(1)	-31(1)	-9(1)
C(12)	50(2)	59(2)	57(2)	4(1)	-24(1)	-4(1)
C(13)	41(1)	48(1)	51(1)	-1(1)	-23(1)	2(1)
B(1)	72(2)	63(2)	46(2)	0(1)	-24(2)	3(2)
Cl(1)	40(2)	54(2)	45(2)	1(2)	-4(2)	8(2)
Cl(1A)	91(5)	117(5)	107(4)	22(3)	-27(3)	-2(3)
Cl(2)	125(5)	101(4)	115(4)	8(3)	-54(4)	4(4)
Cl(2A)	76(3)	40(2)	45(2)	0(1)	-32(2)	8(2)
Cl(3)	105(2)	62(2)	44(2)	-17(2)	-47(2)	6(2)
Cl(3A)	186(6)	118(5)	106(4)	-6(4)	-78(4)	-7(4)
C(1S)	454(24)	174(11)	823(45)	-224(18)	-575(32)	135(12)
C(2S)	287(13)	181(10)	605(27)	-287(16)	-378(18)	195(11)
C(3S)	179(7)	162(7)	303(10)	-87(7)	-195(7)	32(5)
C(4S)	128(8)	135(9)	115(7)	-1(6)	-76(6)	-7(7)

Hydrogen coordinates [x 10^4] and equivalent isotropic displacement parameters [$Å^2$ x 10^3].

	x	y	z	U(eq)
H(3A)	6521(3)	4051(3)	5525(3)	69
H(4A)	8266(3)	5050(3)	2955(3)	79
H(5A)	7978(3)	4408(3)	959(3)	78
H(6A)	6018(3)	2714(3)	1418(3)	70
H(9A)	3655(3)	660(3)	2670(3)	70
H(10A)	1508(3)	-974(3)	4262(3)	77
H(11A)	429(3)	-1320(3)	6907(3)	76
H(12A)	1443(3)	-22(3)	8088(3)	69
H(1SA)	9555(25)	7307(17)	4208(30)	429
H(2SA)	8178(19)	6353(15)	6312(26)	317
H(4SA)	8481(14)	2881(14)	7822(11)	181
H(4SB)	8279(14)	4360(14)	8290(11)	181
H(4SC)	7170(14)	3838(14)	7684(11)	181

$AlBr_3$(9-fluorenone) (**1.2**)

Atomic coordinates [x 10^4] and equivalent isotropic displacement parameters [$Å^2$ x 10^3]. U(eq) is defined as one third of the trace of the orthogonalized Uij tensor.

	x	y	z	U(eq)
Br(1)	405(1)	7209(2)	4572(2)	96(1)
Br(2)	-3341(2)	5979(2)	4941(2)	107(1)
Br(3)	-2547(2)	9484(2)	5192(2)	108(1)
Al(1)	-1857(4)	7191(4)	5544(3)	64(1)
O(1)	-2016(9)	6123(9)	7414(9)	87(3)
C(1)	-88(15)	7984(14)	8310(16)	84(4)
C(2)	586(15)	8552(15)	8973(18)	84(4)
C(3)	342(14)	7915(15)	10450(18)	85(4)
C(4)	-628(14)	6709(15)	11291(14)	77(4)
C(5)	-3002(12)	3951(12)	12492(13)	68(4)
C(6)	-3972(14)	2868(15)	12558(17)	82(4)
C(7)	-4296(14)	2755(14)	11450(17)	78(4)
C(8)	-3680(13)	3742(13)	10085(14)	72(4)
C(9)	-1910(13)	5930(14)	8682(13)	67(4)
C(10)	-1058(12)	6777(12)	9062(12)	57(3)
C(11)	-1316(12)	6132(12)	10625(12)	57(3)
C(12)	-2382(11)	4912(12)	11101(13)	55(3)
C(13)	-2727(12)	4761(12)	9971(12)	53(3)
C(1S)	-5677(26)	-839(26)	11511(25)	184(9)
C(2S)	-6259(22)	268(23)	10355(25)	163(8)
C(3S)	-4208(22)	-973(21)	10848(23)	157(7)
C(4S)	-5998(29)	-1696(30)	12597(27)	112(11)

Bond lengths [Å] and angles [°]

Br(1)-Al(1)	2.256(4)	Br(2)-Al(1)	2.239(4)
Br(3)-Al(1)	2.253(4)	Al(1)-O(1)	1.756(9)
O(1)-C(9)	1.283(14)	C(1)-C(2)	1.33(2)
C(1)-C(10)	1.39(2)	C(2)-C(3)	1.38(2)
C(3)-C(4)	1.40(2)	C(4)-C(11)	1.34(2)
C(5)-C(12)	1.390(14)	C(5)-C(6)	1.43(2)
C(6)-C(7)	1.31(2)	C(7)-C(8)	1.38(2)
C(8)-C(13)	1.35(2)	C(9)-C(10)	1.42(2)
C(9)-C(13)	1.46(2)	C(10)-C(11)	
1.457(14)			
C(11)-C(12)	1.47(2)	C(12)-C(13)	1.36(2)
C(1S)-C(4S)	1.08(2)	C(1S)-C(2S)	1.41(2)
C(1S)-C(3S)	1.51(2)	C(2S)-C(3S)'	1.16(2)

O(1)-Al(1)-Br(2)	102.9(4)	O(1)-Al(1)-Br(3)	105.7(3)
Br(2)-Al(1)-Br(3)	113.1(2)	O(1)-Al(1)-Br(1)	108.2(3)
Br(2)-Al(1)-Br(1)	113.4(2)	Br(3)-Al(1)-Br(1)	112.6(2)
C(9)-O(1)-Al(1)	153.4(10)	C(2)-C(1)-C(10)	122.0(14)
C(1)-C(2)-C(3)	119.1(13)	C(2)-C(3)-C(4)	122.6(14)
C(11)-C(4)-C(3)	118.5(12)	C(12)-C(5)-C(6)	113.4(12)
C(7)-C(6)-C(5)	125.4(13)	C(6)-C(7)-C(8)	119.6(14)
C(13)-C(8)-C(7)	117.1(13)	O(1)-C(9)-C(10)	127.5(12)
O(1)-C(9)-C(13)	122.3(14)	C(10)-C(9)-C(13)	110.2(11)
C(1)-C(10)-C(9)	135.3(13)	C(1)-C(10)-C(11)	118.0(13)
C(9)-C(10)-C(11)	106.7(10)	C(4)-C(11)-C(10)	119.7(11)
C(4)-C(11)-C(12)	134.9(12)	C(10)-C(11)-C(12)	105.4(12)
C(13)-C(12)-C(5)	119.9(12)	C(13)-C(12)-C(11)	111.5(11)
C(5)-C(12)-C(11)	128.6(12)	C(8)-C(13)-C(12)	124.5(11)
C(8)-C(13)-C(9)	129.3(12)	C(12)-C(13)-C(9)	106.2(11)
C(4S)-C(1S)-C(2S)	140(3)	C(4S)-C(1S)-C(3S)	114(3)
C(2S)-C(1S)-C(3S)	104(2)	C(3S)'-C(2S)-C(1S)	132(2)
C(2S)'-C(3S)-C(1S)	124(2)		

Symmetry transformations used to generate equivalent atoms:

' (x,y,z) → (-1-x,-y,1-z)

Anisotropic displacement parameters [$Å^2 \times 10^3$].

	U11	U22	U33	U23	U13	U12
Br(1)	59(1)	132(1)	99(1)	-58(1)	7(1)	-11(1)
Br(2)	68(1)	166(2)	123(2)	-99(1)	-7(1)	-14(1)
Br(3)	98(1)	72(1)	115(1)	-18(1)	19(1)	-1(1)
Al(1)	65(2)	79(3)	40(2)	-24(2)	4(2)	-8(2)
O(1)	119(8)	83(6)	46(6)	-19(5)	-10(5)	2(5)
C(1)	82(11)	65(9)	81(11)	-22(9)	20(9)	-4(8)
C(2)	78(11)	78(10)	93(13)	-40(10)	6(9)	-21(8)
C(3)	75(10)	91(11)	115(14)	-69(11)	-20(9)	-7(8)
C(4)	77(10)	103(11)	75(10)	-63(9)	-5(8)	-1(8)
C(5)	68(9)	59(8)	51(9)	-5(7)	-1(7)	-1(7)
C(6)	50(9)	88(10)	81(12)	-20(9)	12(8)	2(7)
C(7)	68(10)	72(9)	83(12)	-27(10)	-3(9)	-6(7)
C(8)	78(10)	80(9)	49(9)	-22(8)	-9(7)	-3(8)
C(9)	70(9)	78(9)	46(9)	-26(8)	-7(7)	26(7)
C(10)	54(8)	59(8)	55(9)	-28(7)	8(6)	2(6)
C(11)	55(8)	61(7)	41(8)	-17(7)	13(6)	6(6)
C(12)	48(8)	58(8)	53(8)	-22(7)	-5(6)	12(6)
C(13)	52(8)	60(8)	42(8)	-20(7)	0(6)	-5(6)

Hydrogen coordinates [x 10^4] and equivalent isotropic displacement parameters [$Å^2$ x 10^3].

	x	y	z	U(eq)
H(1A)	80(15)	8414(14)	7311(16)	101
H(2A)	1229(15)	9359(15)	8452(18)	101
H(3A)	824(14)	8312(15)	10910(18)	101
H(4A)	-778(14)	6299(15)	12288(14)	92
H(5A)	-2795(12)	4005(12)	13301(13)	81
H(6A)	-4422(14)	2202(15)	13466(17)	98
H(7A)	-4935(14)	2007(14)	11588(17)	94
H(8A)	-3912(13)	3699(13)	9281(14)	86
H(2S)	-7214(22)	469(23)	10615(25)	195
H(3S)	-3665(22)	-1701(21)	11501(23)	188
H(4SA)	-6945(29)	-1525(30)	12917(27)	168
H(4SB)	-5961(29)	-2673(30)	12638(27)	168
H(4SC)	-5391(29)	-1629(30)	13207(27)	168

$AlBr_3$(9-fluorenone)$_2$ (**1.3**)

Atomic coordinates [x 10^4] and equivalent isotropic displacement parameters [$Å^2$ x 10^3]. U(eq) is defined as one third of the trace of the orthogonalized Uij tensor.

	x	y	z	U(eq)
Al(1)	7262(4)	2073(3)	7326(2)	44(1)
Br(1)	4081(2)	2012(1)	7448(1)	69(1)
Br(2)	9298(2)	1852(1)	6104(1)	66(1)
Br(3)	8707(2)	2295(1)	8492(1)	58(1)
O(1)	6244(10)	3995(6)	7125(4)	63(2)
C(1)	4294(15)	5620(11)	8715(6)	58(3)
C(2)	3390(18)	6601(16)	9294(7)	81(4)
C(3)	2753(17)	7964(15)	9050(9)	78(4)
C(4)	3018(17)	8391(12)	8250(8)	70(3)
C(5)	3914(16)	8616(10)	6215(8)	66(3)
C(6)	4435(21)	8383(15)	5374(8)	89(4)
C(7)	5378(18)	7070(14)	5086(7)	77(4)
C(8)	5788(16)	6004(11)	5637(6)	65(3)
C(9)	5442(14)	5270(10)	7158(6)	47(3)
C(10)	4560(14)	6054(10)	7912(5)	44(2)
C(11)	3909(13)	7404(9)	7665(6)	41(2)
C(12)	4324(14)	7543(8)	6787(7)	46(3)
C(13)	5268(14)	6207(9)	6468(6)	44(2)
O(1A)	8097(10)	127(6)	7458(4)	64(2)
C(1A)	9567(15)	-2326(10)	6352(6)	51(3)
C(2A)	10217(16)	-3605(11)	6016(6)	61(3)
C(3A)	10453(17)	-4737(11)	6519(7)	66(3)
C(4A)	9986(14)	-4688(9)	7367(7)	52(3)
C(5A)	8481(15)	-3694(10)	9293(6)	58(3)
C(6A)	7866(17)	-2959(13)	10026(7)	73(4)
C(7A)	7252(16)	-1532(12)	10030(7)	66(3)
C(8A)	7403(15)	-835(10)	9293(6)	56(3)
C(9A)	8352(14)	-1050(10)	7724(6)	50(3)
C(10A)	9081(14)	-2252(9)	7185(6)	47(3)
C(11A)	9264(14)	-3413(9)	7706(6)	47(3)
C(12A)	8623(13)	-2967(9)	8565(6)	43(2)
C(13A)	8061(14)	-1525(9)	8566(6)	41(2)

Bond lengths [Å] and angles [°]

Al(1)-O(1)	1.907(6)	Al(1)-O(1A)	1.913(7)
Al(1)-Br(2)	2.304(3)	Al(1)-Br(1)	2.312(3)
Al(1)-Br(3)	2.323(3)	O(1)-C(9)	1.259(10)
C(1)-C(2)	1.372(14)	C(1)-C(10)	1.365(12)
C(2)-C(3)	1.38(2)	C(3)-C(4)	1.36(2)
C(4)-C(11)	1.381(13)	C(5)-C(12)	1.381(13)
C(5)-C(6)	1.39(2)	C(6)-C(7)	1.39(2)
C(7)-C(8)	1.354(14)	C(8)-C(13)	1.365(12)
C(9)-C(13)	1.425(12)	C(9)-C(10)	1.471(12)
C(10)-C(11)	1.373(12)	C(11)-C(12)	1.429(13)
C(12)-C(13)	1.429(12)	O(1A)-C(9A)	1.230(10)
C(1A)-C(10A)	1.356(12)	C(1A)-C(2A)	1.377(12)
C(2A)-C(3A)	1.361(13)	C(3A)-C(4A)	1.377(12)
C(4A)-C(11A)	1.376(12)	C(5A)-C(12A)	1.372(12)
C(5A)-C(6A)	1.398(13)	C(6A)-C(7A)	1.399(14)
C(7A)-C(8A)	1.368(13)	C(8A)-C(13A)	1.371(12)
C(9A)-C(13A)	1.438(12)	C(9A)-C(10A)	1.481(12)
C(10A)-C(11A)	1.405(12)	C(11A)-C(12A)	1.470(12)
C(12A)-C(13A)	1.415(12)		

O(1)-Al(1)-O(1A)	174.3(3)	O(1)-Al(1)-Br(2)	90.2(2)
O(1A)-Al(1)-Br(2)	89.2(2)	O(1)-Al(1)-Br(1)	88.3(2)
O(1A)-Al(1)-Br(1)	87.4(2)	Br(2)-Al(1)-Br(1)	125.13(13)
O(1)-Al(1)-Br(3)	93.7(2)	O(1A)-Al(1)-Br(3)	91.7(2)
Br(2)-Al(1)-Br(3)	114.17(13)	Br(1)-Al(1)-Br(3)	120.66(13)
C(9)-O(1)-Al(1)	167.5(7)	C(2)-C(1)-C(10)	117.2(10)
C(1)-C(2)-C(3)	120.1(11)	C(4)-C(3)-C(2)	122.5(12)
C(11)-C(4)-C(3)	117.5(11)	C(12)-C(5)-C(6)	120.5(11)
C(7)-C(6)-C(5)	121.0(11)	C(8)-C(7)-C(6)	119.3(10)
C(7)-C(8)-C(13)	120.7(10)	O(1)-C(9)-C(13)	125.6(9)
O(1)-C(9)-C(10)	126.3(9)	C(13)-C(9)-C(10)	108.1(8)
C(1)-C(10)-C(11)	122.9(10)	C(1)-C(10)-C(9)	130.3(9)
C(11)-C(10)-C(9)	106.7(8)	C(4)-C(11)-C(10)	119.7(10)
C(4)-C(11)-C(12)	129.9(10)	C(10)-C(11)-C(12)	110.3(8)
C(5)-C(12)-C(13)	116.9(9)	C(5)-C(12)-C(11)	135.1(10)
C(13)-C(12)-C(11)	107.8(8)	C(8)-C(13)-C(12)	121.5(9)
C(8)-C(13)-C(9)	131.5(9)	C(12)-C(13)-C(9)	107.0(8)
C(9A)-O(1A)-Al(1)	164.4(8)	C(10A)-C(1A)-C(2A)	117.3(9)
C(3A)-C(2A)-C(1A)	120.2(9)	C(2A)-C(3A)-C(4A)	123.5(10)
C(11A)-C(4A)-C(3A)	116.8(9)	C(12A)-C(5A)-C(6A)	117.4(10)
C(5A)-C(6A)-C(7A)	122.6(10)	C(8A)-C(7A)-C(6A)	118.5(10)
C(13A)-C(8A)-C(7A)	120.4(10)	O(1A)-C(9A)-C(13A)	128.7(9)
O(1A)-C(9A)-C(10A)	123.1(10)	C(13A)-C(9A)-C(10A)	108.2(8)
C(1A)-C(10A)-C(11A)	122.8(9)	C(1A)-C(10A)-C(9A)	130.1(9)
C(11A)-C(10A)-C(9A)	107.0(9)	C(4A)-C(11A)-C(10A)	119.3(9)
C(4A)-C(11A)-C(12A)	132.1(9)	C(10A)-C(11A)-C(12A)	108.6(9)
C(5A)-C(12A)-C(13A)	120.3(9)	C(5A)-C(12A)-C(11A)	131.3(9)
C(13A)-C(12A)-C(11A)	108.4(8)	C(8A)-C(13A)-C(12A)	120.6(9)
C(8A)-C(13A)-C(9A)	131.5(9)	C(12A)-C(13A)-C(9A)	107.9(8)

Anisotropic displacement parameters [$Å^2 \times 10^3$].

	U11	U22	U33	U23	U13	U12
Al(1)	45(2)	25(2)	54(2)	2(1)	-4(2)	-2(1)
Br(1)	52(1)	52(1)	101(1)	5(1)	-6(1)	-15(1)
Br(2)	72(1)	55(1)	59(1)	-2(1)	9(1)	-7(1)
Br(3)	68(1)	47(1)	60(1)	0(1)	-15(1)	-17(1)
O(1)	58(5)	19(4)	106(5)	-5(4)	-20(4)	0(3)
C(1)	36(7)	67(8)	68(7)	-1(6)	2(6)	-17(6)
C(2)	61(9)	139(13)	47(7)	-19(9)	1(6)	-37(9)
C(3)	37(8)	98(11)	94(10)	-41(9)	-3(7)	-9(8)
C(4)	54(8)	58(8)	98(9)	-22(8)	-21(7)	-11(7)
C(5)	44(7)	26(6)	127(10)	5(7)	-31(7)	-2(5)
C(6)	99(12)	109(12)	79(9)	47(9)	-40(9)	-61(10)
C(7)	87(11)	84(10)	48(7)	-2(7)	-7(7)	-14(8)
C(8)	65(9)	57(8)	61(7)	-1(6)	-11(6)	0(6)
C(9)	35(6)	43(6)	61(6)	-2(6)	-9(5)	-9(5)
C(10)	39(7)	53(7)	42(6)	-1(5)	1(5)	-20(5)
C(11)	21(6)	26(6)	71(7)	-12(5)	-5(5)	0(4)
C(12)	35(6)	16(5)	87(8)	5(5)	-18(6)	-4(5)
C(13)	41(7)	39(6)	53(6)	10(5)	-15(5)	-12(5)
O(1A)	63(5)	19(4)	101(5)	3(4)	-22(4)	3(3)
C(1A)	48(7)	41(7)	62(7)	7(5)	-4(6)	-12(5)
C(2A)	65(9)	45(7)	68(7)	-12(6)	-3(6)	-11(6)
C(3A)	82(10)	42(7)	75(8)	-16(6)	-2(7)	-22(6)
C(4A)	45(7)	22(6)	89(8)	5(5)	-6(6)	-14(5)
C(5A)	45(7)	49(7)	76(7)	18(6)	-18(6)	-11(6)
C(6A)	66(9)	88(10)	65(8)	25(7)	-17(7)	-26(8)
C(7A)	69(9)	60(8)	68(8)	-19(7)	3(6)	-21(7)
C(8A)	54(8)	42(6)	69(7)	0(6)	-7(6)	-11(6)
C(9A)	29(6)	38(7)	81(8)	-8(6)	-8(5)	-7(5)
C(10A)	44(7)	28(6)	70(7)	8(5)	-13(6)	-13(5)
C(11A)	30(6)	32(6)	78(7)	9(6)	-12(5)	-11(5)
C(12A)	30(6)	38(6)	54(6)	14(5)	-9(5)	-5(5)
C(13A)	31(6)	34(6)	58(6)	-2(5)	-2(5)	-10(5)

Hydrogen coordinates [x 10^4] and equivalent isotropic displacement parameters [$Å^2$ x 10^3].

	x	y	z	U(eq)
H(1A)	4711(15)	4696(11)	8863(6)	69
H(2A)	3206(18)	6335(16)	9847(7)	97
H(3A)	2139(17)	8604(15)	9456(9)	93
H(4A)	2600(17)	9316(12)	8104(8)	84
H(5A)	3299(16)	9500(10)	6401(8)	80
H(6A)	4139(21)	9120(15)	4999(8)	106
H(7A)	5722(18)	6937(14)	4519(7)	92
H(8A)	6437(16)	5127(11)	5447(6)	78
H(1AA)	9447(15)	-1541(10)	6023(6)	62
H(2AA)	10534(16)	-3694(11)	5445(6)	73
H(3AA)	10929(17)	-5591(11)	6279(7)	79
H(4AA)	10152(14)	-5474(9)	7699(7)	62
H(5AA)	8803(15)	-4640(10)	9296(6)	69
H(6AA)	7836(17)	-3440(13)	10528(7)	88
H(7AA)	6776(16)	-1071(12)	10524(7)	79
H(8AA)	7055(15)	112(10)	9289(6)	68

$GaCl_3$(9-fluorenone) (**1.5**)

Atomic coordinates [x 10^4] and equivalent isotropic displacement parameters [$Å^2$ x 10^3]. U(eq) is defined as one third of the trace of the orthogonalized Uij tensor.

	x	y	z	U(eq)
Ga(1)	644(1)	8612(1)	4973(1)	45(1)
Cl(1)	-1290(1)	9093(1)	5451(1)	74(1)
Cl(2)	2590(1)	9019(1)	5488(1)	74(1)
Cl(3)	483(1)	7370(1)	4863(1)	67(1)
O(1)	591(3)	9038(1)	3963(1)	51(1)
C(1)	962(4)	8919(2)	3282(2)	41(1)
C(2)	361(4)	9364(2)	2645(2)	41(1)
C(3)	-612(5)	9978(2)	2648(2)	53(1)
C(4)	-1033(5)	10282(2)	1942(3)	59(1)
C(5)	-489(5)	9973(2)	1279(2)	59(1)
C(6)	487(5)	9352(2)	1269(2)	53(1)
C(7)	904(4)	9051(2)	1962(2)	40(1)
C(8)	1916(4)	8403(2)	2165(2)	40(1)
C(9)	2691(5)	7904(2)	1716(2)	51(1)
C(10)	3563(5)	7345(2)	2071(3)	56(1)
C(11)	3641(5)	7296(2)	2858(3)	56(1)
C(12)	2838(5)	7793(2)	3322(2)	51(1)
C(13)	1964(4)	8336(2)	2967(2)	40(1)

Bond lengths [Å] and angles [°]

Ga(1)-O(1)	1.915(2)	Ga(1)-Cl(2)	2.1248(13)
Ga(1)-Cl(1)	2.1343(12)	Ga(1)-Cl(3)	2.1434(11)
O(1)-C(1)	1.258(4)	C(1)-C(2)	1.463(5)
C(1)-C(13)	1.468(5)	C(2)-C(3)	1.383(5)
C(2)-C(7)	1.404(5)	C(3)-C(4)	1.397(5)
C(4)-C(5)	1.373(5)	C(5)-C(6)	1.392(5)
C(6)-C(7)	1.376(5)	C(7)-C(8)	1.493(5)
C(8)-C(9)	1.364(5)	C(8)-C(13)	1.413(5)
C(9)-C(10)	1.398(5)	C(10)-C(11)	1.383(5)
C(11)-C(12)	1.393(5)	C(12)-C(13)	1.379(5)
O(1)-Ga(1)-Cl(2)	106.79(9)	O(1)-Ga(1)-Cl(1)	101.20(9)
Cl(2)-Ga(1)-Cl(1)	114.20(5)	O(1)-Ga(1)-Cl(3)	107.09(8)
Cl(2)-Ga(1)-Cl(3)	115.01(5)	Cl(1)-Ga(1)-Cl(3)	111.21(5)
C(1)-O(1)-Ga(1)	143.9(3)	O(1)-C(1)-C(2)	122.5(3)
O(1)-C(1)-C(13)	129.7(4)	C(2)-C(1)-C(13)	107.8(3)
C(3)-C(2)-C(7)	121.7(4)	C(3)-C(2)-C(1)	129.8(4)
C(7)-C(2)-C(1)	108.4(3)	C(2)-C(3)-C(4)	117.4(4)
C(5)-C(4)-C(3)	120.3(4)	C(4)-C(5)-C(6)	122.8(4)
C(7)-C(6)-C(5)	117.2(4)	C(6)-C(7)-C(2)	120.6(4)
C(6)-C(7)-C(8)	131.6(4)	C(2)-C(7)-C(8)	107.8(3)
C(9)-C(8)-C(13)	120.5(4)	C(9)-C(8)-C(7)	131.1(4)
C(13)-C(8)-C(7)	108.5(3)	C(8)-C(9)-C(10)	118.3(4)
C(11)-C(10)-C(9)	121.0(4)	C(10)-C(11)-C(12)	121.2(4)
C(13)-C(12)-C(11)	117.4(4)	C(12)-C(13)-C(8)	121.5(4)
C(12)-C(13)-C(1)	131.0(4)	C(8)-C(13)-C(1)	107.4(3)

Anisotropic displacement parameters [$Å^2 \times 10^3$].

	U11	U22	U33	U23	U13	U12
Ga(1)	49(1)	49(1)	37(1)	2(1)	1(1)	2(1)
Cl(1)	65(1)	78(1)	80(1)	7(1)	26(1)	14(1)
Cl(2)	65(1)	72(1)	85(1)	2(1)	-26(1)	-4(1)
Cl(3)	87(1)	49(1)	67(1)	4(1)	-2(1)	-4(1)
O(1)	67(2)	53(2)	35(2)	0(1)	-1(2)	3(2)
C(1)	37(3)	45(2)	41(2)	2(2)	1(2)	-12(2)
C(2)	41(3)	43(2)	40(3)	5(2)	-2(2)	-6(2)
C(3)	55(3)	57(3)	48(3)	1(2)	9(3)	-3(3)
C(4)	53(3)	54(3)	69(3)	16(3)	-3(3)	3(2)
C(5)	55(3)	77(3)	45(3)	17(3)	-8(3)	-5(3)
C(6)	55(3)	66(3)	38(2)	4(2)	-3(3)	-3(3)
C(7)	39(3)	49(2)	33(2)	5(2)	-3(2)	-12(2)
C(8)	39(3)	45(2)	35(2)	0(2)	-2(2)	-9(2)
C(9)	52(3)	58(3)	43(2)	-4(2)	-1(3)	-9(2)
C(10)	48(3)	56(3)	62(3)	-10(3)	5(3)	2(2)
C(11)	49(3)	54(3)	65(3)	12(3)	-1(3)	4(2)
C(12)	52(3)	59(3)	43(2)	4(2)	-2(3)	-4(2)
C(13)	36(3)	43(2)	40(2)	2(2)	-2(2)	-6(2)

Hydrogen coordinates [x 10^4] and equivalent isotropic displacement parameters [$Å^2$ x 10^3].

	x	y	z	U(eq)
H(1A)	149(3)	9472(1)	3983(1)	61
H(3A)	-983(5)	10185(2)	3118(2)	64
H(4A)	-1695(5)	10713(2)	1924(3)	71
H(5A)	-801(5)	10188(2)	801(2)	71
H(6A)	853(5)	9143(2)	799(2)	64
H(9A)	2646(5)	7938(2)	1170(2)	61
H(10A)	4117(5)	6990(2)	1763(3)	67
H(11A)	4263(5)	6914(2)	3089(3)	68
H(12A)	2884(5)	7758(2)	3868(2)	61

$GaBr_3$(9-fluorenone) (**1.6**)

Atomic coordinates [x 10^4] and equivalent isotropic displacement parameters [$Å^2$ x 10^3]. U(eq) is defined as one third of the trace of the orthogonalized Uij tensor.

	x	y	z	U(eq)
Ga(1)	1371(1)	2706(1)	3062(1)	53(1)
Br(1)	297(1)	872(1)	3007(1)	84(1)
Br(2)	4325(1)	2810(1)	2945(1)	75(1)
Br(3)	-388(1)	3971(1)	2425(1)	79(1)
O(1)	1209(6)	3078(4)	3981(2)	54(1)
C(1)	943(9)	2705(7)	5429(3)	56(2)
C(2)	1023(9)	2731(7)	6123(3)	59(2)
C(3)	1699(10)	3701(8)	6458(4)	65(2)
C(4)	2317(9)	4649(7)	6135(3)	56(2)
C(5)	3587(9)	6510(7)	5059(3)	51(2)
C(6)	3986(9)	7112(7)	4494(4)	59(2)
C(7)	3623(9)	6644(7)	3880(4)	58(2)
C(8)	2871(9)	5565(7)	3786(3)	53(2)
C(9)	1693(8)	3834(6)	4407(3)	42(2)
C(10)	1549(8)	3654(6)	5116(3)	37(2)
C(11)	2248(8)	4619(6)	5459(3)	38(2)
C(12)	2821(8)	5445(6)	4979(3)	41(2)
C(13)	2471(8)	4968(6)	4334(3)	41(2)
C(1S)	7532(24)	10427(17)	4264(11)	99(7)
C(2S)	6319(22)	10184(10)	4627(8)	136(5)
C(3S)	4525(30)	10318(14)	4341(8)	177(10)
C(4S)	6663(31)	9852(13)	5285(8)	188(10)

Bond lengths [Å] and angles [°]

Ga(1)-O(1)	1.936(4)	Ga(1)-Br(1)	2.2800(13)
Ga(1)-Br(3)	2.2836(12)	Ga(1)-Br(2)	2.2880(13)
O(1)-C(9)	1.258(7)	C(1)-C(10)	1.379(9)
C(1)-C(2)	1.404(8)	C(2)-C(3)	1.384(10)
C(3)-C(4)	1.391(10)	C(4)-C(11)	1.368(8)
C(5)-C(12)	1.369(9)	C(5)-C(6)	1.406(9)
C(6)-C(7)	1.360(9)	C(7)-C(8)	1.382(9)
C(8)-C(13)	1.375(8)	C(9)-C(13)	1.459(9)
C(9)-C(10)	1.472(8)	C(10)-C(11)	1.392(8)
C(11)-C(12)	1.471(9)	C(12)-C(13)	1.420(8)
C(1S)-C(2S)	1.28(2)	C(2S)-C(4S)	1.39(2)
C(2S)-C(3S)	1.43(2)	C(3S)-C(4S)'	1.26(2)

O(1)-Ga(1)-Br(1)	101.12(13)	O(1)-Ga(1)-Br(3)	107.72(14)
Br(1)-Ga(1)-Br(3)	113.04(5)	O(1)-Ga(1)-Br(2)	105.2(2)
Br(1)-Ga(1)-Br(2)	113.22(5)	Br(3)-Ga(1)-Br(2)	115.06(5)
C(9)-O(1)-Ga(1)	140.7(4)	C(10)-C(1)-C(2)	117.9(7)
C(3)-C(2)-C(1)	118.8(7)	C(2)-C(3)-C(4)	122.6(7)
C(11)-C(4)-C(3)	118.5(7)	C(12)-C(5)-C(6)	118.8(6)
C(7)-C(6)-C(5)	120.7(7)	C(6)-C(7)-C(8)	121.7(7)
C(13)-C(8)-C(7)	118.3(6)	O(1)-C(9)-C(13)	130.5(6)
O(1)-C(9)-C(10)	121.6(6)	C(13)-C(9)-C(10)	107.9(5)
C(1)-C(10)-C(11)	122.8(6)	C(1)-C(10)-C(9)	129.2(6)
C(11)-C(10)-C(9)	107.9(6)	C(4)-C(11)-C(10)	119.4(6)
C(4)-C(11)-C(12)	132.1(6)	C(10)-C(11)-C(12)	108.5(5)
C(5)-C(12)-C(13)	119.5(6)	C(5)-C(12)-C(11)	131.8(6)
C(13)-C(12)-C(11)	108.7(6)	C(8)-C(13)-C(12)	121.0(6)
C(8)-C(13)-C(9)	132.0(6)	C(12)-C(13)-C(9)	107.0(6)
C(1S)-C(2S)-C(4S)	123(2)	C(1S)-C(2S)-C(3S)	117(2)
C(4S)-C(2S)-C(3S)	119.1(14)	C(4S)'-C(3S)-C(2S)	117(2)
C(3S)'-C(4S)-C(2S)	124(2)		

Symmetry transformations used to generate equivalent atoms:

' (x,y,z) → (1-x,2-y,1-z)

Anisotropic displacement parameters [$Å^2$ x 10^3].

	U11	U22	U33	U23	U13	U12
Ga(1)	76(1)	48(1)	34(1)	-8(1)	-2(1)	0(1)
Br(1)	123(1)	58(1)	66(1)	-9(1)	-13(1)	-21(1)
Br(2)	80(1)	78(1)	69(1)	-6(1)	13(1)	3(1)
Br(3)	110(1)	71(1)	52(1)	-5(1)	-11(1)	28(1)
O(1)	78(3)	47(3)	33(2)	-9(2)	-3(2)	-13(3)
C(1)	59(5)	62(6)	46(4)	-2(4)	4(4)	1(4)
C(2)	63(5)	70(6)	45(4)	9(4)	15(4)	10(4)
C(3)	72(6)	80(7)	45(4)	-4(5)	15(4)	23(5)
C(4)	55(5)	66(6)	48(5)	-16(4)	5(4)	2(4)
C(5)	48(5)	47(5)	56(5)	-17(4)	-4(4)	7(4)
C(6)	50(5)	43(5)	82(6)	-1(5)	4(4)	-1(4)
C(7)	61(5)	56(6)	57(5)	6(4)	5(4)	1(4)
C(8)	63(5)	57(6)	40(4)	-4(4)	6(4)	1(4)
C(9)	34(4)	47(5)	44(4)	-1(4)	-2(3)	11(3)
C(10)	40(4)	33(4)	38(4)	-4(3)	1(3)	5(3)
C(11)	39(4)	42(4)	34(4)	-4(3)	4(3)	7(3)
C(12)	39(4)	44(5)	40(4)	-12(3)	0(3)	11(3)
C(13)	37(4)	45(5)	39(4)	-3(3)	-1(3)	6(3)
C(1S)	91(15)	53(14)	158(22)	-26(13)	27(14)	-2(11)
C(2S)	222(19)	47(8)	125(13)	-23(7)	-31(11)	38(9)
C(3S)	364(31)	64(9)	87(12)	-11(9)	-43(15)	46(13)
C(4S)	366(31)	61(9)	103(13)	-20(9)	-113(14)	72(14)

Hydrogen coordinates [x 10^4] and equivalent isotropic displacement parameters [$Å^2$ x 10^3].

	x	y	z	U(eq)
H(1A)	471(9)	2048(7)	5182(3)	67
H(2A)	617(9)	2092(7)	6364(3)	70
H(3A)	1724(10)	3721(8)	6931(4)	78
H(4A)	2818(9)	5303(7)	6378(3)	67
H(5A)	3861(9)	6825(7)	5495(3)	61
H(6A)	4493(9)	7868(7)	4546(4)	70
H(7A)	3930(9)	7073(7)	3506(4)	70
H(8A)	2635(9)	5233(7)	3352(3)	64
H(1SA)	8690(24)	10310(17)	4498(11)	149
H(1SB)	7388(24)	9946(17)	3878(11)	149
H(1SC)	7399(24)	11219(17)	4134(11)	149
H(3SA)	4220(30)	10526(14)	3884(8)	213
H(4SA)	7882(31)	9741(13)	5458(8)	225

$VO(Cl)(9\text{-fluorenone})_2(H_2O)(\mu\text{-}O)(VOCl_2)$ (**1.12**)

Atomic coordinates [x 10^4] and equivalent isotropic displacement parameters [$Å^2$ x 10^3]. U(eq) is defined as one third of the trace of the orthogonalized Uij tensor.

	x	y	z	U(eq)
V(1)	4166(1)	6554(1)	2197(1)	34(1)
V(2)	493(1)	6558(1)	2084(1)	46(1)
Cl(1)	6060(2)	5934(2)	1488(1)	47(1)
Cl(2)	-471(2)	4371(2)	1499(2)	92(1)
Cl(3)	-196(2)	7800(2)	3405(2)	81(1)
O(1A)	3843(4)	7986(4)	1504(3)	41(1)
O(1B)	3928(4)	4760(4)	2521(3)	36(1)
O(2)	4969(4)	7560(4)	3294(3)	40(1)
O(3)	2891(4)	5189(4)	626(3)	45(1)
O(4)	2208(4)	6623(4)	2424(3)	41(1)
O(5)	150(5)	7158(6)	1180(4)	95(2)
C(1A)	6847(7)	9862(7)	2727(5)	42(2)
C(1B)	6953(6)	5598(6)	4084(5)	37(2)
C(2A)	8053(7)	10874(8)	3124(6)	59(2)
C(2B)	8150(7)	5699(7)	4838(5)	47(2)
C(3A)	8096(7)	12026(8)	2811(5)	55(2)
C(3B)	8212(7)	4761(8)	5361(5)	49(2)
C(4A)	6975(8)	12189(7)	2108(6)	51(2)
C(4B)	7087(7)	3697(7)	5140(5)	45(2)
C(5A)	3943(7)	11965(7)	458(5)	44(2)
C(5B)	4148(7)	1406(7)	4213(5)	48(2)
C(6A)	2573(7)	11564(7)	-175(5)	48(2)
C(6B)	2833(8)	653(7)	3677(6)	58(2)
C(7A)	1729(7)	10366(7)	-288(5)	44(2)
C(7B)	1942(7)	1002(7)	2945(6)	54(2)
C(8A)	2220(6)	9468(6)	215(5)	37(2)
C(8B)	2390(7)	2175(7)	2704(5)	46(2)
C(9A)	4320(7)	9129(7)	1473(5)	33(2)
C(9B)	4458(6)	4204(6)	3142(5)	31(2)
C(10A)	5721(6)	10009(6)	2026(5)	32(2)
C(10B)	5841(6)	4571(6)	3876(5)	30(2)
C(11A)	5767(7)	11209(6)	1719(5)	34(2)
C(11B)	5911(7)	3598(7)	4397(5)	36(2)
C(12A)	4423(6)	11100(6)	969(5)	32(2)
C(12B)	4589(7)	2568(7)	3980(5)	35(2)
C(13A)	3560(6)	9844(6)	842(5)	30(2)
C(13B)	3707(6)	2922(6)	3233(5)	29(2)

Bond lengths [Å]

V(1)-O(2)	1.564(4)	V(1)-O(4)	2.014(4)
V(1)-O(1A)	2.013(4)	V(1)-O(1B)	2.031(4)
V(1)-O(3)	2.251(4)	V(1)-Cl(1)	2.336(2)
V(2)-O(5)	1.569(4)	V(2)-O(4)	1.640(4)
V(2)-Cl(2)	2.179(2)	V(2)-Cl(3)	2.187(3)
O(1A)-C(9A)	1.237(6)	O(1B)-C(9B)	1.241(6)
C(1A)-C(10A)	1.376(7)	C(1A)-C(2A)	1.388(8)
C(1B)-C(10B)	1.358(7)	C(1B)-C(2B)	1.385(8)
C(2A)-C(3A)	1.382(8)	C(2B)-C(3B)	1.378(8)
C(3A)-C(4A)	1.382(9)	C(3B)-C(4B)	1.386(8)
C(4A)-C(11A)	1.372(8)	C(4B)-C(11B)	1.362(8)
C(5A)-C(12A)	1.365(7)	C(5A)-C(6A)	1.396(8)
C(5B)-C(6B)	1.373(8)	C(5B)-C(12B)	1.383(8)
C(6A)-C(7A)	1.361(8)	C(6B)-C(7B)	1.369(8)
C(7A)-C(8A)	1.388(7)	C(7B)-C(8B)	1.402(8)
C(8A)-C(13A)	1.370(7)	C(8B)-C(13B)	1.370(8)
C(9A)-C(13A)	1.455(7)	C(9A)-C(10A)	1.484(8)
C(9B)-C(10B)	1.463(8)	C(9B)-C(13B)	1.497(7)
C(10A)-C(11A)	1.424(7)	C(10B)-C(11B)	1.407(7)
C(11A)-C(12A)	1.482(8)	C(11B)-C(12B)	1.480(8)
C(12A)-C(13A)	1.412(7)	C(12B)-C(13B)	1.383(7)

Bond angles [°]

O(2)-V(1)-O(4)	96.2(2)	O(2)-V(1)-O(1A)	98.3(2)
O(4)-V(1)-O(1A)	87.3(2)	O(2)-V(1)-O(1B)	98.8(2)
O(4)-V(1)-O(1B)	83.1(2)	O(1A)-V(1)-O(1B)	161.2(2)
O(2)-V(1)-O(3)	176.2(2)	O(4)-V(1)-O(3)	80.6(2)
O(1A)-V(1)-O(3)	79.6(2)	O(1B)-V(1)-O(3)	82.9(2)
O(2)-V(1)-Cl(1)	100.8(2)	O(4)-V(1)-Cl(1)	162.73(14)
O(1A)-V(1)-Cl(1)	93.21(12)	O(1B)-V(1)-Cl(1)	91.17(12)
O(3)-V(1)-Cl(1)	82.50(11)	O(5)-V(2)-O(4)	108.8(2)
O(5)-V(2)-Cl(2)	107.9(2)	O(4)-V(2)-Cl(2)	106.9(2)
O(5)-V(2)-Cl(3)	110.2(2)	O(4)-V(2)-Cl(3)	108.8(2)
Cl(2)-V(2)-Cl(3)	114.06(9)	C(9A)-O(1A)-V(1)	145.3(4)
C(9B)-O(1B)-V(1)	141.6(4)	V(2)-O(4)-V(1)	155.6(2)
C(10A)-C(1A)-C(2A)	120.0(6)	C(10B)-C(1B)-C(2B)	119.0(6)
C(3A)-C(2A)-C(1A)	119.0(7)	C(3B)-C(2B)-C(1B)	120.3(6)
C(4A)-C(3A)-C(2A)	121.7(7)	C(2B)-C(3B)-C(4B)	120.9(6)
C(11A)-C(4A)-C(3A)	120.1(6)	C(11B)-C(4B)-C(3B)	118.7(6)
C(12A)-C(5A)-C(6A)	117.3(6)	C(6B)-C(5B)-C(12B)	117.3(6)
C(7A)-C(6A)-C(5A)	122.4(6)	C(7B)-C(6B)-C(5B)	123.7(6)
C(6A)-C(7A)-C(8A)	120.6(6)	C(6B)-C(7B)-C(8B)	119.1(7)
C(13A)-C(8A)-C(7A)	117.9(6)	C(13B)-C(8B)-C(7B)	117.4(6)
O(1A)-C(9A)-C(13A)	124.1(6)	O(1A)-C(9A)-C(10A)	128.4(5)
C(13A)-C(9A)-C(10A)	107.5(5)	O(1B)-C(9B)-C(10B)	130.5(5)
O(1B)-C(9B)-C(13B)	122.4(6)	C(10B)-C(9B)-C(13B)	107.1(5)
C(1A)-C(10A)-C(11A)	120.6(6)	C(1A)-C(10A)-C(9A)	132.7(6)
C(11A)-C(10A)-C(9A)	106.7(5)	C(1B)-C(10B)-C(11B)	120.8(6)
C(1B)-C(10B)-C(9B)	131.7(5)	C(11B)-C(10B)-C(9B)	107.5(5)
C(4A)-C(11A)-C(10A)	118.6(6)	C(4A)-C(11A)-C(12A)	132.2(6)
C(10A)-C(11A)-C(12A)	109.2(6)	C(4B)-C(11B)-C(10B)	120.3(6)
C(4B)-C(11B)-C(12B)	130.7(6)	C(10B)-C(11B)-C(12B)	109.0(6)
C(5A)-C(12A)-C(13A)	120.5(6)	C(5A)-C(12A)-C(11A)	132.2(6)
C(13A)-C(12A)-C(11A)	107.3(5)	C(5B)-C(12B)-C(13B)	119.6(6)
C(5B)-C(12B)-C(11B)	131.7(6)	C(13B)-C(12B)-C(11B)	108.7(5)
C(8A)-C(13A)-C(12A)	121.2(5)	C(8A)-C(13A)-C(9A)	129.5(6)
C(12A)-C(13A)-C(9A)	109.3(6)	C(8B)-C(13B)-C(12B)	122.9(5)
C(8B)-C(13B)-C(9B)	129.3(5)	C(12B)-C(13B)-C(9B)	107.8(5)

Anisotropic displacement parameters [$Å^2 \times 10^3$].

	U11	U22	U33	U23	U13	U12
V(1)	31(1)	33(1)	44(1)	23(1)	9(1)	6(1)
V(2)	33(1)	54(1)	63(1)	35(1)	12(1)	8(1)
Cl(1)	37(1)	56(1)	55(1)	24(1)	18(1)	10(1)
Cl(2)	62(1)	61(2)	130(2)	9(2)	20(1)	-9(1)
Cl(3)	59(1)	70(2)	119(2)	23(2)	45(1)	16(1)
O(1A)	41(3)	37(3)	59(3)	33(3)	17(2)	10(2)
O(1B)	34(3)	39(3)	43(3)	26(3)	7(2)	6(2)
O(2)	39(3)	42(3)	37(3)	18(3)	4(2)	1(2)
O(3)	47(3)	46(3)	41(3)	12(3)	8(2)	13(2)
O(4)	30(3)	41(3)	60(4)	26(3)	13(2)	8(2)
O(5)	72(4)	151(6)	105(5)	101(5)	19(3)	38(4)
C(1A)	46(5)	39(5)	48(5)	20(4)	15(4)	8(4)
C(1B)	26(4)	44(5)	44(5)	21(4)	4(4)	6(3)
C(2A)	43(5)	62(6)	74(6)	29(5)	12(4)	1(4)
C(2B)	34(4)	57(5)	50(5)	18(4)	12(4)	9(4)
C(3A)	43(5)	58(6)	52(6)	9(5)	9(4)	-5(4)
C(3B)	40(5)	72(6)	35(5)	17(5)	5(4)	23(4)
C(4A)	62(5)	38(5)	63(6)	21(4)	33(5)	7(4)
C(4B)	42(5)	53(5)	45(5)	24(4)	10(4)	15(4)
C(5A)	62(5)	30(4)	58(6)	28(4)	30(4)	17(4)
C(5B)	58(5)	45(5)	47(5)	24(4)	13(4)	7(4)
C(6A)	52(5)	48(5)	59(6)	32(4)	19(4)	19(4)
C(6B)	84(6)	47(5)	53(6)	30(5)	22(5)	0(5)
C(7A)	39(4)	50(5)	50(5)	25(4)	11(4)	16(4)
C(7B)	58(5)	39(5)	63(6)	17(4)	17(4)	-11(4)
C(8A)	38(4)	32(4)	45(5)	16(4)	16(4)	8(4)
C(8B)	50(5)	44(5)	52(5)	27(4)	15(4)	9(4)
C(9A)	43(4)	37(4)	32(4)	21(4)	16(3)	15(4)
C(9B)	27(4)	32(4)	42(5)	15(4)	18(3)	10(3)
C(10A)	38(4)	34(4)	28(4)	14(4)	8(3)	10(4)
C(10B)	27(4)	31(4)	35(4)	12(4)	12(3)	10(3)
C(11A)	40(4)	29(4)	41(5)	10(4)	27(4)	13(3)
C(11B)	41(4)	34(4)	28(4)	4(4)	9(4)	11(4)
C(12A)	35(4)	35(4)	35(4)	15(4)	20(3)	13(3)
C(12B)	49(5)	36(4)	30(4)	19(4)	15(4)	15(4)
C(13A)	37(4)	28(4)	36(4)	16(4)	17(3)	11(3)
C(13B)	30(4)	27(4)	33(4)	15(4)	9(3)	5(3)

Hydrogen coordinates [x 10^4] and equivalent isotropic displacement parameters [$Å^2$ x 10^3].

	x	y	z	U(eq)
H(3A)	1859(4)	5230(4)	247(3)	55
H(3B)	3215(4)	4675(4)	50(3)	55
H(1AA)	6802(7)	9047(7)	2926(5)	51
H(1BA)	6907(6)	6243(6)	3713(5)	45
H(2AA)	8845(7)	10779(8)	3611(6)	71
H(2BA)	8945(7)	6422(7)	5001(5)	56
H(3AA)	8936(7)	12718(8)	3078(5)	66
H(3BA)	9050(7)	4845(8)	5881(5)	59
H(4AA)	7006(8)	13001(7)	1905(6)	61
H(4BA)	7135(7)	3038(7)	5498(5)	54
H(5AA)	4515(7)	12827(7)	543(5)	53
H(5BA)	4749(7)	1125(7)	4717(5)	58
H(6AA)	2217(7)	12153(7)	-547(5)	58
H(6BA)	2505(8)	-142(7)	3844(6)	70
H(7AA)	786(7)	10149(7)	-719(5)	52
H(7BA)	1030(7)	447(7)	2581(6)	65
H(8AA)	1642(6)	8606(6)	122(5)	44
H(8BA)	1812(7)	2462(7)	2193(5)	55

$[^{t}(Bu)_2Ga(\mu\text{-}O_2CC_6H_4\text{-}2\text{-}NH_2)]_2$ (**2.2**)

Atomic coordinates [x 10^4] and equivalent isotropic displacement parameters [$Å^2$ x 10^3]. U(eq) is defined as one third of the trace of the orthogonalized Uij tensor.

	x	y	z	U(eq)
Ga(1)	9129(1)	1375(1)	5549(1)	38(1)
O(1)	8480(4)	957(3)	4255(2)	59(1)
O(2)	8896(3)	-730(3)	3995(2)	59(1)
N(3)	6051(9)	1857(7)	3107(5)	129(2)
C(1)	8229(5)	131(4)	3766(3)	43(1)
C(2)	7082(5)	183(3)	2904(3)	39(1)
C(3)	6133(6)	1007(5)	2661(4)	58(1)
C(4)	5034(8)	1027(9)	1832(7)	104(3)
C(5)	4928(12)	237(16)	1272(8)	175(9)
C(6)	5847(14)	-618(11)	1456(5)	139(5)
C(7)	6907(7)	-668(5)	2272(4)	74(2)
C(11)	9691(6)	2884(4)	5432(3)	55(1)
C(12)	8296(9)	3503(4)	4962(7)	108(3)
C(13)	10901(8)	2980(5)	4854(6)	101(2)
C(14)	10307(11)	3360(6)	6387(6)	118(3)
C(21)	7682(6)	725(4)	6243(4)	56(1)
C(22)	7614(7)	-462(5)	6150(5)	83(2)
C(23)	6095(7)	1209(6)	5858(6)	94(2)
C(24)	8183(9)	1015(6)	7276(4)	93(2)

Bond lengths [Å] and angles [°]

Ga(1)-O(2)'	1.941(3)	Ga(1)-O(1)	1.946(3)
Ga(1)-C(21)	1.972(5)	Ga(1)-C(11)	1.988(5)
O(1)-C(1)	1.262(5)	O(2)-C(1)	1.255(5)
N(3)-C(3)	1.267(9)	C(1)-C(2)	1.466(6)
C(2)-C(3)	1.347(7)	C(2)-C(7)	1.410(7)
C(3)-C(4)	1.406(10)	C(4)-C(5)	1.28(2)
C(5)-C(6)	1.35(2)	C(6)-C(7)	1.376(11)
C(11)-C(13)	1.501(8)	C(11)-C(12)	1.519(8)
C(11)-C(14)	1.526(9)	C(21)-C(22)	1.507(7)
C(21)-C(24)	1.539(8)	C(21)-C(23)	1.547(8)
O(2)'-Ga(1)-O(1)	107.5(2)	O(2)'-Ga(1)-C(21)	106.8(2)
O(1)-Ga(1)-C(21)	106.8(2)	O(2)'-Ga(1)-C(11)	101.8(2)
O(1)-Ga(1)-C(11)	102.1(2)	C(21)-Ga(1)-C(11)	130.3(2)
C(1)-O(1)-Ga(1)	139.9(3)	C(1)-O(2)-Ga(1)'	144.0(3)
O(2)-C(1)-O(1)	122.9(4)	O(2)-C(1)-C(2)	119.1(4)
O(1)-C(1)-C(2)	118.0(4)	C(3)-C(2)-C(7)	115.6(5)
C(3)-C(2)-C(1)	124.2(4)	C(7)-C(2)-C(1)	120.2(5)
N(3)-C(3)-C(2)	128.0(6)	N(3)-C(3)-C(4)	109.3(7)
C(2)-C(3)-C(4)	122.7(7)	C(5)-C(4)-C(3)	119.4(10)
C(4)-C(5)-C(6)	121.9(10)	C(5)-C(6)-C(7)	119.9(10)
C(6)-C(7)-C(2)	120.5(8)	C(13)-C(11)-C(12)	108.6(6)
C(13)-C(11)-C(14)	108.4(6)	C(12)-C(11)-C(14)	109.3(6)
C(13)-C(11)-Ga(1)	110.4(3)	C(12)-C(11)-Ga(1)	109.6(4)
C(14)-C(11)-Ga(1)	110.6(4)	C(22)-C(21)-C(24)	109.0(5)
C(22)-C(21)-C(23)	110.1(5)	C(24)-C(21)-C(23)	109.6(5)
C(22)-C(21)-Ga(1)	112.8(3)	C(24)-C(21)-Ga(1)	108.3(4)
C(23)-C(21)-Ga(1)	107.0(4)		

Symmetry transformations used to generate equivalent atoms:

' (x,y,z) → (2-x,-y,1-z)

Anisotropic displacement parameters [$Å^2 \times 10^3$].

	U11	U22	U33	U23	U13	U12
Ga(1)	43(1)	35(1)	37(1)	-2(1)	10(1)	-1(1)
O(1)	78(2)	56(2)	39(2)	-2(2)	1(2)	-12(2)
O(2)	46(2)	54(2)	72(2)	13(2)	-1(2)	3(2)
N(3)	129(6)	139(6)	115(6)	40(5)	18(4)	2(5)
C(1)	40(2)	49(3)	41(3)	5(2)	10(2)	-7(2)
C(2)	40(2)	45(3)	33(2)	2(2)	10(2)	-7(2)
C(3)	65(3)	55(3)	57(3)	10(3)	21(3)	-5(3)
C(4)	48(4)	163(8)	94(7)	72(6)	-1(4)	-4(4)
C(5)	85(7)	353(24)	76(7)	85(10)	-15(6)	-97(11)
C(6)	161(9)	220(12)	40(4)	-50(6)	30(5)	-139(9)
C(7)	83(4)	85(4)	60(4)	-5(3)	28(3)	-24(3)
C(11)	73(3)	36(3)	59(3)	-8(2)	17(3)	-8(2)
C(12)	99(5)	44(4)	183(9)	22(4)	30(6)	18(3)
C(13)	119(6)	48(4)	155(7)	0(4)	75(5)	-20(3)
C(14)	159(8)	65(4)	116(7)	-32(4)	-8(6)	-30(5)
C(21)	62(3)	55(3)	57(3)	2(2)	27(2)	-2(2)
C(22)	100(5)	57(3)	111(5)	-5(3)	68(4)	-18(3)
C(23)	63(4)	102(5)	128(7)	11(4)	45(4)	-4(3)
C(24)	125(6)	101(5)	67(4)	-3(4)	51(4)	-22(4)

Hydrogen coordinates [x 10^4] and equivalent isotropic displacement parameters [$Å^2$ x 10^3].

	x	y	z	U(eq)
H(3A)	5358(9)	2353(7)	2875(5)	155
H(3B)	6684(9)	1964(7)	3656(5)	155
H(4A)	4347(8)	1610(9)	1668(7)	125
H(5A)	4202(12)	230(16)	696(8)	210
H(6A)	5788(14)	-1205(11)	1035(5)	167
H(7A)	7547(7)	-1277(5)	2429(4)	89
H(12A)	8578(9)	4230(4)	4911(7)	163
H(12B)	7922(9)	3219(4)	4354(7)	163
H(12C)	7512(9)	3456(4)	5326(7)	163
H(13A)	11174(8)	3709(5)	4804(6)	151
H(13B)	11781(8)	2588(5)	5153(6)	151
H(13C)	10537(8)	2696(5)	4244(6)	151
H(14A)	10572(11)	4085(6)	6304(6)	176
H(14B)	9544(11)	3328(6)	6766(6)	176
H(14C)	11199(11)	2980(6)	6686(6)	176
H(22A)	6900(7)	-744(5)	6499(5)	124
H(22B)	7297(7)	-646(5)	5506(5)	124
H(22C)	8609(7)	-751(5)	6382(5)	124
H(23A)	5352(7)	916(6)	6179(6)	141
H(23B)	6140(7)	1962(6)	5945(6)	141
H(23C)	5809(7)	1052(6)	5206(6)	141
H(24A)	7495(9)	708(6)	7631(4)	140
H(24B)	9193(9)	744(6)	7495(4)	140
H(24C)	8188(9)	1770(6)	7347(4)	140

$[^{t}(Bu)_2Ga(\mu\text{-}O_2CC_6H_4\text{-}2\text{-}OH)]_2$ (**2.3**)

Atomic coordinates [x 10^4] and equivalent isotropic displacement parameters [$Å^2$ x 10^3]. U(eq) is defined as one third of the trace of the orthogonalized Uij tensor.

	x	y	z	U(eq)
Ga(1)	4400(1)	651(1)	6532(1)	50(1)
O(1)	6471(3)	-951(2)	5201(2)	70(1)
O(2)	6136(3)	-12(2)	6475(3)	84(1)
O(3)	8526(5)	-2033(3)	6066(4)	128(2)
C(1)	6734(4)	-639(2)	6255(4)	51(1)
C(2)	7841(4)	-1024(2)	7269(3)	52(1)
C(3)	8645(5)	-1676(3)	7113(5)	78(1)
C(4)	9685(6)	-2024(4)	8143(8)	107(2)
C(5)	9822(8)	-1683(6)	9254(8)	132(3)
C(6)	9107(9)	-1032(7)	9440(6)	134(3)
C(7)	8109(6)	-687(3)	8478(5)	97(2)
C(11)	5385(5)	1635(3)	7251(4)	70(1)
C(12)	4394(43)	2292(12)	6676(37)	160(16)
C(13)	6987(18)	1729(13)	7103(15)	110(6)
C(14)	5470(27)	1607(16)	8679(17)	156(12)
C(12A)	4277(38)	2290(18)	7239(38)	179(19)
C(13A)	6381(27)	1941(14)	6376(22)	173(11)
C(14A)	6386(31)	1551(12)	8441(18)	174(14)
C(21)	2834(5)	-17(3)	6999(4)	75(1)
C(22)	3401(8)	-313(4)	8345(6)	132(2)
C(23)	1405(6)	469(4)	6901(7)	128(2)
C(24)	2460(8)	-731(3)	6138(6)	118(2)

Bond lengths [Å] and angles [°]

Ga(1)-O(2)	1.938(3)	Ga(1)-O(1)'	1.963(3)
Ga(1)-C(21)	1.968(4)	Ga(1)-C(11)	1.975(4)
O(2)-C(1)	1.244(4)	O(1)-C(1)	1.253(5)
O(3)-C(3)	1.290(6)	C(1)-C(2)	1.471(5)
C(2)-C(3)	1.357(6)	C(2)-C(7)	1.424(7)
C(3)-C(4)	1.425(7)	C(4)-C(5)	1.338(10)
C(5)-C(6)	1.322(10)	C(6)-C(7)	1.357(9)
C(11)-C(14A)	1.42(2)	C(11)-C(12)	1.48(3)
C(11)-C(13)	1.49(2)	C(11)-C(12A)	1.49(3)
C(11)-C(13A)	1.55(3)	C(11)-C(14)	1.56(2)
C(21)-C(23)	1.510(7)	C(21)-C(24)	1.533(7)
C(21)-C(22)	1.543(7)		

O(2)-Ga(1)-O(1)'	105.22(13)	O(2)-Ga(1)-C(21)	107.5(2)
O(1)'-Ga(1)-C(21)	105.0(2)	O(2)-Ga(1)-C(11)	102.6(2)
O(1)'-Ga(1)-C(11)	102.3(2)	C(21)-Ga(1)-C(11)	131.7(2)
C(1)-O(1)-Ga(1)'	138.2(3)	C(1)-O(2)-Ga(1)	153.3(3)
O(2)-C(1)-O(1)	123.3(4)	O(2)-C(1)-C(2)	118.6(4)
O(1)-C(1)-C(2)	118.1(4)	C(3)-C(2)-C(7)	118.1(4)
C(3)-C(2)-C(1)	123.6(4)	C(7)-C(2)-C(1)	118.4(4)
O(3)-C(3)-C(2)	124.4(4)	O(3)-C(3)-C(4)	115.1(5)
C(2)-C(3)-C(4)	120.5(5)	C(5)-C(4)-C(3)	117.3(6)
C(6)-C(5)-C(4)	124.2(7)	C(5)-C(6)-C(7)	119.9(8)
C(6)-C(7)-C(2)	120.0(7)	C(12)-C(11)-C(13)	112(2)
C(14A)-C(11)-C(12A)	111(2)	C(14A)-C(11)-C(13A)	106.2(13)
C(12A)-C(11)-C(13A)	103(2)	C(12)-C(11)-C(14)	110(2)
C(13)-C(11)-C(14)	106.9(10)	C(14A)-C(11)-Ga(1)	114.6(9)
C(12)-C(11)-Ga(1)	107.4(11)	C(13)-C(11)-Ga(1)	113.6(8)
C(12A)-C(11)-Ga(1)	113.3(12)	C(13A)-C(11)-Ga(1)	107.6(8)
C(14)-C(11)-Ga(1)	107.1(9)	C(23)-C(21)-C(24)	109.2(5)
C(23)-C(21)-C(22)	109.5(5)	C(24)-C(21)-C(22)	108.5(5)
C(23)-C(21)-Ga(1)	108.2(3)	C(24)-C(21)-Ga(1)	111.2(4)
C(22)-C(21)-Ga(1)	110.2(3)		

Symmetry transformations used to generate equivalent atoms:

' (x,y,z) → (1-1,-y,1-z)

Anisotropic displacement parameters [$Å^2 \times 10^3$]

	U11	U22	U33	U23	U13	U12
Ga(1)	57(1)	50(1)	43(1)	-1(1)	9(1)	2(1)
O(1)	95(2)	66(2)	42(2)	2(1)	3(2)	7(2)
O(2)	80(2)	65(2)	99(2)	-9(2)	5(2)	25(2)
O(3)	149(4)	119(3)	114(3)	3(3)	25(3)	62(3)
C(1)	49(2)	45(2)	59(3)	7(2)	12(2)	-4(2)
C(2)	47(2)	54(2)	54(2)	14(2)	8(2)	-3(2)
C(3)	68(3)	81(3)	89(4)	20(3)	27(3)	7(3)
C(4)	68(3)	98(4)	150(6)	50(4)	14(4)	21(3)
C(5)	86(4)	168(8)	123(6)	72(6)	-16(5)	-26(5)
C(6)	129(6)	191(8)	66(4)	18(5)	-9(4)	-36(6)
C(7)	79(3)	136(5)	62(3)	30(3)	-11(3)	-22(3)
C(11)	74(3)	57(3)	76(3)	-10(2)	15(3)	-1(2)
C(12)	187(25)	40(8)	208(32)	-56(11)	-48(21)	6(10)
C(13)	78(9)	142(14)	116(14)	-56(12)	34(9)	-54(9)
C(14)	242(28)	167(20)	73(10)	-72(11)	65(17)	-99(21)
C(12A)	111(14)	138(19)	244(42)	-122(22)	-49(17)	42(11)
C(13A)	189(25)	117(17)	213(26)	-74(18)	48(18)	-90(17)
C(14A)	225(27)	91(10)	133(22)	-30(13)	-110(19)	-2(15)
C(21)	78(3)	81(3)	68(3)	10(2)	21(2)	-13(2)
C(22)	149(6)	156(6)	95(4)	37(4)	39(4)	-34(5)
C(23)	84(4)	153(6)	159(7)	16(5)	54(4)	-6(4)
C(24)	138(5)	99(5)	121(5)	-14(3)	43(4)	-61(4)

Hydrogen coordinates [x 10^4] and equivalent isotropic displacement parameters [$Å^2$ x 10^3].

	x	y	z	U(eq)
H(3)	7789	-1638	5221	80
H(4A)	10246(6)	-2470(4)	8052(8)	129
H(5A)	10454(8)	-1921(6)	9941(8)	159
H(6A)	9294(9)	-804(7)	10225(6)	160
H(7A)	7596(6)	-231(3)	8606(5)	116
H(12A)	4849(43)	2781(12)	7005(37)	240
H(12B)	4333(43)	2272(12)	5799(37)	240
H(12C)	3384(43)	2253(12)	6823(37)	240
H(13A)	7409(18)	2216(13)	7464(15)	165
H(13B)	7603(18)	1301(13)	7506(15)	165
H(13C)	6975(18)	1726(13)	6233(15)	165
H(14A)	5945(27)	2072(16)	9086(17)	234
H(14B)	4470(27)	1549(16)	8839(17)	234
H(14C)	6082(27)	1157(16)	8991(17)	234
H(12D)	4772(38)	2765(18)	7586(38)	269
H(12E)	3712(38)	2387(18)	6404(38)	269
H(12F)	3591(38)	2115(18)	7731(38)	269
H(13D)	6885(27)	2421(14)	6690(22)	259
H(13E)	7132(27)	1542(14)	6361(22)	259
H(13F)	5778(27)	2025(14)	5549(22)	259
H(14D)	6795(31)	2061(12)	8693(18)	261
H(14E)	5856(31)	1354(12)	9038(18)	261
H(14F)	7206(31)	1200(12)	8390(18)	261
H(22A)	4305(8)	-625(4)	8407(6)	198
H(22B)	2619(8)	-625(4)	8574(6)	198
H(22C)	3633(8)	130(4)	8894(6)	198
H(23A)	1635(6)	915(4)	7443(7)	192
H(23B)	628(6)	157(4)	7137(7)	192
H(23C)	1046(6)	645(4)	6060(7)	192
H(24A)	3363(8)	-1044(3)	6198(6)	176
H(24B)	2100(8)	-552(3)	5298(6)	176
H(24C)	1681(8)	-1041(3)	6374(6)	176

$[^{t}(Bu)_2Ga(\mu\text{-}O_2CC_6H_4\text{-}2\text{-}Me)]_2$ (**2.4**)

Atomic coordinates [x 10^4] and equivalent isotropic displacement parameters [$Å^2$ x 10^3]. U(eq) is defined as one third of the trace of the orthogonalized Uij tensor.

	x	y	z	U(eq)
Ga	922(1)	2108(1)	1418(1)	39(1)
O(1)	1470(3)	655(2)	2147(2)	51(1)
O(2)	1203(3)	-921(2)	348(2)	49(1)
C(1)	1673(3)	-418(3)	1597(3)	40(1)
C(2)	2620(4)	-1081(3)	2506(3)	41(1)
C(3)	2274(4)	-1329(3)	3577(3)	49(1)
C(3A)	817(6)	-1048(5)	3877(4)	76(1)
C(4)	3309(5)	-1899(4)	4385(3)	63(1)
C(5)	4648(6)	-2176(4)	4156(4)	73(1)
C(6)	4966(5)	-1947(4)	3090(4)	69(1)
C(7)	3943(4)	-1427(3)	2249(3)	53(1)
C(11)	-172(4)	2848(3)	2528(3)	49(1)
C(12)	-643(6)	4029(5)	2091(4)	77(1)
C(13)	1203(6)	3479(5)	4035(4)	77(1)
C(14)	-1911(5)	1635(4)	2307(4)	67(1)
C(21)	2976(4)	3195(3)	1067(3)	50(1)
C(22)	2424(6)	4170(5)	331(5)	84(1)
C(23)	3485(5)	2216(4)	215(4)	71(1)
C(24)	4663(5)	4114(4)	2436(4)	79(1)

Bond lengths [Å] and angles [°]

Ga-O(2)'	1.954(2)	Ga-O(1)	1.966(2)
Ga-C(11)	1.987(3)	Ga-C(21)	1.988(3)
O(1)-C(1)	1.262(3)	O(2)-C(1)	1.256(3)
C(1)-C(2)	1.493(4)	C(2)-C(3)	1.388(4)
C(2)-C(7)	1.402(4)	C(3)-C(4)	1.396(4)
C(3)-C(3A)	1.505(5)	C(4)-C(5)	1.367(5)
C(5)-C(6)	1.367(6)	C(6)-C(7)	1.370(5)
C(11)-C(14)	1.518(5)	C(11)-C(12)	1.529(5)
C(11)-C(13)	1.529(5)	C(21)-C(22)	1.518(5)
C(21)-C(24)	1.528(5)	C(21)-C(23)	1.531(5)
O(2)'-Ga-O(1)	102.57(10)	O(2)'-Ga-C(11)	103.01(11)
O(1)-Ga-C(11)	102.58(11)	O(2)'-Ga-C(21)	107.38(12)
O(1)-Ga-C(21)	109.02(11)	C(11)-Ga-C(21)	129.31(14)
C(1)-O(1)-Ga	129.4(2)	C(1)-O(2)-Ga'	143.0(2)
O(2)-C(1)-O(1)	124.2(3)	O(2)-C(1)-C(2)	118.2(2)
O(1)-C(1)-C(2)	117.6(2)	C(3)-C(2)-C(7)	120.1(3)
C(3)-C(2)-C(1)	123.4(3)	C(7)-C(2)-C(1)	116.4(3)
C(2)-C(3)-C(4)	117.7(3)	C(2)-C(3)-C(3A)	123.2(3)
C(4)-C(3)-C(3A)	119.1(3)	C(5)-C(4)-C(3)	121.5(3)
C(4)-C(5)-C(6)	120.5(3)	C(5)-C(6)-C(7)	119.8(3)
C(6)-C(7)-C(2)	120.3(3)	C(14)-C(11)-C(12)	109.2(3)
C(14)-C(11)-C(13)	109.4(3)	C(12)-C(11)-C(13)	109.4(3)
C(14)-C(11)-Ga	110.1(2)	C(12)-C(11)-Ga	108.8(2)
C(13)-C(11)-Ga	109.9(2)	C(22)-C(21)-C(24)	109.6(3)
C(22)-C(21)-C(23)	109.1(3)	C(24)-C(21)-C(23)	108.2(3)
C(22)-C(21)-Ga	108.4(2)	C(24)-C(21)-Ga	108.2(2)
C(23)-C(21)-Ga	113.3(2)		

Symmetry transformations used to generate equivalent atoms:

' (x,y,z) → (-x,-y,-z)

Anisotropic displacement parameters [$Å^2$ x 10^3].

	U11	U22	U33	U23	U13	U12
Ga	39(1)	45(1)	37(1)	20(1)	17(1)	22(1)
O(1)	66(1)	63(1)	43(1)	31(1)	26(1)	42(1)
O(2)	42(1)	71(1)	33(1)	21(1)	15(1)	24(1)
C(1)	31(1)	48(2)	41(2)	22(1)	15(1)	15(1)
C(2)	42(2)	40(2)	36(1)	16(1)	12(1)	17(1)
C(3)	54(2)	49(2)	41(2)	21(1)	16(1)	22(1)
C(3A)	83(3)	114(3)	66(2)	55(2)	48(2)	53(2)
C(4)	82(2)	63(2)	47(2)	33(2)	23(2)	33(2)
C(5)	85(3)	71(3)	66(2)	33(2)	15(2)	51(2)
C(6)	68(2)	72(2)	73(3)	24(2)	24(2)	47(2)
C(7)	55(2)	56(2)	50(2)	19(2)	19(2)	31(2)
C(11)	55(2)	60(2)	44(2)	21(1)	25(1)	34(2)
C(12)	92(3)	81(3)	89(3)	38(2)	48(2)	60(2)
C(13)	82(3)	101(3)	47(2)	15(2)	27(2)	47(2)
C(14)	67(2)	87(3)	70(2)	32(2)	47(2)	40(2)
C(21)	46(2)	47(2)	59(2)	23(2)	25(1)	19(1)
C(22)	75(3)	84(3)	115(3)	61(3)	53(2)	31(2)
C(23)	62(2)	70(2)	86(3)	25(2)	50(2)	19(2)
C(24)	51(2)	75(3)	82(3)	10(2)	21(2)	12(2)

Hydrogen coordinates [x 10^4] and equivalent isotropic displacement parameters [$Å^2$ x 10^3]. U(eq) is defined as one third of the trace of the orthogonalized Uij tensor.

	x	y	z	U(eq)
H(3AA)	249(6)	-643(5)	3248(4)	114
H(3AB)	-93(6)	-1936(5)	3782(4)	114
H(3AC)	1368(6)	-381(5)	4789(4)	114
H(4A)	3053(5)	-2122(4)	5104(3)	76
H(5A)	5383(6)	-2520(4)	4757(4)	88
H(6A)	5878(5)	-2179(4)	2917(4)	82
H(7A)	4157(4)	-1275(3)	1494(3)	64
H(12A)	-1174(6)	4390(5)	2623(4)	115
H(12B)	452(6)	4802(5)	2232(4)	115
H(12C)	-1507(6)	3634(5)	1145(4)	115
H(13A)	669(6)	3833(5)	4569(4)	116
H(13B)	1518(6)	2744(5)	4308(4)	116
H(13C)	2289(6)	4260(5)	4173(4)	116
H(14A)	-2439(5)	1991(4)	2844(4)	101
H(14B)	-2777(5)	1248(4)	1362(4)	101
H(14C)	-1610(5)	891(4)	2570(4)	101
H(22A)	3399(6)	4704(5)	151(5)	126
H(22B)	1341(6)	3580(5)	-513(5)	126
H(22C)	2170(6)	4831(5)	878(5)	126
H(23A)	4479(5)	2792(4)	74(4)	106
H(23B)	3860(5)	1624(4)	703(4)	106
H(23C)	2445(5)	1612(4)	-649(4)	106
H(24A)	5674(5)	4647(4)	2290(4)	119
H(24B)	4397(5)	4774(4)	2972(4)	119
H(24C)	4978(5)	3492(4)	2908(4)	119

$(^{t}Bu)_2Al(\mu\text{-}O_2CC_6H_4\text{-}2\text{-}NH_2)(^{t}Bu)_3$ (**2.5**)

Atomic coordinates [x 10^4] and equivalent isotropic displacement parameters [$Å^2$ x 10^3]. U(eq) is defined as one third of the trace of the orthogonalized Uij tensor.

	x	y	z	U(eq)
Al(1)	6223(1)	8837(1)	3469(1)	61(1)
Al(2)	7328(1)	8144(1)	1115(1)	60(1)
O(1)	6536(2)	8516(1)	2677(1)	60(1)
O(2)	7064(2)	7775(1)	1933(1)	68(1)
N(1)	5314(3)	7938(1)	3678(1)	69(1)
C(1)	6827(3)	7914(2)	2497(1)	56(1)
C(2)	6954(3)	7350(1)	2965(1)	54(1)
C(3)	6264(3)	7366(2)	3541(1)	56(1)
C(4)	6498(4)	6852(2)	3975(1)	74(1)
C(5)	7383(4)	6313(2)	3850(2)	87(1)
C(6)	8061(4)	6282(2)	3283(2)	88(1)
C(7)	7834(4)	6797(2)	2842(2)	72(1)
C(11)	8065(4)	8952(2)	4000(2)	78(1)
C(12)	7762(5)	8872(3)	4701(2)	158(2)
C(13)	9304(4)	8453(2)	3864(2)	103(1)
C(14)	8677(6)	9663(2)	3900(3)	174(3)
C(21)	4628(4)	9517(2)	3405(2)	72(1)
C(22)	3213(4)	9213(2)	3092(2)	110(1)
C(23)	4257(5)	9799(2)	4055(2)	124(2)
C(24)	5091(4)	10115(2)	2999(2)	111(1)
C(31)	8031(4)	7286(2)	691(2)	82(1)
C(32)	9617(5)	7091(2)	907(2)	135(2)
C(33)	7968(5)	7377(2)	-39(2)	129(2)
C(34)	7064(5)	6666(2)	820(2)	113(2)
C(41)	5322(4)	8481(2)	793(2)	85(1)
C(42)	4553(4)	8900(3)	1285(2)	135(2)
C(43)	4227(5)	7918(3)	583(2)	139(2)
C(44)	5449(5)	8945(3)	205(2)	133(2)
C(51)	8883(4)	8865(2)	1262(2)	73(1)
C(52)	10078(4)	8651(2)	1754(2)	110(1)
C(53)	9621(4)	9037(2)	644(2)	119(2)
C(54)	8234(5)	9533(2)	1511(2)	115(1)
C(2S)	3020(6)	11846(4)	1671(3)	128(2)
C(3S)	2932(6)	12291(3)	2147(4)	133(2)
C(4S)	2122(8)	12097(5)	2633(3)	152(3)
C(1S)	2120(25)	11224(8)	1832(8)	84(5)
C(5S)	1225(15)	11684(11)	2767(7)	123(7)
C(6S)	1230(33)	11133(17)	2329(14)	108(9)
C(7S)	2250(15)	10668(6)	1311(5)	155(4)
C(1SA)	2436(20)	11292(11)	1515(8)	125(6)
C(5SA)	1533(26)	11382(11)	2512(12)	95(7)
C(6SA)	1736(28)	11009(16)	2002(13)	142(14)
C(7SA)	592(12)	11032(7)	3001(6)	202(7)

Bond lengths [Å]

Al(1)-O(1)	1.822(2)	Al(1)-C(21)	1.958(3)
Al(1)-C(11)	1.960(4)	Al(1)-N(1)	2.003(3)
Al(2)-O(2)	1.896(2)	Al(2)-C(51)	2.001(3)
Al(2)-C(41)	2.005(4)	Al(2)-C(31)	2.021(3)
O(1)-C(1)	1.270(3)	O(2)-C(1)	1.250(3)
N(1)-C(3)	1.450(3)	C(1)-C(2)	1.481(4)
C(2)-C(7)	1.375(4)	C(2)-C(3)	1.397(4)
C(3)-C(4)	1.367(4)	C(4)-C(5)	1.359(4)
C(5)-C(6)	1.374(5)	C(6)-C(7)	1.380(4)
C(11)-C(14)	1.516(5)	C(11)-C(13)	1.523(5)
C(11)-C(12)	1.525(5)	C(21)-C(22)	1.522(5)
C(21)-C(24)	1.523(5)	C(21)-C(23)	1.533(4)
C(31)-C(32)	1.523(5)	C(31)-C(34)	1.530(5)
C(31)-C(33)	1.547(5)	C(41)-C(42)	1.521(5)
C(41)-C(43)	1.528(5)	C(41)-C(44)	1.546(5)
C(51)-C(52)	1.511(5)	C(51)-C(53)	1.532(4)
C(51)-C(54)	1.539(5)	C(2S)-C(1SA)	1.24(2)
C(2S)-C(3S)	1.334(7)	C(2S)-C(1S)	1.51(2)
C(3S)-C(4S)	1.346(8)	C(4S)-C(5S)	1.19(2)
C(4S)-C(5SA)	1.51(2)	C(7S)-C(1S)	1.56(2)
C(1S)-C(6S)	1.37(3)	C(5S)-C(6S)	1.42(3)
C(1SA)-C(6SA)	1.35(2)	C(5SA)-C(6SA)	1.32(3)
C(5SA)-C(7SA)	1.53(2)		

Bond angles [°]

O(1)-Al(1)-C(21)	108.90(12)	O(1)-Al(1)-C(11)	113.08(12)
C(21)-Al(1)-C(11)	123.7(2)	O(1)-Al(1)-N(1)	89.07(10)
C(21)-Al(1)-N(1)	107.82(13)	C(11)-Al(1)-N(1)	108.62(13)
O(2)-Al(2)-C(51)	104.63(12)	O(2)-Al(2)-C(41)	105.96(12)
C(51)-Al(2)-C(41)	115.4(2)	O(2)-Al(2)-C(31)	98.33(12)
C(51)-Al(2)-C(31)	114.9(2)	C(41)-Al(2)-C(31)	115.0(2)
C(1)-O(1)-Al(1)	129.8(2)	C(1)-O(2)-Al(2)	145.0(2)
C(3)-N(1)-Al(1)	112.5(2)	O(2)-C(1)-O(1)	122.4(3)
O(2)-C(1)-C(2)	117.4(3)	O(1)-C(1)-C(2)	120.2(2)
C(7)-C(2)-C(3)	118.1(3)	C(7)-C(2)-C(1)	119.1(3)
C(3)-C(2)-C(1)	122.8(3)	C(4)-C(3)-C(2)	120.5(3)
C(4)-C(3)-N(1)	120.4(3)	C(2)-C(3)-N(1)	119.2(3)
C(5)-C(4)-C(3)	120.8(3)	C(4)-C(5)-C(6)	119.9(3)
C(5)-C(6)-C(7)	119.8(3)	C(2)-C(7)-C(6)	121.0(3)
C(14)-C(11)-C(13)	106.7(3)	C(14)-C(11)-C(12)	108.4(4)
C(13)-C(11)-C(12)	106.8(3)	C(14)-C(11)-Al(1)	109.2(3)
C(13)-C(11)-Al(1)	115.1(2)	C(12)-C(11)-Al(1)	110.3(3)
C(22)-C(21)-C(24)	107.9(3)	C(22)-C(21)-C(23)	107.9(3)
C(24)-C(21)-C(23)	107.9(3)	C(22)-C(21)-Al(1)	110.9(2)
C(24)-C(21)-Al(1)	109.7(2)	C(23)-C(21)-Al(1)	112.4(2)
C(32)-C(31)-C(34)	106.3(3)	C(32)-C(31)-C(33)	107.8(3)
C(34)-C(31)-C(33)	106.3(3)	C(32)-C(31)-Al(2)	112.9(3)
C(34)-C(31)-Al(2)	112.7(2)	C(33)-C(31)-Al(2)	110.5(3)
C(42)-C(41)-C(43)	106.0(3)	C(42)-C(41)-C(44)	106.7(3)
C(43)-C(41)-C(44)	105.5(3)	C(42)-C(41)-Al(2)	112.6(2)
C(43)-C(41)-Al(2)	114.5(3)	C(44)-C(41)-Al(2)	111.0(2)
C(52)-C(51)-C(53)	108.5(3)	C(52)-C(51)-C(54)	105.7(3)
C(53)-C(51)-C(54)	107.2(3)	C(52)-C(51)-Al(2)	112.0(2)
C(53)-C(51)-Al(2)	111.0(2)	C(54)-C(51)-Al(2)	112.1(2)
C(1SA)-C(2S)-C(3S)	136.7(10)	C(3S)-C(2S)-C(1S)	107.6(8)
C(2S)-C(3S)-C(4S)	116.5(6)	C(5S)-C(4S)-C(3S)	141.2(11)
C(3S)-C(4S)-C(5SA)	109.5(10)	C(6S)-C(1S)-C(2S)	129(2)
C(6S)-C(1S)-C(7S)	121(2)	C(2S)-C(1S)-C(7S)	110(2)
C(4S)-C(5S)-C(6S)	110(2)	C(1S)-C(6S)-C(5S)	115(2)
C(2S)-C(1SA)-C(6SA)	111(2)	C(6SA)-C(5SA)-C(4S)	126(2)
C(6SA)-C(5SA)-C(7SA)	114(2)	C(4S)-C(5SA)-C(7SA)	120(2)
C(5SA)-C(6SA)-C(1SA)	119(3)		

Anisotropic displacement parameters [$Å^2 \times 10^3$].

	U11	U22	U33	U23	U13	U12
Al(1)	75(1)	64(1)	45(1)	-5(1)	19(1)	6(1)
Al(2)	75(1)	64(1)	41(1)	-3(1)	21(1)	-3(1)
O(1)	84(1)	59(1)	39(1)	0(1)	22(1)	6(1)
O(2)	94(2)	73(1)	39(1)	-4(1)	26(1)	1(1)
N(1)	80(2)	84(2)	46(1)	3(1)	25(1)	1(2)
C(1)	62(2)	67(2)	42(2)	-5(2)	17(1)	-3(2)
C(2)	67(2)	54(2)	42(2)	-3(1)	10(1)	-4(2)
C(3)	69(2)	57(2)	42(2)	-2(2)	13(1)	-5(2)
C(4)	106(3)	73(2)	43(2)	4(2)	12(2)	-8(2)
C(5)	135(3)	65(2)	60(2)	6(2)	-2(2)	3(2)
C(6)	123(3)	62(2)	78(3)	-8(2)	6(2)	17(2)
C(7)	98(2)	66(2)	54(2)	-8(2)	15(2)	7(2)
C(11)	84(2)	82(2)	68(2)	-17(2)	9(2)	3(2)
C(12)	141(4)	268(7)	63(3)	-30(3)	-7(3)	42(4)
C(13)	82(3)	120(3)	105(3)	-17(3)	-5(2)	6(2)
C(14)	148(4)	92(3)	274(7)	1(4)	-72(4)	-21(3)
C(21)	86(2)	71(2)	59(2)	-6(2)	19(2)	11(2)
C(22)	85(3)	115(3)	129(3)	-21(3)	6(2)	29(2)
C(23)	155(4)	127(3)	91(3)	-28(3)	34(3)	54(3)
C(24)	131(3)	92(3)	110(3)	23(3)	19(3)	22(3)
C(31)	112(3)	77(2)	61(2)	-8(2)	43(2)	-5(2)
C(32)	141(4)	99(3)	170(5)	-27(3)	59(3)	28(3)
C(33)	208(5)	117(3)	69(2)	-27(2)	71(3)	-24(3)
C(34)	171(4)	83(3)	89(3)	-20(2)	50(3)	-26(3)
C(41)	87(3)	112(3)	57(2)	-1(2)	9(2)	-2(2)
C(42)	102(3)	204(5)	98(3)	-22(3)	3(2)	61(3)
C(43)	110(3)	188(5)	117(4)	-13(4)	-1(3)	-25(3)
C(44)	130(4)	180(5)	89(3)	45(3)	-9(3)	16(3)
C(51)	83(2)	69(2)	68(2)	1(2)	17(2)	-2(2)
C(52)	93(3)	135(3)	102(3)	-2(3)	-13(2)	-20(3)
C(53)	123(3)	143(4)	95(3)	18(3)	30(3)	-54(3)
C(54)	136(4)	77(3)	133(4)	-16(3)	26(3)	-16(2)
C(2S)	110(4)	159(6)	114(5)	4(4)	-9(3)	-4(4)
C(3S)	118(4)	116(4)	162(6)	11(5)	-23(4)	-17(3)
C(4S)	110(5)	232(10)	114(5)	-7(5)	-1(4)	13(5)
C(7S)	226(13)	127(9)	116(8)	-51(7)	40(8)	-9(9)
C(1S)	126(15)	73(10)	53(8)	-8(8)	9(8)	14(9)
C(5S)	69(8)	206(19)	98(9)	-4(10)	38(6)	37(10)
C(6S)	71(14)	104(18)	149(20)	29(14)	0(12)	8(11)
C(1SA)	123(11)	167(16)	83(10)	-35(12)	-15(9)	-11(10)
C(5SA)	63(11)	110(18)	116(17)	34(11)	40(12)	10(11)
C(6SA)	84(14)	99(17)	241(40)	43(17)	9(15)	-2(11)
C(7SA)	150(9)	263(15)	207(12)	154(12)	115(9)	81(10)

Hydrogen coordinates [x 10^4] and equivalent isotropic displacement parameters [$Å^2$ x 10^3].

	x	y	z	U(eq)
H(1A)	5129(3)	7932(1)	4093(1)	83
H(1B)	4440(3)	7893(1)	3452(1)	83
H(4A)	6047(4)	6870(2)	4361(1)	89
H(5A)	7547(4)	5971(2)	4152(2)	105
H(6A)	8656(4)	5909(2)	3195(2)	105
H(7A)	8283(4)	6770(2)	2457(2)	87
H(12A)	7368(5)	8423(3)	4761(2)	237
H(12B)	7057(5)	9207(3)	4826(2)	237
H(12C)	8674(5)	8923(3)	4955(2)	237
H(13A)	9526(4)	8487(2)	3426(2)	154
H(13B)	8998(4)	7995(2)	3954(2)	154
H(13C)	10174(4)	8565(2)	4128(2)	154
H(14A)	8855(6)	9721(2)	3459(3)	261
H(14B)	9592(6)	9723(2)	4151(3)	261
H(14C)	7966(6)	9995(2)	4024(3)	261
H(22A)	2902(4)	8833(2)	3339(2)	165
H(22B)	3391(4)	9063(2)	2670(2)	165
H(22C)	2448(4)	9555(2)	3073(2)	165
H(23A)	3965(5)	9438(2)	4329(2)	185
H(23B)	3463(5)	10124(2)	4000(2)	185
H(23C)	5126(5)	10021(2)	4242(2)	185
H(24A)	5333(4)	9955(2)	2587(2)	166
H(24B)	5945(4)	10331(2)	3204(2)	166
H(24C)	4289(4)	10437(2)	2953(2)	166
H(32A)	10277(5)	7464(2)	832(2)	202
H(32B)	9905(5)	6700(2)	668(2)	202
H(32C)	9671(5)	6981(2)	1351(2)	202
H(33A)	6984(5)	7510(2)	-190(2)	193
H(33B)	8225(5)	6953(2)	-233(2)	193
H(33C)	8664(5)	7724(2)	-147(2)	193
H(34A)	6040(5)	6758(2)	700(2)	169
H(34B)	7166(5)	6564(2)	1266(2)	169
H(34C)	7397(5)	6282(2)	583(2)	169
H(42A)	5189(4)	9262(3)	1444(2)	202
H(42B)	4322(4)	8605(3)	1629(2)	202
H(42C)	3650(4)	9090(3)	1095(2)	202
H(43A)	4657(5)	7640(3)	267(2)	208
H(43B)	3324(5)	8121(3)	407(2)	208
H(43C)	4012(5)	7641(3)	942(2)	208
H(44A)	6143(5)	9305(3)	311(2)	200
H(44B)	4492(5)	9137(3)	87(2)	200
H(44C)	5791(5)	8685(3)	-144(2)	200
H(52A)	9632(4)	8549(2)	2146(2)	166
H(52B)	10775(4)	9019(2)	1821(2)	166
H(52C)	10586(4)	8255(2)	1610(2)	166
H(53A)	8885(4)	9173(2)	321(2)	179
H(53B)	10133(4)	8639(2)	506(2)	179
H(53C)	10321(4)	9401(2)	722(2)	179

Hydrogen coordinates [x 10^4] and equivalent isotropic displacement parameters [$Å^2$ x 10^3].

	x	y	z	U(eq)
H(54A)	7460(5)	9697(2)	1218(2)	172
H(54B)	9012(5)	9867(2)	1556(2)	172
H(54C)	7835(5)	9453(2)	1917(2)	172
H(2SA)	3596(6)	11940(4)	1312(3)	154
H(3SA)	3435(6)	12722(3)	2138(4)	160
H(4SA)	2098(8)	12407(5)	2984(3)	183
H(7SA)	1598(15)	10319(6)	1454(5)	232
H(7SB)	1937(15)	10799(6)	885(5)	232
H(7SC)	3248(15)	10495(6)	1319(5)	232
H(5SA)	613(15)	11716(11)	3106(7)	148
H(6SA)	670(33)	10739(17)	2377(14)	130
H(1SA)	2474(20)	11096(11)	1114(8)	150
H(6SB)	1405(28)	10560(16)	1978(13)	170
H(7SD)	492(12)	11331(7)	3357(6)	303
H(7SE)	1070(12)	10617(7)	3143(6)	303
H(7SF)	-374(12)	10929(7)	2809(6)	303